Altiplanic aquifer exploration by multidisciplinary methods

Addressing the basis of sustainable use of groundwater

Gomez Lopez, Etzar

2019

Document Version:
Publisher's PDF, also known as Version of record

Altiplanic aquifer exploration by multidisciplinary methods:

Addressing the basis of sustainable use of groundwater

ETZAR GÓMEZ
ENGINEERING GEOLOGY | FACULTY OF ENGINEERING | LUND UNIVERSITY

Printed by Media-Tryck, Lund 2019 NORDIC SWAN ECOLABEL 3041 0903

"The greatest crime in a desert is to find water and keep silent about it"
- African proverb

Division of Engineering Geology
Faculty of Engineering
Lund University
ISBN (print) 978-91-7895-265-6
ISRN LUTVDG/(TVDG-1043)/(1-134)/(2019)

Altiplanic aquifer exploration by multidisciplinary methods

Altiplanic aquifer exploration by multidisciplinary methods:

Addressing the basis of sustainable use of groundwater

Etzar Gómez

LUND
UNIVERSITY

DOCTORAL DISSERTATION

by due permission of the Faculty of Engineering, Lund University, Sweden.
To be defended at V-huset, John Ericsson väg 1, Lund, Sweden, Lecture hall V:D,
on October 25, 2019 at 10:15 a.m.

Faculty opponent
Dr. Anne Coudrain, Director of Research, Institut de Recherche pour le Développement, France

Organization LUND UNIVERSITY	Document name: Doctoral dissertation
Faculty of Engineering	Date of issue: 2019-08-30
Author: Etzar Gómez	Sponsoring organization: Swedish International Development Cooperation Agency (SIDA)

Altiplanic aquifer exploration by multidisciplinary methods:
Addressing the basis of sustainable use of groundwater

Abstract

The sustainable use of groundwater relies on building up three stages: exploration, development and management. The exploration is crucial to understand the capabilities and limitations of aquifer units; e.g. volume of available water and potential yield, distinction of recharge and discharge zones, and the groundwater quality are developed in this stage. In the Altiplano, groundwater is probably the most important water resource to supply domestic consumption and irrigation, since surficial bodies have been affected by reductions linked to drought events.

The city of Oruro, Bolivia, in the Central Altiplano, is supplied solely with groundwater from a porous aquifer that has been utilized for decades; however, its hydrogeological characteristics are not fully understood due to the scarcity of data and limited resources to conduct long-term research. In order to develop the exploration of the aquifer units to the north of Oruro, this thesis presents studies aiming to fill gaps in the knowledge about their hydrogeological characteristics. A multidisciplinary approach including analysis of isotopic data and geoelectrical surveys was applied in this thesis; results and interpretations are based on data from previous studies and from sampling and measurements conducted recently within this work. The study subjects in this thesis include groundwater flow patterns inferred through isotopic characteristics, deduction of some geological features (fault mapping and delineation of bedrock) from changes in resistivity and estimation of aquifer parameters relating hydraulic properties and resistivity. Data acquisition during this work consisted of sampling and analysing isotopic compositions in water from precipitation, rivers and wells. Likewise, resistivity was obtained from surveys using electrical resistivity tomography and transient electromagnetic methods.

Two aquifers were identified in the study area: unconsolidated sediments storing freshwater, currently under exploitation, overlying fractured bedrock that holds hydrothermal flows characterised by high temperature and salinity. Groundwater in the aquifers comes mainly from precipitation on the mountains, forming rivers that infiltrate laterally into the top aquifers, the natural discharge could have been located outside the limits of the study area, to the southwest; however, the cone of depression created by the wellfield supplying Oruro captures a substantial part of this groundwater. Isotopic characteristics of water in precipitation and groundwater at different depths were analysed to infer four circulation systems: (1) a shallow one receiving minor vertical infiltration, (2) the main system circulating through the unconsolidated sediments, (3) a transitional system between sediments and bedrock and (4) the deepest one, circulating through the bedrock fractures.

Resistivity models obtained from geoelectrical surveys were analysed to infer the depth of the contact between sediments and bedrock; in the selected study area, it varies from a couple of meters to ~200 m. The shape of the bedrock is interpreted as complex and irregular. Likewise, extensions of faults underneath the sediments were detected by tracking changes in resistivity; some of them seem to be connected to the hydrothermal sources in the region. Finally, an empirical relationship between hydraulic conductivity (from pumping test) and resistivity in the porous aquifer was used to estimate aquifer parameters (hydraulic conductivity and transmissivity) in areas with available resistivity data.

The outcomes from this thesis help to improve the basic comprehension of the hydrogeological characteristics of the studied aquifer system and fill gaps in the exploration stage; the results can be incorporated into the technical analyses aiming for the sustainable use of groundwater in the Altiplano. The applied methods have proven to be adequate to the local conditions and the multidisciplinary approach used in this thesis, can serve as an example for other studies dealing with similar conditions and limitations. Extensive surveys covering bigger areas with the same methodology, presented un this thesis, would permit the completion of the exploration stage and would make possible to shift the focus to the development and management stages of the aquifer units.

Key words: Bolivia; Geochemistry; Geophysics; Groundwater; Hydrogeology; Isotopes; Resistivity

Classification system and/or index terms (if any): -

Supplementary bibliographical information: -		Language: English
ISSN and key title: -		ISBN: 978-91-7895-265-6
Recipient's notes	Number of pages: 134	Price:
	Security classification: -	

Signature  Date 2019-08-23

Altiplanic aquifer exploration by multidisciplinary methods:

Addressing the basis of sustainable use of groundwater

Etzar Gómez

Coverphoto by Etzar Gómez

Faculty of Engineering
Division of Engineering Geology

ISBN (print) 978-91-7895-265-6
ISBN (pdf) 978-91-7895-266-3
ISRN LUTVDG/(TVDG-1043)/(1-134)/(2019)

Printed in Sweden by Media-Tryck, Lund University
Lund 2019

Preface

This thesis summarises almost five years of work dedicated to set a scientific research concerning groundwater in a semiarid region. A subject that is relevant but lacks awareness and support. Despite the achievements and results obtained, there is a lot to do to establish hydrogeology as an important issue for the society. The work presented in this thesis intends to be a reference for the stakeholders and researchers that might plan future investigations in more efficient ways.

The present research was supported and funded by the Swedish International Development Agency (SIDA) and the Society of Exploration Geophysicists (SEG) through the Geoscientists Without Borders (GWB) programme. The work was carried out at the Division of Engineering Geology, Lund University in Sweden with the participation of the Institute of Hydraulics and Hydrology, San Andrés Major University in Bolivia.

This work was made possible only because of the commitment and guidance of my supervisors Gerhard Barmen, Torleif Dahlin and Jan-Erik Rosberg, who were always able to contribute with their knowledge, resources and time to overcome the challenges encountered in the way. I express my gratitude to them and to all the staff of Engineering Geology for hosting me in a working environment where I found the motivation to always do my best. Against all odds.

Eternal gratitude to my family for their endless love and support.

Etzar Gómez

Lund, July 2019

Table of contents

Abstract

The sustainable use of groundwater relies on building up three stages: exploration, development and management. The exploration is crucial to understand the capabilities and limitations of aquifer units; e.g. volume of available water and potential yield, distinction of recharge and discharge zones, and the groundwater quality are developed in this stage. In the Altiplano, groundwater is probably the most important water resource to supply domestic consumption and irrigation, since surficial bodies have been affected by reductions linked to drought events.

The city of Oruro, Bolivia, in the Central Altiplano, is supplied solely with groundwater from a porous aquifer that has been utilized for decades; however, its hydrogeological characteristics are not fully understood due to the scarcity of data and limited resources to conduct long-term research. In order to develop the exploration of the aquifer units to the north of Oruro, this thesis presents studies aiming to fill gaps in the knowledge about their hydrogeological characteristics. A multidisciplinary approach including analysis of isotopic data and geoelectrical surveys was applied in this thesis; results and interpretations are based on data from previous studies and from sampling and measurements conducted recently within this work. The study subjects in this thesis include groundwater flow patterns inferred through isotopic characteristics, deduction of some geological features (fault mapping and delineation of bedrock) from changes in resistivity and estimation of aquifer parameters relating hydraulic properties and resistivity. Data acquisition during this work consisted of sampling and analysing isotopic compositions in water from precipitation, rivers and wells. Likewise, resistivity was obtained from surveys using electrical resistivity tomography and transient electromagnetic methods.

Two aquifers were identified in the study area: unconsolidated sediments storing freshwater, currently under exploitation, overlying fractured bedrock that holds hydrothermal flows characterised by high temperature and salinity. Groundwater in the aquifers comes mainly from precipitation on the mountains, forming rivers that infiltrate laterally into the top aquifers, the natural discharge could have been located outside the limits of the study area, to the southwest; however, the cone of depression created by the wellfield supplying Oruro captures a substantial part of this groundwater. Isotopic characteristics of water in precipitation and groundwater at different depths were analysed to infer four circulation systems: (1) a shallow one

receiving minor vertical infiltration, (2) the main system circulating through the unconsolidated sediments, (3) a transitional system between sediments and bedrock and (4) the deepest one, circulating through the bedrock fractures.

Resistivity models obtained from geoelectrical surveys were analysed to infer the depth of the contact between sediments and bedrock; in the selected study area, it varies from a couple of meters to ~200 m. The shape of the bedrock is interpreted as complex and irregular. Likewise, extensions of faults underneath the sediments were detected by tracking changes in resistivity; some of them seem to be connected to the hydrothermal sources in the region. Finally, an empirical relationship between hydraulic conductivity (from pumping test) and resistivity in the porous aquifer was used to estimate aquifer parameters (hydraulic conductivity and transmissivity) in areas with available resistivity data.

The outcomes from this thesis help to improve the basic comprehension of the hydrogeological characteristics of the studied aquifer system and fill gaps in the exploration stage; the results can be incorporated into the technical analyses aiming for the sustainable use of groundwater in the Altiplano. The applied methods have proven to be adequate to the local conditions and the multidisciplinary approach used in this thesis, can serve as an example for other studies dealing with similar conditions and limitations. Extensive surveys covering bigger areas with the same methodology, presented un this thesis, would permit the completion of the exploration stage and would make possible to shift the focus to the development and management stages of the aquifer units.

Sammanfattning

En hållbar användning av grundvattenresurser bygger på tre steg: prospektering, utveckling och förvaltning. Prospektering är avgörande för att förstå möjligheter och begränsningar hos akvifersenheter; t.ex. volym av tillgängligt vatten och potentiell uttagskapacitet, nybildnings- och utflödeszoner, och grundvattenkvalitet är undersöks i detta steg. På Altiplano är grundvatten förmodligen den viktigaste resursen för att leverera vatten för hushållsändamål och bevattning, eftersom ytvattensamlingar har påverkats av minskningar i samband med torkhändelser.

Staden Oruro, belägen centralt i Altiplano, Bolivia, försörjs sedan årtionden enbart med grundvatten från en porakvifer. Dess hydrogeologiska egenskaper är inte fullt ut förstådda på grund av knappheten i data och begränsade resurser för att genomföra långsiktig forskning. För att utveckla prospekteringen av akvifers-enheterna norr om Oruro, presenterar denna avhandling studier som fokuserar på att fylla luckor i kunskapen om deras hydrogeologiska karaktärsdrag och egenskaper. Ett multidisciplinärt tillvägagångssätt, inkluderande analys av isotopdata och geoelektriska undersökningar tillämpades i denna avhandling; resultat och tolkningar baseras på data från tidigare studier och från provtagning och mätningar som nyligen genomförts inom ramen för detta arbete. Grundvattenflödesmönster bedöms genom variation i isotopsammansättning, några geologiska egenskaper (kartläggning av förkastningar och avgränsning av berggrund) studeras genom förändringar i resistivitet och akviferparametrar uppskattas genom att relatera hydrauliska egenskaper till resistivitet. Under doktorandarbetet provtags vatten från nederbörd, floder och brunnar och dess isotopkomposition analyserades. Vidare erhölls marklagrens resistivitetsfördelning från undersökningar med elektrisk resistivitetstomografi och transienta elektromagnetiska metoder.

Två akviferer identifierades i studieområdet: okonsoliderade sediment som lagrar sötvatten och som för närvarande används för vattenförsörjningen. De överlagrar uppsprucken berggrund som på vissa platser innehåller hydrotermiska flöden kännetecknade av hög temperatur och salthalt. Grundvattnet i akvifererna kommer huvudsakligen från nederbörd i omgivande bergsområden. Detta vatten bildar floder som infiltreras lateralt till ytliga akviferer och det naturliga utflödesområdet kunde ha varit beläget utanför studieområdets gränser i sydväst. Emellertid fångar den avsänkningstratt som skapas av brunnsfältet som levererar vatten till Oruro en betydande del av detta grundvatten. Isotopegenskaperna hos vatten i nederbörd och

grundvatten från olika djup analyserades och ledde till en konceptuell modell med fyra cirkulationssystem: (1) ett ytligt som mottar mindre mängder infiltration vertikalt, (2) huvudsystemet som cirkulerar genom de okonsoliderade sedimenten, (3) ett övergångssystem mellan sediment och berggrund och (4) det djupaste, som cirkulerar genom spricksystem i berggrunden.

Resistivitetsmodeller erhållna från geoelektriska undersökningar analyserades för att utläsa djupet till kontakten mellan okonsoliderade sediment och berggrund; i det valda studieområdet varierar det från ett par meter till ~200 meter. Formen på berggrundens överyta tolkas som komplex och oregelbunden. På samma sätt detekterades förlängningar av förkastningar under sedimenten genom att spåra förändringar i resistivitet. Vissa av förkastningarna verkar vara kopplade till hydrotermiska källor i regionen. Slutligen användes ett empiriskt förhållande mellan hydraulisk ledningsförmåga (från provpumpningar) och resistivitet i porakviferen för att uppskatta akviferparametrar (hydraulisk ledningsförmåga och transmissivitet) i områden med tillgänglig resistivitetsdata.

Resultaten från denna avhandling bidrar till att förbättra den grundläggande förståelsen för det studerade akviferssystemets hydrogeologiska egenskaper och fylla luckor i prospekteringsstadiet. De kan också införlivas i de tekniska analyser som syftar till en hållbar användning av grundvatten i Altiplano-området. De tillämpade metoderna har visat sig vara lämpliga för de lokala förhållandena och det multidisciplinära tillvägagångssättet som används i denna avhandling kan tjäna som exempel för andra studier som behandlar liknande förhållanden med motsvarande begränsningar. Omfattande undersökningar, som täcker större områden med samma metod som presenteras i denna avhandling, skulle möjliggöra ett slutförande av prospekteringsstadiet och göra det möjligt att flytta fokus till utveckling och förvaltning av akviferersenheterna.

Resumen

El uso sostenible del agua subterránea se basa en el emplazamiento de tres etapas: exploración, desarrollo y gestión. La exploración es crucial para entender las capacidades y limitaciones de las unidades acuíferas; p.ej. el volumen de agua disponible y el rendimiento potencial, la distinción de las zonas de recarga y descarga y la calidad del agua subterránea se desarrollan en esta etapa. En el Altiplano, el agua subterránea es probablemente el recurso hídrico más importante para abastecer el consumo doméstico y el riego, ya que los cuerpos superficiales se han visto afectados por reducciones relacionadas con eventos de sequía.

La ciudad de Oruro, Bolivia, en el Altiplano Central, se suministra únicamente con agua subterránea de un acuífero poroso que ha sido utilizado durante décadas; sin embargo, sus características hidrogeológicas no se comprenden completamente debido a la escasez de datos y los recursos limitados para llevar a cabo investigaciones a largo plazo. Con el fin de desarrollar la exploración de las unidades acuíferas al norte de Oruro, esta tesis presenta estudios con el objetivo de llenar los vacíos en el conocimiento sobre sus características hidrogeológicas. En esta tesis se aplicó un enfoque multidisciplinario que incluye el análisis de datos isotópicos y levantamientos geo-eléctricos; Los resultados y las interpretaciones se basan en datos de estudios anteriores y de muestreos y mediciones realizados recientemente en este trabajo. Los temas de estudio en esta tesis incluyen patrones de flujo de agua subterránea inferidos a través de características isotópicas, deducción de algunas características geológicas (mapeo de fallas y delimitación del lecho rocoso) sobre cambios en la resistividad y estimación de parámetros acuíferos que relacionan las propiedades hidráulicas y la resistividad. La adquisición de datos durante este trabajo consistió en muestrear y analizar composiciones isotópicas en agua de precipitaciones, ríos y pozos. Del mismo modo, la resistividad se obtuvo de las encuestas utilizando tomografía de resistividad eléctrica y métodos electromagnéticos transitorios.

Dos acuíferos se identificaron en el área de estudio: sedimentos no consolidados que almacenan agua dulce, actualmente en explotación, yacen sobre roca fracturada que contiene flujos hidrotermales caracterizados por su alta temperatura y salinidad. El agua subterránea en los acuíferos proviene principalmente de la precipitación en las montañas, formando ríos que se infiltran lateralmente en los acuíferos someros, la descarga natural podría haberse ubicada fuera de los límites del área de estudio,

hacia el suroeste; sin embargo, el cono de abatimiento creado por el campo de pozos que abastece a Oruro captura una parte sustancial de estas aguas subterráneas. Las características isotópicas del agua en precipitación y en agua subterránea a diferentes profundidades se analizaron para inferir cuatro sistemas de circulación: (1) el somero que recibe una reducida infiltración vertical, (2) el sistema principal que circula a través de los sedimentos no consolidados, (3) un sistema de transición entre los sedimentos y la roca de fondo y (4) la más profunda, que circula a través de las fracturas de la roca madre.

Se analizaron modelos de resistividad obtenidos de estudios geo-eléctricos para inferir la profundidad del contacto entre los sedimentos y la roca de fondo; en el área de estudio seleccionada esta varía desde un par de metros hasta ~200 m. La forma de la roca de fondo se interpreta como compleja e irregular. Asimismo, se detectaron extensiones de fallas debajo de los sedimentos mediante un rastreo de los cambios en la resistividad; algunos de ellos parecen estar conectados a las fuentes hidrotermales de la región. Finalmente, se utilizó una relación empírica entre la conductividad hidráulica (de pruebas de bombeo) y la resistividad en el acuífero poroso para estimar los parámetros acuíferos (conductividad hidráulica y transmisividad) en áreas con datos de resistividad disponibles.

Los resultados de esta tesis ayudan a mejorar la comprensión básica de las características hidrogeológicas del sistema acuífero en estudio y llenar los vacíos en la etapa de exploración; Los resultados pueden incorporarse en los análisis técnicos que apuntan al uso sostenible de las aguas subterráneas en el Altiplano. Los métodos aplicados han demostrado ser adecuados para las condiciones locales y el enfoque multidisciplinario utilizado en esta tesis puede servir como ejemplo para otros estudios que lidian con similares condiciones y limitaciones. Levantamientos extensivos cubriendo áreas más grandes, con la misma metodología presentada en esta tesis, permitirían completar la etapa de exploración y haría posible cambiar la atención hacia las etapas de desarrollo y gestión de las unidades acuíferas.

Popular summary

In regions affected by drought and shortages of water, groundwater reservoirs tend to be more resilient than surface bodies as supply sources. In recent years such are the conditions of the aquifers that supply water to the city of Oruro, Bolivia. The capabilities and limitations of these reservoirs need to be understood by conducting investigations that ultimately aid to the sustainable use of groundwater.

Due to limited resources and the extent and depth of the aquifers, this study has focused on a representative locality where features of the freshwater aquifer (unconsolidated sediments) and the saline aquifer (fractured bedrock) can be explored. The methods applied in this study, i.e. analysis of isotopic data and geoelectrical surveys, are efficient, non-invasive and able to incorporate results from previous studies to make wider interpretations of the hydrogeological characteristics around the study area.

Percentages of light and heavy elements of the water molecule (stable isotopes) are used as "fingerprints" holding information about the origin and the travel paths of water samples. In this study, isotopic characteristics of precipitation, river waters and groundwater were analysed to infer four circulation systems: (1) a shallow one receiving modest vertical infiltration, (2) the main system circulating through the unconsolidated sediments, (3) a transitional system between sediments and bedrock and (4) a deep system circulating through the bedrock fractures. Results from geoelectrical surveys are expressed as resistivity, which is a property of geological formations indicating the capacity to allow electric currents to flow through them. It is highly influenced by the salinity of water present in the subsoil. Resistivity was used to infer which type of geological formations lie in the study area, the contact between sediments and bedrock (which seems uneven and complex) and to track extensions of faults with saline water beneath the sediments. Another outcome from the study consists of estimations of hydraulic properties of the sediments by an empirical relationship found between resistivity and hydraulic conductivity (the capacity to allow water flowing).

The study improves the knowledge about the hydrogeological characteristics of aquifers supplying Oruro. However, the exploration of these reservoirs needs to be expanded and extended to other parts of the aquifer system, perhaps using similar methods to those presented in this thesis, since they were proven to be efficient and well suited to the characteristics of the study area.

Appended papers

Paper I

Gómez, E., Barmen, G., Rosberg, J.-E., 2016. Groundwater Origins and Circulation Patterns Based on Isotopes in Challapampa Aquifer, Bolivia. *Water*, 8, 207. https://doi.org/10.3390/w8050207

Paper II

Gómez, E., Larsson, M., Dahlin, T., Barmen, G., Rosberg, J.-E., 2019. Alluvial aquifer thickness and bedrock structure delineation by electromagnetic methods in the highlands of Bolivia. *Environmental Earth Sciences*, 78, 84. https://doi.org/10.1007/s12665-019-8074-x

Paper III

Gómez, E., Svensson, E., Dahlin, T., Barmen, G., Rosberg, J.-E., 2019. Tracking of geological structures and detection of hydrothermal intrusion by geo-electrical methods in the highlands of Bolivia. *Journal of South American Earth Sciences*, 91, 214–226. https://doi.org/10.1016/j.jsames.2019.02.002

Paper IV

Gómez, E., Broman, V., Dahlin, T., Barmen, G., Rosberg, J.-E., 2019. Quantitative estimations of aquifer properties from resistivity in the Bolivian highlands. *H2Open Journal*, 2, 113–124. https://doi.org/10.2166/h2oj.2019.007

Author contribution

Paper I

The author planned the study, obtained archive data and collected water samples. He performed most of the data analysis, paper writing, revision and correspondence with the journal.

Paper II

The author designed the geoelectrical survey, organized the fieldwork and participated during the data acquisition. He performed most of the data analysis, paper writing, revision and correspondence with the journal.

Paper III

The author planned the geoelectrical survey, organized the fieldwork and participated during the data acquisition. He performed most of the data analysis, paper writing, revision and correspondence with the journal.

Paper IV

The author planned the study, participated during the data acquisition, performed most of the data analysis, paper writing, revision and correspondence with the journal.

1 Introduction

There is no doubt about the importance of water for life. As a resource, it is a key factor to sustain economic activities and development, in rural areas as well as in densely populated urban areas that can grow and prosper only if the water supply is guaranteed (Hubbard and Rubin, 2005; Maliva and Missimer, 2012). However, continuous growth of cities without proper planning poses challenges for water supply, enhanced nowadays by the effects of climate change (Canedo-Rosso et al., 2019). This is a common situation among cities in developing countries, such as Bolivia.

Providing enough and safe water is the main goal for authorities and decision-makers involved in the water sector. Water utilities are responsible of supply and sanitation, striving constantly to satisfy the demand of existing and new settlements (ANESAPA, 2019). In Bolivia, water services were established as a human right in the Constitution of 2009 (GOB, 2009), meaning that the state and regional governments are required to take care of the supply, subsidizing costs, protecting sources and guaranteeing the services. This promotes a relaxed attention towards the water services; people tend to forget about the importance of water after the services are implemented and have been running for a certain time, taking for granted that water will always come from the tap (Salina and Berger, 2008).

Public water awareness tends to only happen when the services are interrupted and people suffer seriously from it (Ekmekçi and Günay, 1997). The immediate antecedent of this situation in Bolivia goes back to 2016, when the country declared a national emergency due to a water supply deficit in at least three major cities (GOB, 2016), as a consequence of the most severe drought in the last twenty-five years (Marengo et al., 2017; Satgé et al., 2017). The crisis severely impacted La Paz city, located in the Altiplano, where the water stored in dams and surficial reservoirs depleted to very low levels. After the rainy season arrived, the reservoirs were refilled and the crisis was relieved, and the people went back to a passive state with regards water awareness.

One of the cities that did not report any reduction on its water supply volumes, during the crisis of 2016, was Oruro (also located in the Altiplano). The city is supplied solely with groundwater and the main aquifers are located to the north of the urban area. However, the most dramatic effect of the mentioned drought was seen just to the south of the city; the lake Poopo, the largest lake located within the

Bolivian territory, dried up completely (Allen, 2016). This environmental crisis triggered the water awareness to a peak among people in Oruro but concerns regarding the freshwater aquifers were never in the spotlight.

Compared to surface water, groundwater resources are in general difficult to ascertain due to the fact that they cannot be observed directly (Kimura et al., 2018). In terms of investments generated after the national emergency (GOB, 2016), most of these were allocated to construct new surficial reservoirs and repair others. Small investments in the field of groundwater were used to implement new wells in sites where the resource is available. Finally, even smaller investments were aimed for groundwater investigations to improve the knowledge about the quantity, quality and management of these "unseen" resources. Although some aquifers have been under study, there is still a lot to do to achieve basic knowledge for the sustainable use of groundwater in the country. Moreover, the technical work must be accompanied by awareness of local authorities and users, well informed about basic concepts of groundwater resources (Ekmekçi and Günay, 1997).

The knowledge about Oruro's freshwater aquifers is of capital importance to prevent water crises in the future. Aspects like aquifer geometry, size, recharge and discharge, quality of water and flow directions need to be understood and put together to develop a sound management plan of the groundwater resources. Unfortunately, the lack of awareness towards this aquifer system and the weak research capacity of local institutions pose major problems for implementing long term investigation projects, impeding the growth of research initiatives and limiting the access to resources: human and financial. Under these circumstances, short-term investigations can be useful to set the basis for longer research projects, making use of the available information and applying efficient techniques able to provide new and relevant data.

The sustainable use of groundwater can be achieved by establishing three stages: exploration, development and management, each one standing on the previous, as shown in Figure 1. Different branches of science and engineering can address those stages (Niwas et al., 2011). In the present study, a multidisciplinary approach, based on isotopes and geophysics, is used to assess and improve the exploration stage of the aquifers around Oruro.

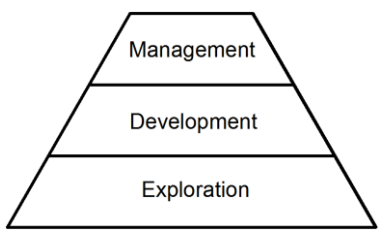

Figure 1 Stages of groundwater sustainable projects.

The two most relevant subjects on which this research is focused are: (1) Isotopic characteristics of water. Representative samples of water from the aquifers hold information about its origin and flow patterns through geological environments. Environmental isotopes (stable and radioactive) in different stages of the hydrological cycle are powerful tools in groundwater investigations (Mook, 2000). (2) Resistivity of geological formations obtained from geoelectrical tests (electrical resistivity tomography and transient electromagnetic soundings) that have evolved during the more recent years, becoming suitable tools for hydrogeological investigations (Christiansen et al., 2009; Kirsch and Yaramanci, 2009a; Slater and Lesmes, 2002). The mentioned studies are focused on a representative sector of the aquifer system around Oruro; the alluvial fan of River Paria. New results are complemented with existing information and data from geology, hydraulics and hydrochemistry (Banks et al., 2002; Dames & Moore Norge, 2000; Guérin et al., 2001; Lizarazu et al., 1987; Rigsby et al., 2005) to set the basis of the sustainable use of groundwater in Oruro.

1.1 Research purpose

The overall purpose of this thesis is to improve the knowledge about the studied aquifers, which later could aid the establishment of strategies to promote the sustainable use of groundwater in complex hydrogeological environments like in the Altiplano. The applied methodology intends to serve as an example for investigations dealing with similar conditions and limitations. The aquifer system to the north of Oruro is the main study area. It has been investigated using data from different sources of hydrogeological information; from previous studies and recently acquired data.

1.2 Research objectives

The overall objective of this thesis is to refine the hydrogeological knowledge of the central part of the alluvial fan of River Paria by adding new information from isotopic and geoelectrical techniques.

The specific objectives can be formulated as follows:

- To test the applicability of exploration methods like stable isotopes and geoelectrical surveys to the semiarid conditions of the central Altiplano.
- To combine the available sources of information, obtained from previous studies and recently acquired, in a consistent and complementary way.

- To develop the knowledge regarding the hydrothermal activity in the eastern part of the investigated area.
- To correlate resistivity values with local geological formations and hydraulic parameters to establish relationships valid for the rest of the investigated area.

1.3 Limitations

This thesis is mainly focused on the application of isotopic data analysis and geoelectrical surveys as exploration techniques to improve the understanding of hydrogeological settings in a sector of the studied aquifer system. Due to the extensive size of the aquifers of interest and the lack of information about them, the data acquisition strategy using different techniques was designed to cover as much area as possible rather than to focus a detailed exploration on a small area; hence, correlations between results from different methods (e.g. mutual constrain resistivity inversions or interdisciplinary analyses) are not included in this thesis. Although outcomes and conclusions of this study aim to support future management plans for sustainable use of groundwater, aquifer management is mentioned in the thesis mainly as a motivation but not as a topic of study.

Limitations regarding specific challenges to conduct research in the study area can be divided in two main aspects: technical and social.

Among the technical limitations, one of the toughest pitfalls is the difficulty to gather information and the lack of archives; most of the studies conducted in the study area were never properly saved and reported, some of them are dispersed in universities, institutions and private collections with limited access. Consequently, many research attempts tend to repeat tests and measurements that were conducted previously. In the recent years, the Ministry of Environment and Water of Bolivia is trying to unify the available information concerning groundwater in the country in a single database; however, the progress in this task is still slow.

Most of the methods applied in this study are indirect and non-invasive. The hypothesis formulated based on the results from these methods needs to be confirmed with ground truth information. Unfortunately, lack of equipment, laboratories and limited budgets prohibit the application of complementary tests; e.g. core and grain size analyses, pumping tests, hydrochemical sampling at different levels and borehole drilling that can provide ground truth information.

Concerning the limitations in the social context, due to the weak research capacity of local institutions and scarce scientific tradition in Bolivia, many research projects cannot create links and connections between institutions due to the heavy

bureaucracy involved. In the field of groundwater, scientific investigations are rare and commonly misunderstood regarding their scopes and goals. Consequently, it is difficult to join forces with other universities and institutions, although the common benefit can be easily recognized, the bureaucratic pitfalls prohibit such collaborations.

Other social limitations directly concern people living around the study area. Since the access to groundwater for consumption and irrigation in the region has caused several conflicts in the past, the villagers became reluctant to cooperate with any kind of investigation concerning groundwater. Consequently, the access to some places was not allowed, impeding extending some measurements over larger areas in connection with other sources of information such as wells and dug pits.

1.4 Thesis outline and content

This thesis is composed of six chapters and four appended papers, which contain the research outcomes in detail.

- Chapter 1. Introduces the context related to challenges that the water sector face in Bolivia, especially groundwater investigations that need to be adapted to the local conditions and limitations.
- Chapter 2. Presents an overview of the study area and the available information to establish the basis of a conceptual model.
- Chapter 3. Describes the theory behind isotopic and geoelectrical methods applied to complement and update the hydrogeological knowledge in the study area. Remarks on the applicability of these methods to the Altiplano conditions are mentioned.
- Chapter 4. Presents the results from the specific study subjects enclosed in this thesis. Each of them provides new knowledge to improve the understanding of the hydrogeological processes in the selected study area.
- Chapter 5. Discusses briefly about specific results coming from each investigation enclosed in this thesis.
- Chapter 6. Summarizes the conclusions and indicates directives for future investigations.

2 Study area

The initial settlement and growing of Oruro city are closely related to the mining activity in the region. Some surficial water bodies and springs were used to supply water in the past. As the city was growing, dug wells were implemented taking advantage of the shallow water table. Since the middle of the last century deep drilled wells (up to ~100 m deep) have been supplying water to the city (SELA, 2018). Nowadays, Oruro has about 300,000 inhabitants and depends solely on the closest aquifers to supply water for domestic consumption, irrigation, mining and industry (D'Elia, 2013; GITEC and COBODES Ltda., 2014). The sustainable use of groundwater in the region should be the main goal for the coming years. For this purpose, a complete description of the aquifers is needed, putting together all the available pieces of information and filling the gaps with new surveys.

2.1 General description

The Challapampa aquifer system encompasses all the geological formations storing water in the region to the north of Oruro (Figure 2). Unconsolidated sediments in an almost flat terrain are the most productive aquifers currently under exploitation. The area on which this aquifer system is emplaced is ~500 km^2 according to previous studies (Banks et al., 2002; D'Elia, 2013; Dames & Moore Norge, 2000) between latitudes 17″35' S – 18″00' S and longitudes 66″59' W – 67″12' W. The average altitude of this flat area is ~3700 meters above sea level (masl), surrounded by mountains and hard rock outcrops. The climate in the region is semi-arid with an average temperature of 10 °C and annual precipitation in the range of 300 to 500 mm. About 80% of the precipitation occurs between December and March, driven by the high-reaching anticyclones over the subtropical Andes (Coudrain et al., 1995), which transports humidity from the Atlantic and the Amazon.

The land over the aquifer system is mainly used for small-scale agriculture, especially during the rainy season. Although some sectors have continuous crops if irrigation is available, typically supplied by shallow dug wells or less commonly, deep drilled wells. In the central part of the alluvial fan of River Paria a well field operated by the local water supply company SELA (Servicio Local de Acueductos y Alcantarillado de Oruro), exploits the freshwater aquifer to supply the urban area

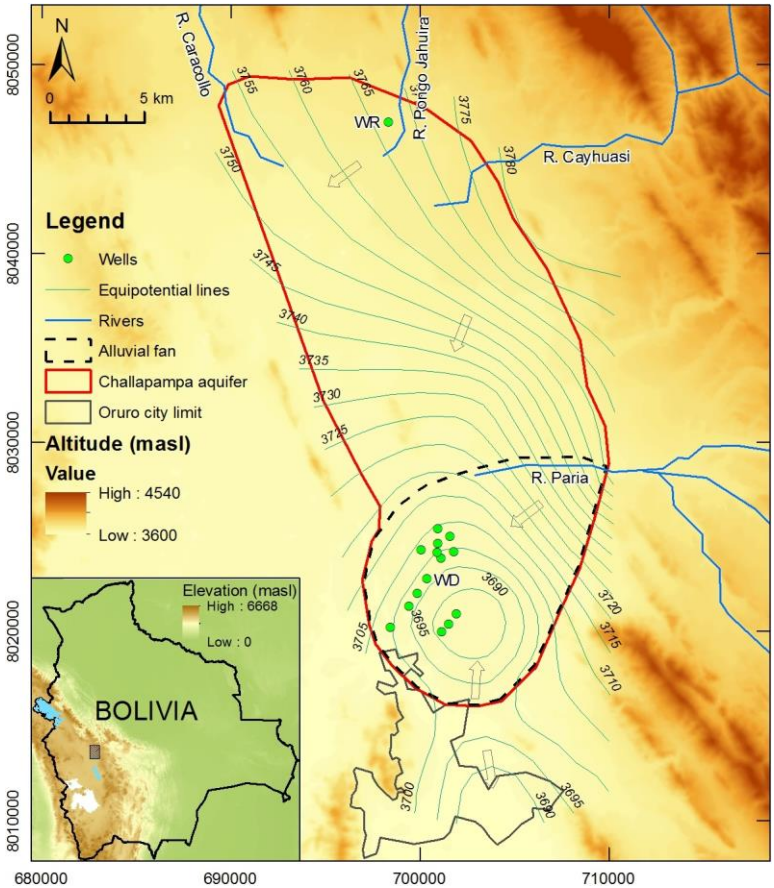

Figure 2 Location of the study area. Equipotential lines and arrows correspond to the porous aquifer. Modified from GEOBOL and Swedish Geological AB (1992); GITEC and COBODES Ltda. (2014).

of Oruro. Around this sector a cone of depression has been lowering the piezometric levels in other wells (D'Elia, 2013; GITEC and COBODES Ltda., 2014), leading to disputes and conflicts between SELA and the villagers living in the vicinity.

2.2 Geological settings

The regional geology is comprised of three groups of formations: (1) Consolidated rocks of Silurian age in the bedrock, outcrops and mountain ranges. In chronological order these formations are Cancañiri, Llallagua, Uncía and Catavi. They are comprised of sedimentary rocks like sandstones, siltstones and shales, as well as metamorphic rocks, like quartzite, in the oldest formations (GEOBOL and Swedish

Geological AB, 1992; Suarez Soruco, 2000). The secondary porosity of these formations, varying from small fractures to large faults, is assumed to be more significant than the primary porosity. (2) Volcanic formations from the Tertiary like the Oruro Complex and the Escalera Volcanics, that are comprised of dacitic tuffs and dacitic, rhyodacitic and porphyritic lavas (GEOBOL and Swedish Geological

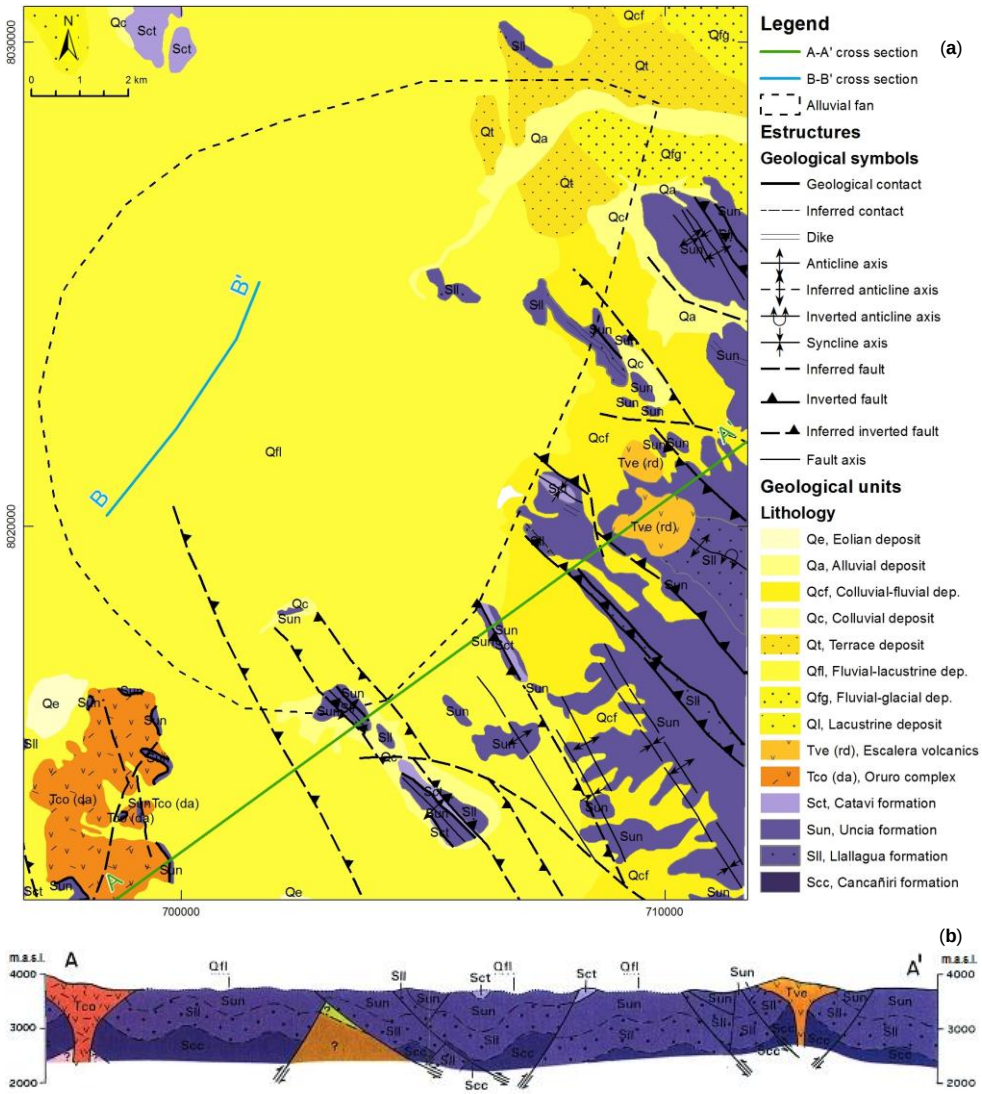

Figure 3 Geological formations around the alluvial fan of River Paria. (**a**) Geological map. (**b**) A-A' cross section. The scale in this cross section does not allow to show the Quaternary sediments (yellow); the thickness of these units in this part is just a few meters and the hard rock is shallow. Modified from GEOBOL and Swedish Geological AB (1992).

AB, 1992; Rigsby et al., 2005; Suarez Soruco, 2000). These formations have strong influence on the hydrothermal activity in the region. (3) Unconsolidated deposits from the Quaternary, consisting of clays, silts, sands, gravels and pebbles sorted in complex arrangements (GEOBOL and Swedish Geological AB, 1992; Rigsby et al., 2005; Suarez Soruco, 2000). The primary porosity of these formations depends on the grain size and the depositional environment, e.g. lacustrine, fluvial-glacial, fluvial-lacustrine, colluvial and alluvial. These sediments are likely to be interconnected, forming a single porous aquifer, which is assumed heterogeneous and anisotropic.

The oldest sedimentary formations were deposited in marine environments. Compressive tectonic forces folded these units resulting in synclines and anticlines with NW-SE direction forming mountain ranges. Volcanic intrusions intensified the compression resulting in faults with the same NW-SE direction, as shown in Figure 3. The products of the erosion of the mountains filled the valleys forming plateaus, which are the main aquifers in the Altiplano (Rigsby et al., 2005; Suarez Soruco, 2000).

The sedimentary rocks hold and enclose the unconsolidated sediments, around as mountain ranges and outcrops, and beneath as bedrock. The faults in the bedrock are assumed part of the deepest fractured aquifers. Some of these faults reach geothermal sources and hence, they are saturated with saline and hot water. The characteristics of the bedrock and the fractured aquifer have scarcely been investigated and they are out of the scope of this study due to limitations in the depth of investigation of the applied methods. Previous studies attempted to describe the contact between the bedrock and the unconsolidated sediments by combining drilling logs and refraction seismic surveying in the alluvial fan of River Paria (e.g. Dames & Moore Norge, 2000; Banks et al., 2002). They indicate that the deepest contact between bedrock and sediments is located in the centre and south-western part of the alluvial fan (Paper II).

The characteristics of shallow sediments have been studied more than those of the bedrock. However, the package of sediments is still not fully understood because the overlapping depositional processes ended in complex arrangements. As shown in Figure 4, lateral and vertical variability (e.g. erratic changes in lithology and clay lenses embedded in more granular coarser backgrounds) impede the continuity of large layers with the same characteristics. Only the top silty-clay layer is almost omnipresent, covering the aquifer with a thickness varying from a few centimeters to a couple of meters. The thickness of the complete sediment deposits increases from zero at the foot of the outcrops to more than ~150 m, as it is indicated in Figure 4. This cross section is the result of the interpolation of lithological columns from drilling logs in the alluvial fan; none of these drillings reached the bedrock, hence, the total thickness of the sediments needs to be estimated with other methods.

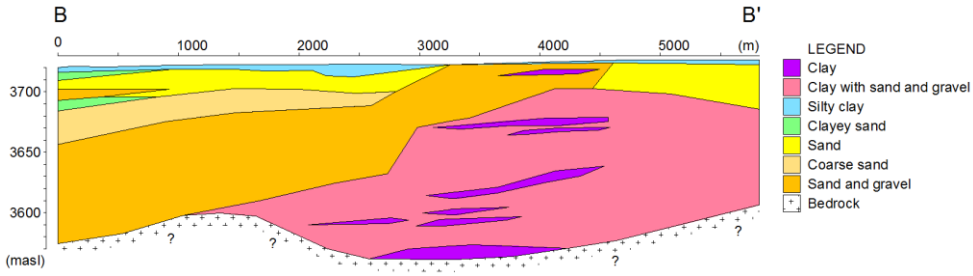

Figure 4 Lithological cross section B-B' corresponding to the porous aquifer from drilling logs (location in Figure 3). Modified from Dames & Moore Norge (2000).

2.3 Hydrogeological background

The unconsolidated sediments in the study area can store and transmit water; however, different proportions in the content of gravel, sand and clay affect the hydraulic response. Consequently, the location of the screens in completed wells coincides with layers of favourable granulometry to ensure good groundwater production. The electrical response, important for some geophysical methods, is also influenced by the arrangement of sediments, especially by layers with high clay content. The hydraulic characteristics of the porous aquifer have been previously estimated by conducting pumping tests in some wells located in the alluvial fan. Transmissivity (T) has values in the range of 5.8×10^{-4} to 7.6×10^{-3} m^2/s with an average of 3.0×10^{-3} m^2/s. The hydraulic conductivity (K) was also estimated dividing T by the length of screens, resulting in values in the range of 4.4×10^{-5} to 2.9×10^{-4} m/s with an average of 1.4×10^{-4} m/s (Dames & Moore Norge, 2000; SCIDE et al., 1996). The variation in both parameters, T and K, relates to the heterogeneity of sediments. In the rest of the aquifer, the hydraulic characteristics remain unknown due to the limited or non-existent wells to conduct more hydraulic tests; however, T and K can be expected to be in the ranges indicated above.

The potentiometric surface shown in Figure 2 might not be very accurate considering the size of the aquifer and the few data points available to interpolate groundwater levels. However, recharge and discharge zones can be identified. The main discharge zone is in the centre of the alluvial fan where the well field is located; the water table in this sector remains stable throughout the year. On the other hand, fluctuations of groundwater levels are more evident in the recharge zones around the rivers Caracollo, Pongo Jahuira, Cayhuasi and Paria, due to seasonality of precipitation, as shown in Figure 5. Even though the measurements correspond to a short period (14 months) the critical drought in the Altiplano

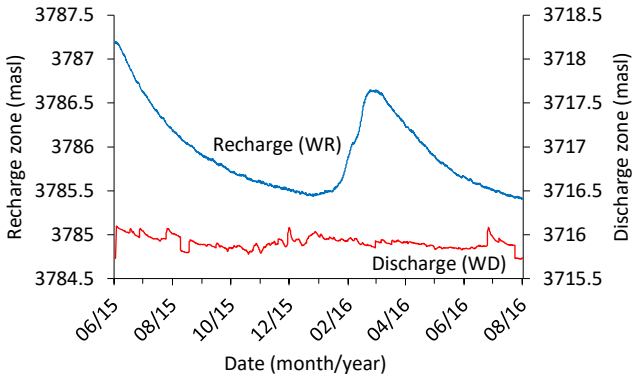

Figure 5 Groundwater levels corresponding to the recharge and discharge zones. Locations of wells WR and WD are marked in Figure 2.

(between 2015 and 2016) affected recharge of the aquifer system, since the peak reached in March 2016 seems lower than the projection of the previous recharge.

The hydrochemical characteristics of groundwater in the porous aquifer can be used to reinforce the circulation model formulated in previous studies (see Figure 2). The salinity of water increases along its path from the recharge zones (rivers), to the wells in the discharge zone. On the other hand, the isotopic composition in both zones correspond to the same range of values (for $\delta^{18}O$), therefore, they are assumed to be interconnected. Figure 6 shows both parameters: salinity expressed as Electrical Conductivity (EC) and $\delta^{18}O$ to expose the hydrochemical evolution of water in the aquifer.

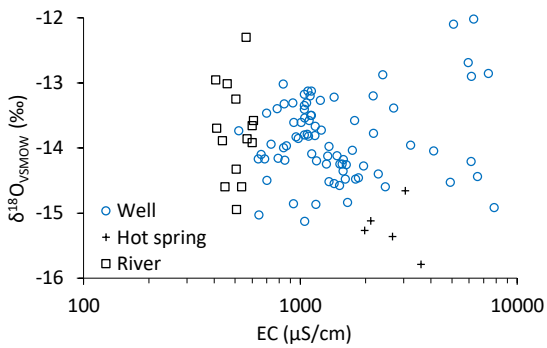

Figure 6 Process of dissolved elements enrichment for groundwater in the porous aquifer: from low salinity in rivers to high salinity in wells and hot springs (GITEC and COBODES Ltda., 2014; Lizarazu et al., 1987; Swedish Geological AB, 1996).

2.4 Hydrogeological conceptual model

Based on the available information, the groundwater in the porous aquifer has its origins in the precipitation over the mountains. The runoff reaches rivers at the head of the plateau, which later infiltrate laterally into the aquifers. This infiltration process constitutes the main water input of the aquifer system, estimated to be 104.9 million m^3 per year. On the other hand, annual vertical infiltration from precipitation over the area of the aquifers was estimated to be only 6.8 million m^3, for a total recharge of 111.7 million m^3 per year (GITEC and COBODES Ltda., 2014). After infiltration, water incorporates dissolved elements due to the contact with the geological environment; the longer the path and residence time, the greater the salinity (as shown in Figure 6). According to the topography, the slope of the unconsolidated sediments is southward. The Lake Poopo, the lowest sector in the Central Altiplano catchment, is assumed the natural discharge zone of surficial water and groundwater. However, the constant abstraction from the well field has changed the natural flow patterns, which currently flows towards the central part of the alluvial fan (see Figure 2), creating a cone of depression of about 5 km radius (Banks et al., 2002; D'Elia, 2013). The annual abstraction from the well field was estimated to be 9.5 million m^3 (SELA, 2018) without considering volumes for irrigation from other wells. Regarding the flow patterns in the fractured aquifer, the existence of hydrothermal activity in the middle of the alluvial fan might indicate

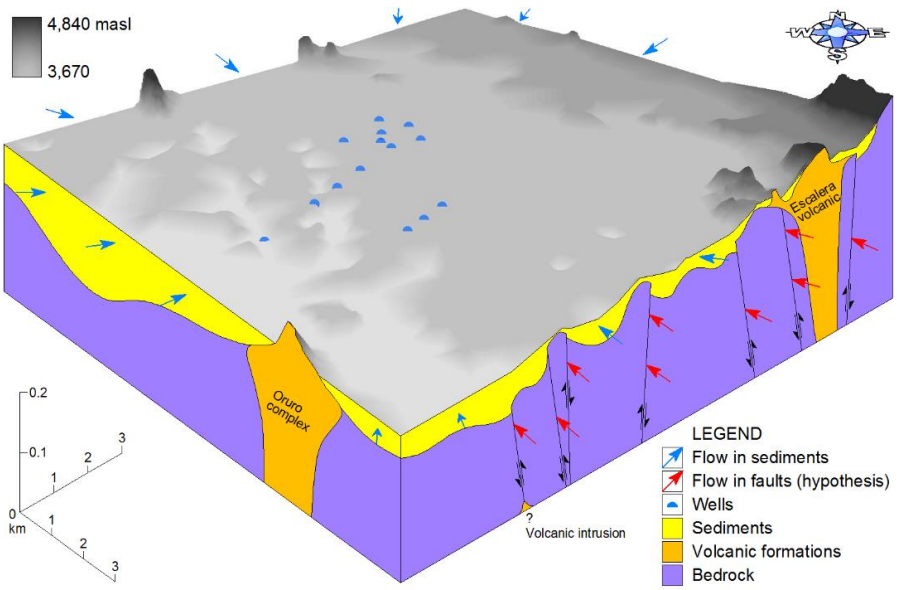

Figure 7 Hydrogeological conceptual model in the central part of the alluvial fan.

that the water in the faults circulates towards the NW from the SE, where the volcanic intrusions are located. This hypothesis needs to be confirmed. Figure 7 shows the hypothesised flow patterns corresponding to the porous aquifer and the fractured aquifer in the middle of the alluvial fan.

3 Exploration methods and methodology

The available information and data from different sources and studies comprise the basis of the hydrogeological description of the aquifers to the north of Oruro. Results and interpretations from additional methods aim to fill gaps in the hydrogeological knowledge of the aquifer units. Environmental isotopes analyses and geoelectrical surveys were applied to improve the knowledge in subjects like groundwater flow patterns (as e.g. Aravena et al., 1999; Scheihing et al., 2017; Uribe et al., 2015), geological structures underlying sediments (as e.g. Haile and Abiye, 2012; Kumar et al., 2011; Navarro et al., 2004) and estimations of aquifer parameters (as e.g. Perdomo et al., 2018; Soupios et al., 2007; Tizro et al., 2010). These methods were selected due to their diverse applications in hydrogeological studies dealing with complex hydrogeological conditions and scarcity of data (as e.g. Boiero et al., 2010; Pacheco-Guerrero et al., 2019; Yin et al., 2011). Previous studies have used these methods in the region; isotopes to expose characteristics of different types of waters in the catchment (e.g. GITEC and COBODES Ltda., 2014; Lizarazu et al., 1987; Swedish Geological AB, 1996) and geoelectrical tests, mainly Vertical Electrical Soundings (VES), to find suitable sites for boreholes and production wells (e.g. Canaviri, 2011; Guérin et al., 2001; SCIDE et al., 1996). In this chapter, the theory and issues regarding the application of these methods in the Altiplano are described.

3.1 Isotopic methods

Hydrologic studies using isotopes require a good understanding of the precipitation characteristics and other processes affecting isotopic compositions (e.g. Scheihing et al., 2017). In the case of the study area, it belongs to the Altiplano basin (Central Altiplano sub-basin), an enclosed catchment that receives the main water input from precipitation (~350 mm/y), which ultimately evaporates back to the atmosphere (potential evaporation ~1800 mm/y) (SENAMHI, 2015). Aquifers are part of the hydrologic cycle, especially those receiving recharge from direct infiltration and lateral infiltration from rivers. In order to improve the understanding of the origin and flow patterns of water in the aquifer system around Oruro, the first study (Paper

I) investigated the isotopic characteristics in different stages of the water cycle (precipitation, surface water and groundwater).

In hydrological studies, the most abundant and stable form of a chemical element (an isotope) is evaluated in relation to other isotopes; which have the same atomic number (number of protons) but different mass number (total number of protons and neutrons). Environmental isotopes can be either stable, used as tracers due to their quality of remaining unaltered over time, or radioactive, used for dating because they decay over time. The isotopic data used in this study include mainly deuterium and oxygen-18.

3.1.1 Stable isotopes

Hydrogen and oxygen atoms form the water molecule; each element has its own isotopes. In hydrological studies, the isotopes of interest are deuterium (^{2}H) and oxygen-18 (^{18}O). The isotopic compositions of these elements are expressed as deviations (δ) respect to the Vienna-Standard Mean Ocean Water (V-SMOW) in per mil units (‰) (Mook, 2000).

The correlation between $\delta^{2}H$ and $\delta^{18}O$ in samples from meteoric origin around the world follows a linear relationship described by Craig (1961), known as the Global Meteoric Water Line (GMWL), $\delta^{2}H = 8 \cdot \delta^{18}O + 10$. This relationship in the Central Altiplano is slightly different because it is affected by latitude, altitude, distance from the coast and seasonality of precipitation among others. The Global Network for Isotopes in Precipitation (GNIP) has data to determine the Local Meteoric Water Line (LMWL) corresponding to the region (Figure 8), using records from stations located in the Altiplano with similar characteristics like elevation and precipitation regimes. These stations are Laica Cota, El Alto, Oruro and Quillacas.

The slope of LMWL is similar to GMWL, but its deuterium excess is greater, most likely because of the additional deuterium-rich moisture in the atmosphere from the

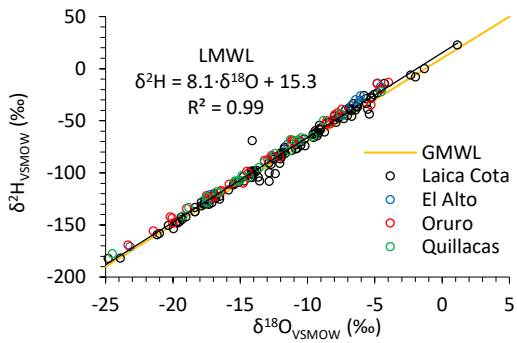

Figure 8 Local Meteoric Water Line for the Central Altiplano. Data from IAEA (2015).

inland water bodies (Fiorella et al., 2015). The ranges of isotopic compositions in precipitation in the Altiplano are quite large over the year; however, aquifer recharge mainly occurs during and just after the rainy months (as shown in Figure 5). The distribution of the average isotopic compositions by month, shown in Figure 9, aids to visualize the typical isotopic range of precipitation during the rainy season (from December to March), which ends recharging the aquifers.

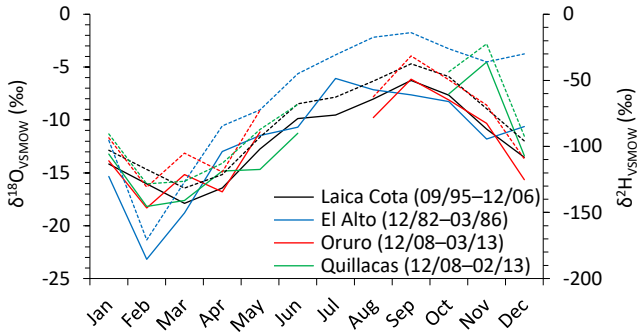

Figure 9 Monthly average isotopic compositions in precipitation for GNIP stations in the Altiplano. Continuos ($\delta^{18}O$) and dashed ($\delta^{2}H$) lines in the same colour correspond to the same station. Data from IAEA (2015).

From the isotopes in precipitation in Figure 9, the depleted values that most likely reach surface bodies and later aquifers are clearly visible, as well as the parallel behaviour of $\delta^{2}H$ and $\delta^{18}O$ compositions through the year. Nevertheless, the relationship between stable isotopes in surface water and groundwater might be different from that in precipitation, due to the high potential evapotranspiration in the region that enriches isotopic concentrations at the surface and shallow levels underground. After scrutiny of isotopes in precipitation, the next step is to analyse isotopic compositions in groundwater, which is presented in the next chapter.

The methods to estimate isotopic compositions in water samples are based on gas-source mass-spectrometry. For example, Picarro Cavity Ringdown Spectrometer L2120 was used to analyse precipitation samples from stations Oruro and Quillacas (IAEA, 2015). The samples collected between 2014 and 2015 from deep wells, shallow dug wells and rivers in the study area, were analysed at the laboratory of the Geological Survey of Denmark and Greenland (GEUS), applying the methodology described above.

3.1.2 Radioactive isotopes

In radioactive isotopes, the nuclear forces are unbalanced due to an excess of one of its components, driving to a release of energy to stabilise the nucleus. This radioactive decay takes a specific time which varies according to the element.

Relative variations in concentrations permits the use of these elements for dating and estimations of residence times. For hydrological investigations the radioactive isotopes most commonly used are tritium and radiocarbon (Mook, 2000; Seiler and Gat, 2007). In the present investigation, radioactive isotopes are used to support some findings and interpretations (Paper I).

3.2 Geoelectrical methods

When it comes to exploration of aquifers, geoelectrical methods are suitable given their advantages and wide range of applications, e.g. discrimination between solid rock and fractured rock, between saturated and dry sediments, between freshwater and saline water, as well as mapping of contaminants and mapping of geological features in general (Kirsch and Yaramanci, 2009a). These methods expose changes in physical properties of the ground, and one of the most important among them is resistivity.

Resistivity (ρ) is the property that indicates the capacity of materials to allow electric current to flow through them. It is the inverse of conductivity (σ) and can be expressed as proportional to resistance (R) (voltage over current, from Ohm's law) times the cross-section area (A) divided by the section length (L), $\rho = R \cdot A / L$. Resistivity is commonly expressed in Ω·m. Different types of materials have different ranges of resistivity, as shown in Figure 10. Water is a natural electrolyte, hence, the saturation degree and the salinity of water filling the voids of geological formations play a major role in the resistivity obtained by geoelectrical methods. Field measurements and data collection obtain information of the ground as apparent resistivity, which is not the real representation of the subsoil settings; it needs to be processed and inverted before obtaining an estimation of the true

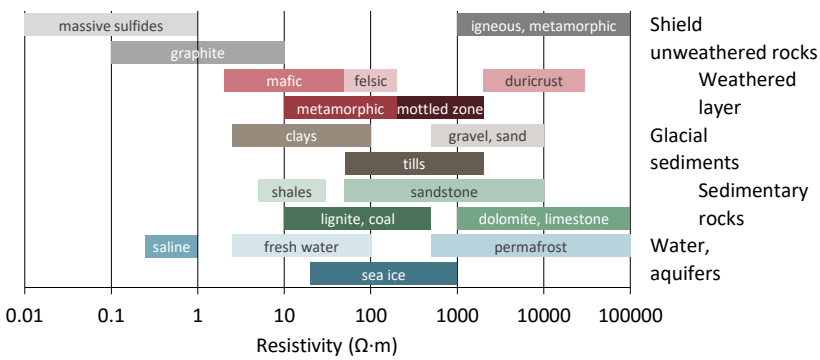

Figure 10 Typical resistivity and conductivity ranges for geological materials. Modified from Palacky (1987).

resistivity. This inversion process varies according to the applied method. Two main methods were used in this research, transient electromagnetic soundings and electrical resistivity tomography.

3.2.1 Transient ElectroMagnetics (TEM)

The TEM method is point-based and consists in sending a current through a transmitter antenna that generates a primary electromagnetic (EM) field that is incident on the ground (Figure 11a). When the current in the transmitter is abruptly interrupted (Figure 11b) its primary EM field induces an electromotoric force producing eddy currents flowing through conductive bodies in the ground (Figure 11c). Those eddy currents generate a secondary EM field that reaches the surface where it is detected by receiver antennas (Figure 11d). The receivers acquire time-dependent decaying voltage signals at different times (gates) during the off-time of the measurement (Figure 11d). The process continues alternating the direction of the current in the transmitter. During the data acquisition, those signals are transformed to apparent resistivity, varying according to the type of materials and the geological settings (Christiansen et al., 2009; Reynolds, 2011).

The equipment used for the TEM surveys was an ABEM WalkTEM, which handle dual moment electrical pulses; a high moment (HM) pulse and a low moment (LM) pulse. The setup was an offset array consisting of a transmitter loop (50 × 50 m), in the centre the RC-5 receiver (0.5 × 0.5 m) and the RC-200 receiver (10 × 10 m) was 50 m offset from the centre of the transmitter (Figure 11a). Part of the measurements did not use the RC-200 receiver. The acquired data need to be conditioned before being inverted; the shallow part of the resistivity models was resolved with the LM obtained from the RC-5, and the deepest part with the HM obtained from the RC-200.

The inversion process aims to find a model that reproduces the obtained data and is representative of the resistivity distribution of the test site. For TEM it is based on 1-D layered models matching as closely as possible scattered points from the measurements (Nabighian, 1991). Two types of models can be used for the inversion, a layered model (few resistivity layers) and a smooth model (gradual resistivity transitions corresponding to a greater number of layers increasing in thickness by depth) (Christiansen et al., 2009). A model is considered reliable until the Depth Of Investigation (DOI) (Christiansen and Auken, 2012). The TEM raw data were processed with SPIA (Aarhus GeoSoftware, 2017a), running 1-D inversions of individual measurements. Resistivity images as maps and cross-sections using inverted 1-D models were made with Aarhus Workbench (Aarhus GeoSoftware, 2017b).

Figure 11 Schematic representation of the TEM principles. On-time and off-time curves. (**a**) 3-D surveying scheme. (**b**) Current in the transmitter. (**c**) Electromotoric force in the ground. (**d**) Secondary EM decay in the receiver. Modified from Christiansen et al. (2009).

3.2.2 Electrical Resistivity Tomography (ERT)

This method is based on the principles of Direct Current (DC) resistivity surveying, in which the resistivity of the ground is evaluated by injecting a current through a pair of electrodes (A B) and measuring the potential difference in another pair of electrodes (M N). The intensity of the current and the geometry of the quadrupole arrangement (set of electrodes A B M N), together with the subsoil characteristics,

determine the measured potential difference (Figure 12a). DC measurements aim to obtain apparent resistivity (ρ_a), as a punctual value (usually at the centre of the quadruple at a certain depth, as shown in Figure 12b) assuming homogeneity of the ground that is proportional to the quadruple geometric factor (K) times the current (I) divided by the potential difference (U), $\rho_a = K \cdot I / U$. Repeated measurements with consistent but progressively larger quadruple arrangement (maintaining the same target) produce a 1-D Vertical Electrical Sounding (VES), which is a vertical section of the resistivity of the ground at different depths. If the quadruple remains unaltered but displaced along a line, the measurements will provide a resistivity profiling, also called Constant Separation Traversing (CST) (Reynolds, 2011). A combination of VES and CST is known as Electrical Resistivity Tomography (ERT), whose ρ_a measurements are presented in 2-D sections (Kirsch and Yaramanci, 2009a). Multi-electrode and multi-channel equipment (as shown in Figure 12b) have improved this method making it more efficient in terms of resolution, time and cost (Dahlin and Zhou, 2006).

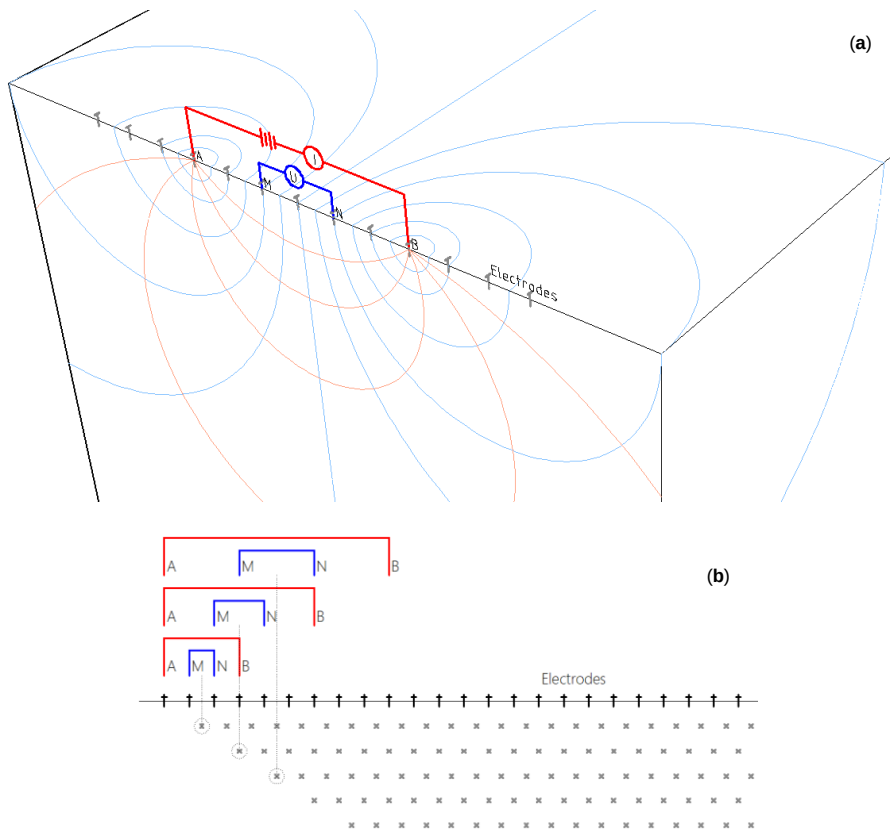

Figure 12 Schematic representation of the ERT principles of. (**a**) DC surveying scheme (single resistivity datum). (**b**) ERT surveying scheme (multiple resistivity data). Modified from Reynolds (2011).

The ERT surveys in the study area were conducted with ABEM Terrameter LS equipment including four cables, each one with 21 take outs. The electrode separation was 10 and 20 m, reaching a total spread length of 800 and 1,600 m respectively. Some traverses were extended using the roll-along technique, consisting of placing a new cable at the end of the line after the measurements are completed in one station. For most of the measurements a Multiple Gradient array was selected given its good signal-to-noise ratio and stable and fast field data acquisition (Dahlin and Zhou, 2006).

The inverse numerical modelling process for ERT consists of iterations based on finite elements (or finite differences), comparing the resistivity obtained from a model with the apparent resistivity from the field data (pseudo section). Residual errors between these two sections are calculated and minimized by refinements in the model until obtaining the most likely representation of the resistivity distribution through the final model (Dahlin, 2001; Loke, 2004; Loke et al., 2003). The inversion processes for ERT were carried out using Res2Dinvx64 (v. 4.05). The robust constraint inversion (L1–norm) was selected due to its ability to handle sharp transitions in models. The vertical to horizontal flatness ratio 1.0 was selected, since both vertical and horizontal changes in resistivity and chargeability were expected.

3.2.3 Induced Polarization (IP)

This method is based on the principle that geological formations are capable of retaining electrical charges after an injected current is removed. IP depends on the lithology and the conductivity of the fluid in the formation. This property can be determined either in time or in frequency domain and it is expressed as chargeability (Slater and Lesmes, 2002). The IP data acquisition in the corresponding study comes from the full waveform records conducted mainly to get resistivity; they also contain IP decay signals in time domain, available to be extracted following the procedure proposed by Olsson et al. (2015). Potentials from the decay curve were measured at different times (gates) during the “on” of the current, since the full waveform was recorded in 100% duty cycle (no “off” time) (Olsson et al., 2016). Another way to handle IP data that permits the examination of areas saturated with saline water at the surface and in some faults, is dividing the chargeability by the resistivity to obtain the Normalized IP (NIP), which is a parameter proportional to the surface conductivity (Slater and Lesmes, 2002).

3.2.4 Practical remarks

Some characteristics of the study area, which are similar over all the Altiplano, determine the applicability of the used geoelectrical methods. They are mentioned as follows:

- The scarce or non-existing vegetation of the Altiplano is an advantage to deploy equipment and components indiscriminately.
- The planar terrain where most of the sediments and alluvial aquifers lie is also beneficial for rapid field procedures.
- The aridity of the surface might pose a problem, especially for the ERT method, since the contacts between electrodes and the ground were registered with high resistive values; hence, the use of contact-additives is imperative. This issue is not important for TEM.
- More conductive saturated sediments overlying more resistive hard rock, as in the study area, might be unfavourable to visualise the contact between these formations with TEM, for which the opposite (resistive overlying conductive) is more suitable.
- Very conductive shallow features like saline saturated layers and faults with saline intrusions can produce 3-D effects during the data acquisition, difficult to handle for point-based methods like the TEM. The ERT technique is able to handle these features if traverses are deployed perpendicularly.

4 Results and interpretations

The different exploration methods applied in this research provide new data and information used to improve the understanding of the hydrogeological characteristics of the study area, exposing deep features in the bedrock and supporting rough estimations of hydraulic parameters of the top aquifer.

New results and interpretations aim to fill gaps in the knowledge about hydrogeological processes and are presented in three study subjects: (1) groundwater flow patterns, (2) geological structures beneath sediments and (3) aquifer parameters estimations, including as well important remarks about data and sources of information.

4.1 Data sources and field measurements

As mentioned before, the well field located within the study area continuously extracts groundwater to supply the urban area of Oruro (see Figure 2). Hydraulic properties of the top porous aquifer were obtained from pumping tests conducted in some of those wells (blue circles in Figure 13); typically, their penetration reaches depths < 100 meters below the surface (mbs). This information was obtained from SCIDE et al. (1996) and Dames & Moore Norge (2000).

Some isotopic sampling points are shown as purple dots in Figure 13. Part of the isotopic data was obtained from previous studies (e.g. GITEC and COBODES Ltda., 2014; Lizarazu et al., 1987; Swedish Geological AB, 1996), complemented with new samples collected in 2014 and 2015, analysed later as part of this research.

Geoelectrical surveys with TEM and ERT were conducted between 2015 and 2017 as part of this investigation, they are also shown in Figure 13 (in red lines the ERT traverses from 2015, obtained using different equipment, electrode array, electrode separation, etc; in blue lines ERT traverses from 2017, conducted with the same equipment and standardized procedures, e.g. gradient array and 10 m electrode separation). Dots represent the TEM soundings in the study area; green dots correspond to 2016 field work using two receivers, orange dots are from 2017 using only the small central receiver RC-5.

4.2 Groundwater flow patterns

The first study in this research propose the existence of four flow systems in the alluvial fan of River Paria (Paper I), based on the isotopic characteristics of groundwater in this area. As indicated before, the top clay layer in the aquifer system reduces the vertical infiltration and the water retained at the surface is affected by evaporation; hence, the small amount of water reaching the water table is isotopically enriched. For example, two groundwater samples from the same site

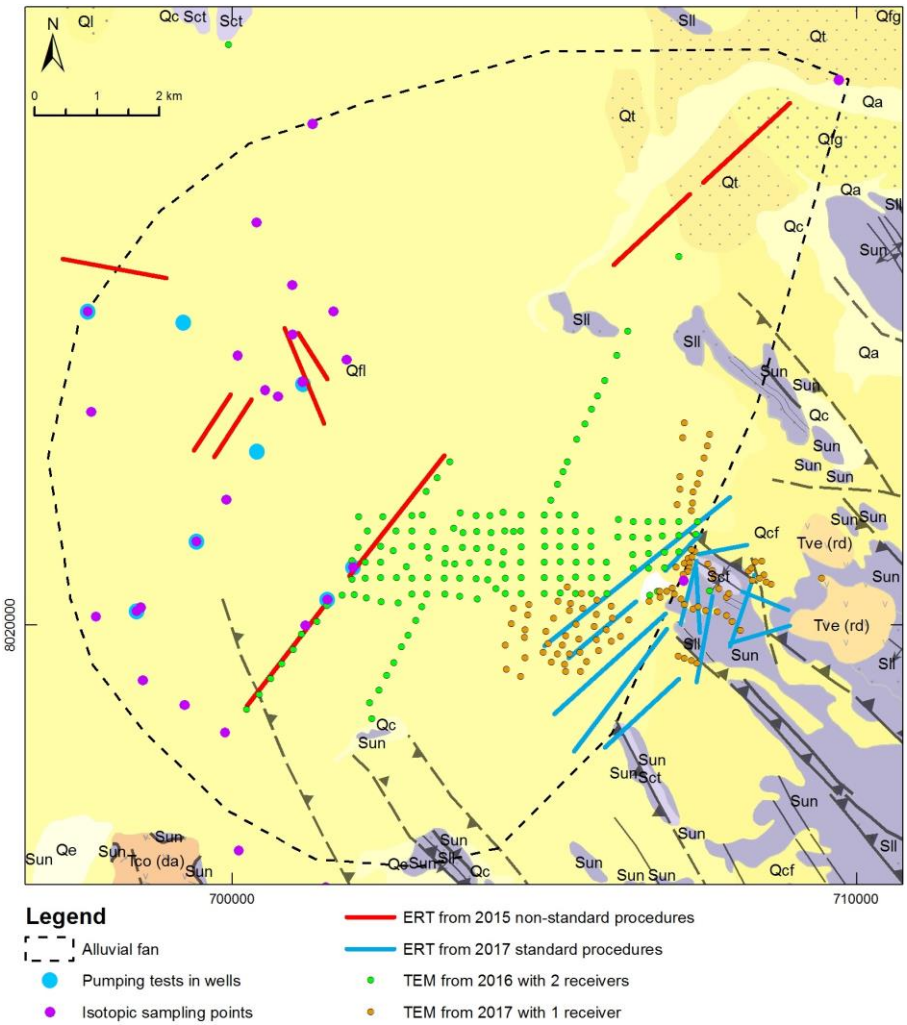

Figure 13 Location of wells, sampling points and geoelectrical measurements around the alluvial fan of River Paria. The semi-transparent background showing geological structures and geological formations is the same as in Figure 3a.

but corresponding to different levels in the middle of the aquifer have different isotopic compositions: $\delta^{18}O$ from a dug well (<10 mbs) is -13.9 ‰ and from a deep well (~65 mbs) is -14.9 ‰ (Paper I). Therefore, the very shallow part of the porous aquifer is assumed as the top flow system mainly recharged by direct infiltration.

The relationship between the stable isotopes in samples from boreholes align a tendency less steep than the LMWL, which indicates the effect of evaporation. Some samples from rivers are located in between these lines (Figure 14). From the isotopes in precipitation, the recharge signature is located in the range from -12.6 to -17.5 ‰ for $\delta^{18}O$, corresponding to the 25th and 75th percentile of precipitation samples for the rainy season (Paper I). After recharge, groundwater is unaffected by evaporation and the isotopic composition remains relatively unaltered, however salinity increases along the flow's pathways: from rivers (EC ~500 µS/cm) to wells (EC between ~600 to ~2000 µS/cm) which capture groundwater circulating in levels between 35 to 100 mbs.

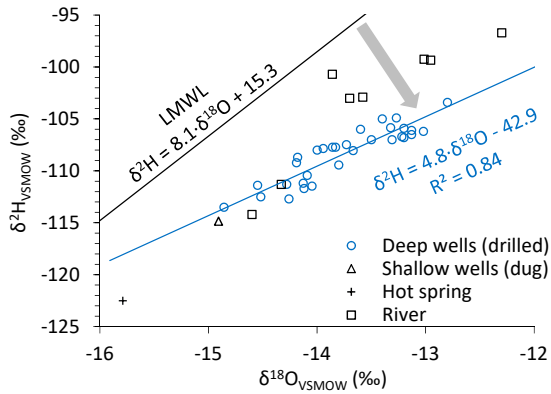

Figure 14 Isotopic trend line of groundwater in the porous aquifer (blue line). The arrow indicates the effect of evaporation on the water from precipitation.

Groundwater samples with much depleted $\delta^{18}O$ values were reported in previous studies (e.g. Lizarazu et al., 1987; Swedish Geological AB, 1996), corresponding to wells outside the study area and from deeper levels (~400 mbs) flowing mainly through the sedimentary bedrock. They might indicate recharge at higher altitudes and longer residence times. A transitional zone is assumed in between 100 and 400 mbs, where the contact of sediments and bedrock is located. Flows below 100 mbs that are not captured by pumping wells might continue towards the Lake Poopo, with NE–SW flow direction. The assumed four flow systems in the middle of the alluvial fan are indicated in the Table 1.

Radioactive isotopes were also used to confirm the pathways in the porous aquifer. Tritium decay occurs from compositions of ~7.4 TU, in River Paria, to values of

Table 1 Summary of flow systems and hydrogeological parameters in the alluvial fan of River Paria (Banks et al. 2002; Dames & Moore Norge 2000; Gómez et al. 2016; Lizarazu et al. 1987).

Flow system depth (mbs)	Stratigraphic approach	Origin of water	Scheme
0 – 20	Unconsolidated sediments	Direct infiltration	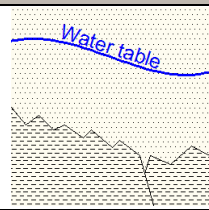
20 – 100	Unconsolidated sediments	Lateral recharge	
100 – 400	Transitional zone	Lateral recharge	
> 400	Consolidated rock	Unknown	

~0.2 TU or even below detection levels around the well field, as it is shown in Figure 15. Hence, it is assumed that residence times of groundwater in the sediments are longer than the active life of tritium. Groundwater dating was approached using isotopic compositions of ^{13}C and ^{14}C (Lizarazu et al., 1987). Ages from modern (<30 years) to 7200 years were found in the study area. The oldest waters show a high salinity corresponding to deep flow patterns, probably ascending through faults.

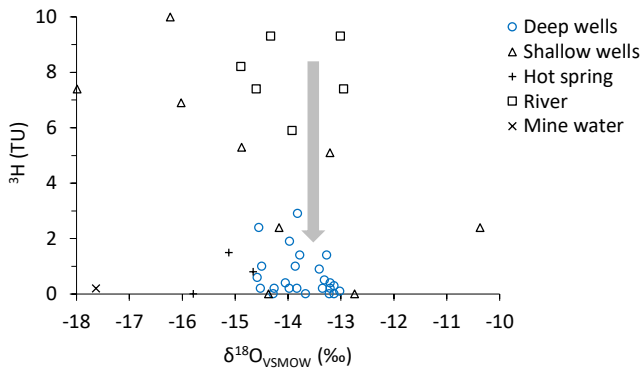

Figure 15 Tritium content in surficial water and groundwater. The arrow indicates tritium decay along the flow of water in the sediments. Modified from Lizarazu et al. (1987).

4.3 Geological structures beneath sediments

Geoelectrical methods were used to expose deep geological features that play important roles in the occurrence of groundwater in the alluvial fan of River Paria. Two types of investigations were conducted on this matter: TEM was applied to map the contact between sediments and the bedrock and ERT/IP to investigate the faults in the eastern part of the study area.

The results from the TEM and ERT surveys are expressed as resistivity. The geological settings and the saturation characteristics are used to propose a classification based on their distinctive resistivity values (Table 2); among them, the lowest values most likely correspond to the hydrothermal activity around faults and shallow parts, medium values might indicate freshwater aquifers in sediments and fractured rocks, high resistivity values might be related to dry formations. This classification is based on measurements conducted on geologically well-defined sites like rocky outcrops and around hot springs. Interpretations from previous studies were also taken into account for this proposed classification (e.g. Palacio, 1993; Dames and Moore, 2000; Guérin et al., 2001; Canaviri, 2011; GITEC and COBODES Ltda., 2014; Broman and Svensson, 2017).

Table 2 Classification of geological formations according to resistivity in the study area.

Resistivity (Ω·m)	Classification	Geological characteristics
< 5	Very conductive	Soils saturated with saline waters from hydrothermal sources, also in contact with preferential flow paths where this type of water is present
5 to 20	Conductive	Fully saturated formations, mainly unconsolidated sediments. High content of saline water coming from hydrothermal flows or very shallow levels of saturated sediments where vertical infiltration dissolved salts encrusted close to the surface
20 to 80	Medium	Porous aquifers and top parts of the fractured bedrock. Water in these geological formations is assumed less saline than the hydrothermal one, therefore this might correspond to meteoric water laterally infiltrated
80 to 200	Resistive	Hard rocks (sedimentary and volcanic) with low effective porosity and therefore low water content
> 200	Very resistive	Dry hard rock with very little to insignificant porosity

4.3.1 Contact between sediments and bedrock

Changes in resistivity from low to high values in the middle of the alluvial fan (i.e. from conductive to resistive), were used to address the porous aquifer thickness and the relief of the bedrock. TEM measurements distributed in a rectangular grid (sounding separation ~250 m) allowed mapping of the contact between unconsolidated sediments saturated with freshwater and the bedrock with low water content (Paper II). The DOI (depth of investigation) applying TEM varies from 100 to 400 m, the geological contact is expected in this depth range. Some ERT profiles and VES soundings also expose this contact between geological facies; although measurements that are located far away from the TEM grid are not included in this study (e.g. the northernmost ERT lines shown in Figure 13).

Resistivity maps at different levels, shown in Figure 16, expose two distinctive parts on the top slice: values ≥ 30 Ω·m most likely correspond to dry shallow sediments to the west (unsaturated zone); the high clay content in this layer would be responsible for the relatively low resistivity values despite the small water content.

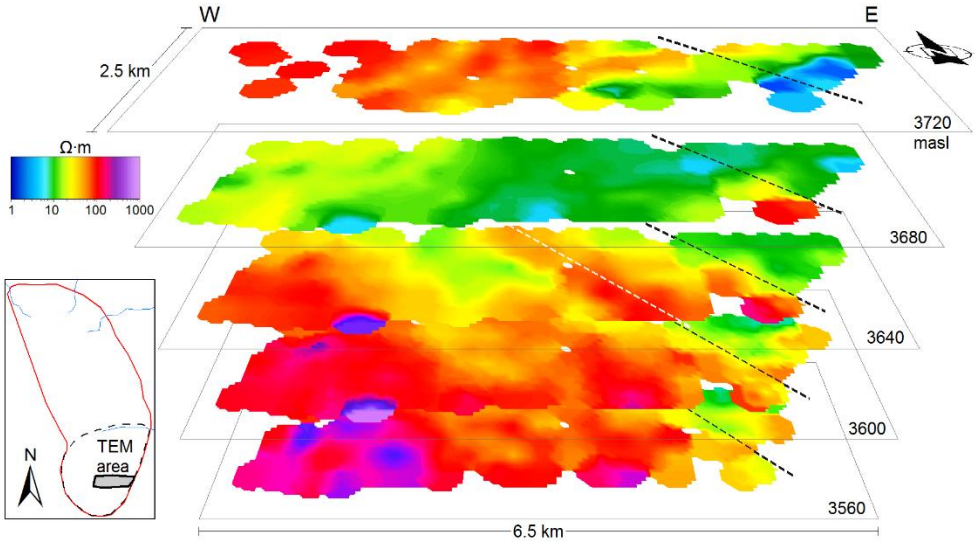

Figure 16 Resistivity maps at different levels (slices) from interpolated TEM smooth models. Black dashed lines indicate a trending low values corresponding to a fault with saline water. White dashed line in slice 3640 m indicates a bedrock fold.

On the east side, values between 5 and 10 Ω·m are in accordance with the location of some hot springs and saline water in this sector. In the next resistivity slice (3680 masl); homogenous values around 10 Ω·m indicate fully saturated sediments. The most eastern sector still exposes lower values linked with the hydrothermal activity. In the next slice (3640 masl), high values indicate the relief of the bedrock protruding as folds with SE-NW direction. The rest of the slices below 3600 masl, do not have significant changes in resistivity. Values ≥ 100 Ω·m to the west indicate consolidated dry rock. On the other side, low values remain indicating saline water intrusion in a fault (Paper II).

The distinction between alluvial sediments and the bedrock through resistivity is relatively consistent except in those sectors in contact with hydrothermal flows, where it is difficult to address the contact between geological formations. In the TEM grid sector, the thickness of the sediments increases from a few meters (around hard rock outcrops) to ~80 m in the centre of the grid. The slope of the bedrock was indicated in previous studies (e.g. Banks et al., 2002) as a smooth depression from east to west. However, the bedrock relief seems more complex, considering the existence of buried folds appearing at 40 to 80 mbs. These folds have a SE-NW fold axis orientation, similar to the other geological structures and faults in the region (Paper II). A more detailed resolution of the bedrock relief in this sector, from TEM surveys, is shown in Figure 17.

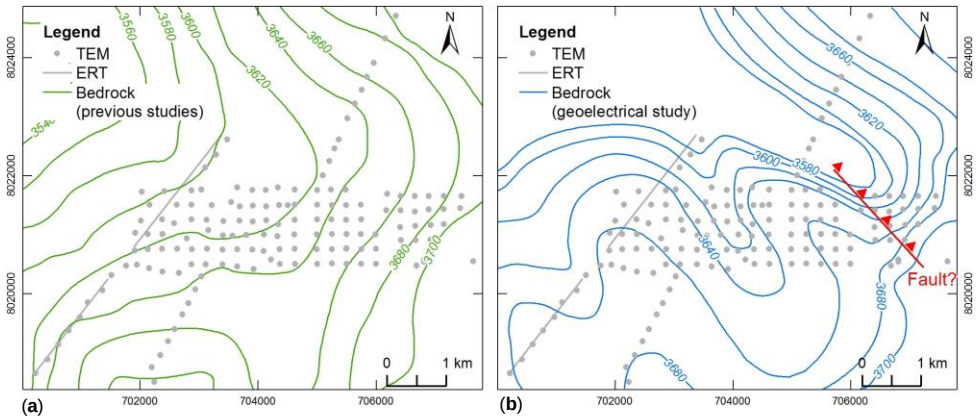

Figure 17 Contour bedrock maps. (**a**) From previous studies based on seismic and VES tests (Banks et al., 2002; Dames & Moore Norge, 2000). (**b**) Inferred from TEM soundings in this study.

4.3.2 Fault mapping

According to the regional geological map, a fault system is located next to the eastern limit of the aquifer. Some of these faults apparently continue north-westwards, beneath the unconsolidated sediments. Low resistive traces from TEM suggest the existence of fractures holding saline water in connection with hydrothermal pathways (Paper III). ERT/IP measurements perpendicular to three faults were deployed to identify the continuation of these structures by tracking low resistivity in the subsoil. The results are grouped into two zones: Zone 1, in the NE part of the study area where hard rock outcrops and two faults are located; and Zone 2, to the SW where the terrain is flat and the remaining fault is located (Figure 18).

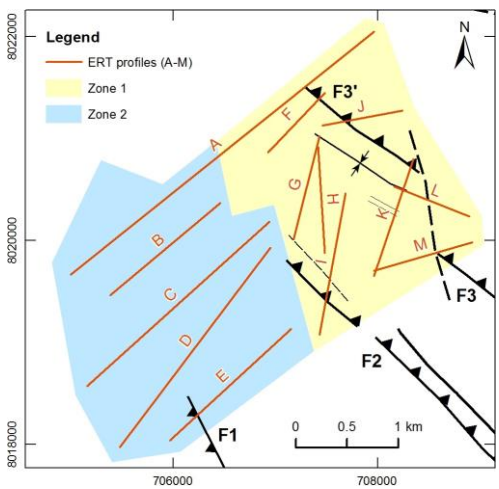

Figure 18 Distribution of ERT/IP measurements. Black marks are faults and structures, same as in Figure 3a.

Zone 1

This sector is rocky and highly resistive; small conductive patches can be seen in shallow sediments of profiles K, L and M (Figure 19). Profiles G, H and I show conductive parts appearing near the hot springs. The southern part of profile I exposes conductive areas close to fault F2. The last three profiles A, F and J, located in the flat terrain, show very conductive parts (almost vertical) assumed as faults crossing profiles A and F, aligning with a similar feature in profile G. This feature could be another fault with hydrothermal flows, F4 (Figure 19).

The normalized chargeability sections in this zone (Figure 20) also show the fault F4 crossing profiles A, F and G in those parts where the normalized chargeability is higher than the background. The profile F is located at the foot of the outcrops and the NIP model shows high saline water content around the middle part, just in front of the hot spring HS3. Profile A exposes similar features through normalized chargeability as in profile F.

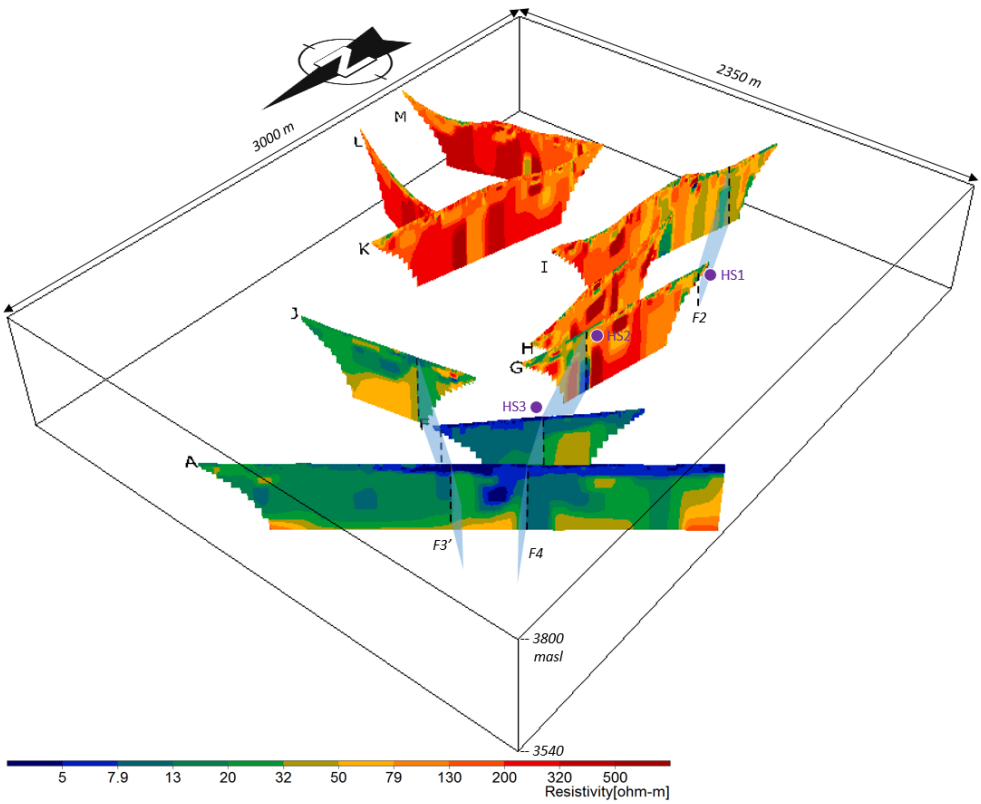

Figure 19 3-D view of resistivity models corresponding to Zone 1. Dashed lines indicate inferred faults; lines in profiles I and the southernmost part of G align with the fault F2, lines in profiles A, F and the northern part of G are aligned with the fault F4. Blue shadows indicate the direction of the inferred faults.

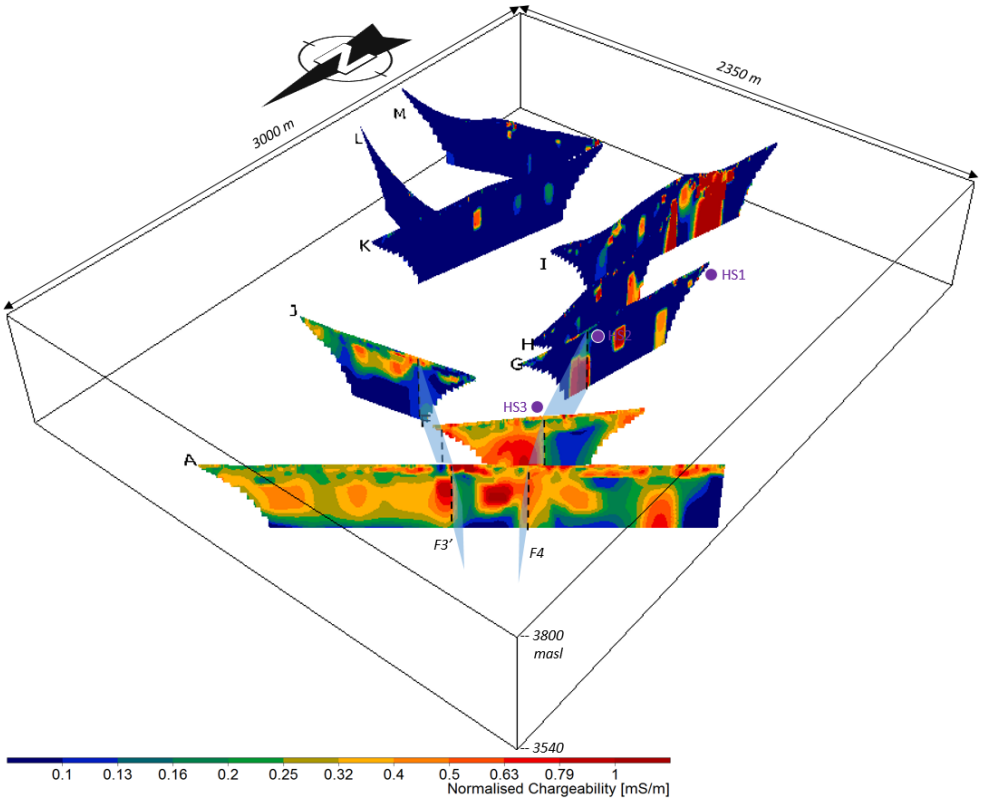

Figure 20 3-D view of normalised chargeability models corresponding to Zone 1. Dashed lines indicate inferred faults from resistivity. Blue shadows indicate the direction of the inferred faults.

Zone 2

In this sector, groundwater from the hot springs saturates the shallow subsurface. ERT profiles A, B, C, D and E belong to this zone (Figure 21). High resistivity below the top ~50 m in profiles A, B, C and D show traces of a fold in the bedrock with N to S axis orientation. Very conductive patches to the NE side of profile C, near hot spring HS1, seems aligned with hydrothermal flows in the fault F2. Low resistivity trending downwards in profile E, agrees with the location of fault F1; however, it does not appear clearly in profile D. Hence, this fault seems not to continue below the sediments (as shown in Figure 21).

The normalized chargeability in this zone (Figure 22) shows high values related to saturated sediments in the first ~50 m (profiles A, B, C and D); lower values, assumed as hard rock, are in the rest of the NIP models. In the NE part of profile A and below those saturated sediments, patches of normalized chargeability, slightly higher than the background, might indicate a fracture with saline water. Slightly high normalized chargeability is also present in the NE part of profile C, near the

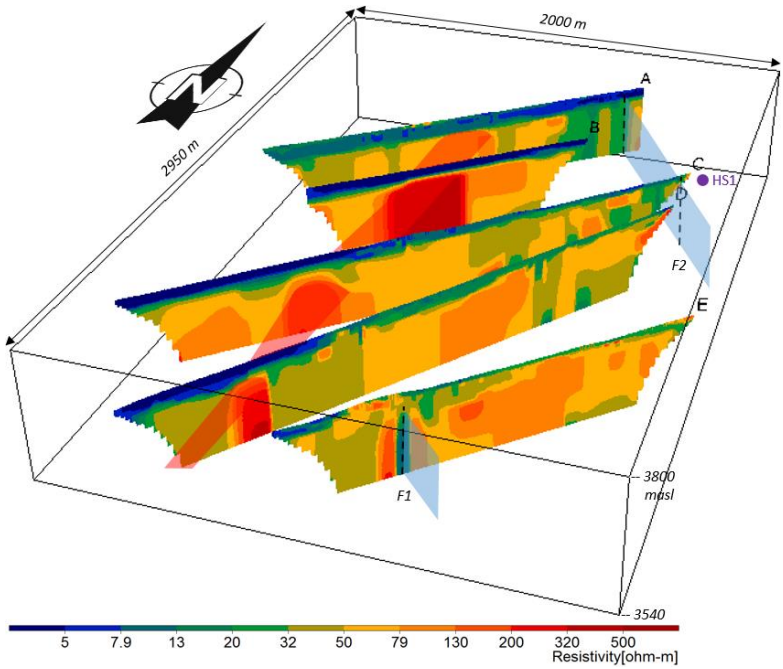

Figure 21 3-D view of resistivity models corresponding to Zone 2. Dashed lines indicate faults; in A and C aligning with the fault F2; in E aligning with the fault F1. Blue shadows indicate the direction of the inferred faults. Red shadow indicates an alignment of a bedrock fold in profiles A, B, C and D.

hot spring HS1. A similar feature appears also in the NIP model of profile E; it resembles the resistivity model with higher values indicating a fault with altered rocks and mineralization.

Some TEM soundings in the same area provide results to support the existence of the features inferred with the ERT profiles. The resistivity is low at shallow levels due to the presence of saline water, but it increases gradually with depth. Low resistivity patches indicate fractures with saline water in the bedrock, linked to a projection of fault F2. Deeper tracking of this type of features is limited by the DOI of the applied methods (until ~200 mbs).

The three major faults in the investigated area were tracked as shown in Figure 21; F1 seems not to continue north-westward much beyond the profile E. A buried fold with north to south orientation was detected. Traces of F2 appear in profiles A, C, G and I. Patches showing conductive zones appear in profiles C and G, near HS1. They might indicate preferential hydrothermal flows going upwards in this site. Resistivity in profiles A, F and J contain traces of fault F3 crossing them. The most conductive parts in profiles A, F and G correspond to F4, a second order fracture. This fracture is not indicated in the geological map (Figure 3a); however, it seems to be connected almost vertically with the fault F2, which in turn might reach a

volcanic intrusion (likely the Escalera volcanic formation, shown in Paper III: Fig. 9b). All these newly inferred geological structures are shown in Figure 23.

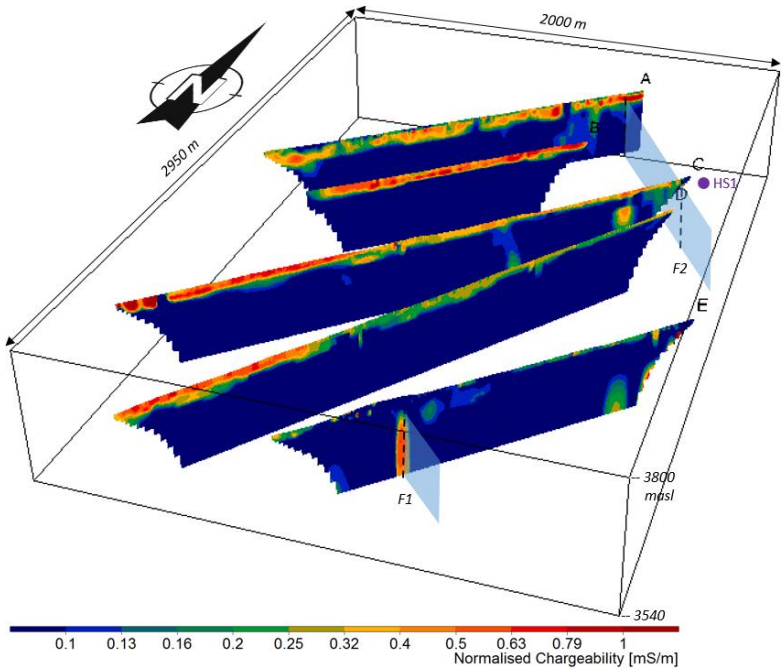

Figure 22 3-D view of normalised chargeability models corresponding to Zone 2. Dashed lines indicate faults inferred from resistivity. Blue shadows indicate the direction of the inferred faults.

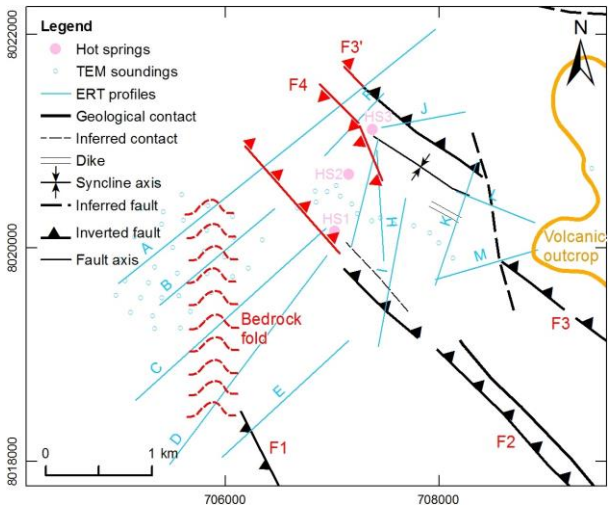

Figure 23 Map of geological structures and faults in the study area. In black from the geological map, in red newly inferred in this study.

4.4 Aquifer parameters estimations

With the purpose of making wider use of geoelectrical measurements to fill the gaps in the exploration stage of the porous aquifer, this study subject proposes an empirical relationship between hydraulic conductivity (K) and resistivity (ρ) to estimate aquifer parameters in the central part of the alluvial fan of River Paria. To establish an empirical relationship between K and ρ, the hydraulic conductivity input data was adopted from pumping tests. The corresponding resistivity comes from the closest geoelectrical station, which can be from TEM, ERT or VES tests (Kirsch and Yaramanci, 2009b; Mazáč et al., 1985). Figure 24 shows K vs. ρ, where the scatter points seem align with a linear relationship used to predict K values in sites with resistivity results. Most of the points fit in a linear correlation except WP10. This well might be above a fault with hydrothermal flows, which makes the resistivity lower than in the rest of the investigated area.

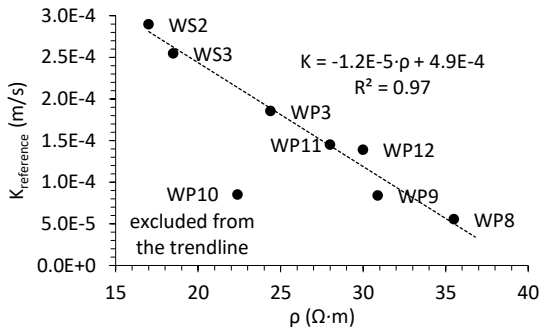

Figure 24 Empirical linear correlation between hydraulic conductivity from pumping tests and resistivity from the closest geoelectrical station.

Hydraulic conductivity values were estimated in other areas around geoelectrical stations using the linear relationship shown in Figure 24. Transmissivity was also estimated using the equation $T = K \cdot h$ (Fetter, 2001), where h is the thickness of the saturated sediments obtained from the inverted resistivity models as well. The distribution of calculated T permits to locate the most promising areas for groundwater production; values were interpolated with the Kriging method, as it is shown in Figure 25. The highest transmissivity values are located in the middle of the investigated area and the lowest values correspond to the southwestern part, where the bedrock was detected at shallow levels.

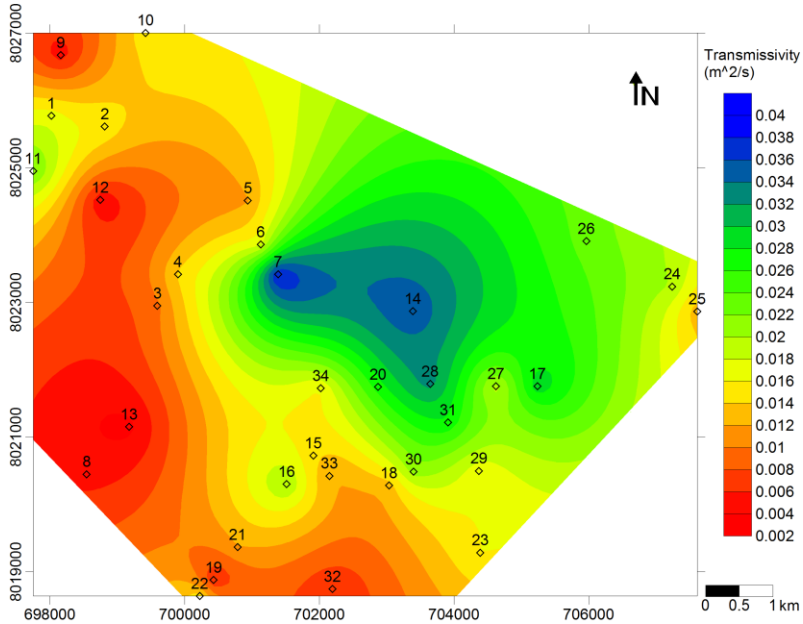

Figure 25 Calculated transmissivity distribution in the porous aquifer. Central part of the alluvial fan of River Paria shown in Figure 2.

5 Discussion

There is still a long way to go before reaching sustainable use of groundwater in developing countries like Bolivia. Despite the importance of aquifers in semi-arid regions such as the Altiplano, those "unseen" resources need more attention to ensure that exploration, development and management stages are completed in the best possible way, putting together advances in the technical work with the development of social awareness towards water resources. Any attempt to generate knowledge in this subject is valuable per se.

The studies presented in this thesis contribute with results and interpretations aiming to improve the understanding of the hydrogeological characteristics in the alluvial fan of River Paria. The overall outcome of this research intends to exemplify the use of non-invasive methods that can be applicable in similar study cases in need of efficient data acquisition. Likewise, the multidisciplinary approach including geoelectrical surveys and isotopic data analysis, can be beneficial since the physical characteristics addressed by resistivity interpretations (e.g. geological settings, geometry and aquifer properties), can be complemented the hydraulic properties obtained from isotopic interpretations (e.g. distinction of flow paths).

5.1 Study outcomes

The results from the studies included in this thesis prove the applicability of the isotopic data analysis and geoelectrical surveys to the semiarid conditions of the study area. Data retrieved from previous studies complemented the recently acquired data. In the case of the isotopic data, new groundwater compositions of deuterium and oxygen-18 (related to the V-SMOW standard) were added to the available database for the subsequent analyses. Likewise, 1-D and 2-D resistivity models from the recent TEM and ERT surveys were analysed together with the 1-D resistivity models obtained from previous VES measurements; although there are some considerations arising when it comes to interpreting resistivity from mixed methods, they were acknowledged in the Papers II, III and IV. The most relevant outcomes from the appended papers can be summarized as follows:

- The first study proposes the existence of four circulation patterns in the aquifer system to the north of Oruro (Paper I). The distinction is based on the isotopic signatures related to origins and recharge processes (see Table 1). The flows in the porous aquifer (unconsolidated sediments) are mainly recharged by lateral infiltration from the rivers around the flatland. Deeper flows in the bedrock faults might have different origins and longer residence times, and some of them are in contact with hydrothermal sources.
- There are indications of the complex and irregular shape of the bedrock from geoelectrical interpretations (Paper II). The tectonic forces behind the shape of the mountains around Oruro have influenced on the bedrock shape and geological structures as well (see Figure 17). Hence, the thickness of the unconsolidated sediments varies from a couple of meters, near the rock outcrops, to ~200 m in the middle of the alluvial fan of River Paria (Paper IV). Likewise, the NW-SE direction of faults and mountain ranges is replicated in folds and fractures beneath the sediments (Paper III).
- Two major faults have projections towards the NW coming from the eastern side of the study area (see Figure 23). An additional second order fault was also located in parallel with the other two faults previously mentioned (Paper III). These structures host hydrothermal flows discharging upwards around the hot springs of Capachos (eastern limit of the alluvial fan).
- The most promising site for groundwater production is in the centre of the alluvial fan of River Paria (Paper IV), where the package of sediments is thicker than in the rest of the investigated area (see Figure 25). This site also holds groundwater with adequate quality for consumption and irrigation. On the other hand, places around faults might be affected by hydrothermal flows, which in turn could increase the salinity of water.

5.2 Integrating interpretations to the hydrogeological conceptual model

In the Altiplano basin, sedimentary deposits are commonly good aquifers since the water table is relatively shallow and groundwater can be extracted by either dug or drilled wells; however, the boundaries of these aquifers are not always defined. In the present case study, the unconsolidated sediments occupy an area of ~500 km^2, from which ~150 km^2 are delimited by the alluvial fan of River Paria. In the northern part of this alluvial fan (i.e. the apex), the thickness of the sediments might be just a couple of meters (according to resistivity images from two ERT lines). On the other hand, the sediments thickness is greater in the intermediate and distal part of

the same alluvial fan. Despite the gap in data cover between these two sectors (see Figure 13), it is possible to assume that the thickness increases south-westwards.

Previous studies proposed a sound depiction of the bedrock relief below the sediments in the alluvial fan, to which new details like faults and folds from the recent geoelectrical surveys were added. The study provides more evidences of the existence of a fractured aquifer underlying the top porous alluvial aquifer. Some faults were traced further than the initial indication of the regional geological map. However, the real length of these structures could be even longer since the fault traces seem to cross the site where the geoelectrical data were acquired (central part of the alluvial fan). Some hydrothermal flows near the hot springs most likely go upwards, however the hydraulic characteristics of the fractured aquifer need further study. While the most important freshwater aquifers lie in the shallow unconsolidated sediments, saline flows linked to deep hydrothermal activity around the recently inferred faults, could affect the quality of water in the nearby wells. This has happened in other wells around the study area.

Despite the complex arrangement of sediments in the porous aquifer, the water quality and salinity remain relatively stable in the alluvial fan (e.g. EC $\leq$ 1000 µS/cm). The applied geoelectrical methods have limitations at shallow depths to improve the stratification of sediments in detail, except for some patches of low resistivity protruding from a higher background, likely related to high clay content lenses. Nevertheless, assuming the unconsolidated sediments to be a single porous aquifer, the geoelectrical methods have provided useful results to complete an initial round of exploration, especially in the central part of the alluvial fan.

The close correlation between resistivity and hydraulic conductivity in the porous aquifer permitted the estimation of hydraulic properties (K and T) in the central part of the alluvial fan. Additional estimations can be done in other areas with similar geological settings to obtain preliminary results of K and T that otherwise would be expensive and time consuming to obtain through traditional tests in wells. On the other hand, key characteristics that influence on the electrical response of geological formations must be considered (e.g. clay content, porosity, bulk chemistry), because in sites heavily influenced by any of them, the application of the methodology presented in Paper IV has limitations and the accuracy of estimations based on an empirical relationship might be questionable.

The outcomes from the application of different exploration techniques may provide enough data to step into the development stage of the aquifer system. A numerical model of the porous aquifer based on its geometry (thickness), the calculated hydraulic parameters (K and T), the salinity of water, the location of hydrothermal flows, the groundwater levels and flow directions would be valuable tools for the water resources management. However, to define the boundary conditions without similar information around the investigated area might carry uncertainties that

would make the numerical model less reliable. Hence, the exploration methods applied in this research might be repeated to cover larger areas and eventually the entire aquifer system.

6 Conclusions

The sustainable use of water resources in the Altiplano should be prioritized to guarantee the supply for domestic consumption as well as for irrigation in the future. In the case of the aquifers to the north of Oruro, they have been reliable water sources. However, they may become vulnerable to recharge reduction, overabstraction and contamination. The studies presented in this thesis aim to fill gaps in the exploration stage and to improve the hydrogeological knowledge in the study area. The outcomes of this thesis can be described as follows:

- Despite the challenges in conducting exploration tests in a remote area with limited resources, the applied methods have proven to be suitable to the local conditions. The data acquisition was efficient, and the results improved the understanding of the hydrogeological settings in the study aquifer system.
- The hydrogeological knowledge about the central part of the alluvial fan of River Paria has been refined to include distinction of groundwater flow paths from isotopic data analysis, and clarification of geological settings and estimation of aquifer properties from resistivity data analysis.
- Another topic that requires further investigations concerns the hydrothermal characteristics to the east of the alluvial fan. Despite this thesis has provided more evidences regarding the existence of a fractured aquifer beneath the top porous aquifer, its hydraulic characteristics remain unknown. Just a few hydrothermal flows discharging upwards in some faults were inferred from resistivity interpretations.

Advances in the understanding of hydrogeological characteristics are valuable contributions filling gaps in the exploration stage of sustainable use of groundwater in the study area. However, due to the extensive size of the aquifer system, exploration methods from different branches of engineering and science should be applied over the entire area before shifting to the development and later to the management stages.

Although the results from this research are specific and valid only for the study area, the methodology of applying isotopic and resistivity data analyses can serve as an example of a hydrogeological approach for studies with similar environmental conditions and limitations. Each case study may have their own characteristics

making them more suitable for some techniques compared to others; however, a multidisciplinary approach is always recommended for groundwater exploration, since it is a complex subject involving geology, hydraulics, physics and chemistry that may even vary over time.

6.1 Recommendations

One of the critical issues that need to be addressed in parallel with the advances in the technical work is the social component. A society well aware of the importance of the groundwater resources is open to be engaged in roles of protection and correct use of water. However, the current social conflicts in the study area impede access to some areas to conduct tests. Other alternatives may also help in this matter, such as airborne geophysics which would allow data acquisition without disturbing villagers.

In order to improve the outcomes from the applied exploration methods, some recommendations can be mentioned:

- The isotopic database should be updated. In the case of the isotopes in precipitation, the most recent reports are from 2013; however, the data contain gaps in all of the stations. For groundwater, continuous sampling would allow making discretized analyses including seasonal variations in the recharge process.
- To consolidate interpretations from the resistivity analysis, more ground truth information is needed; this may come from exploration drilling in strategic and representative sites over the study aquifer. In fact, reliable interpretations are achieved correlating geoelectrical interpretations with other sources of information.
- The accuracy of the aquifer parameters estimation, included in Paper IV, can be improved with additional information like groundwater electrical conductivity and porosity. There are other approaches to estimate hydraulic properties in the porous aquifer that use this additional information (e.g. Archie's law, Dar-Zarrouk parameters, Kozeny-Carman-equation).

6.2 Future research

In order to improve the description of the aquifer system around Oruro, many other exploration techniques can be applied. Some suggestions that can be mentioned for future studies are:

Study of contamination regarding wastewater and mining from the urban area of Oruro. It can be addressed by hydrochemical and isotopic analyses, as well as geophysics. Although previous studies indicated that no contamination traces exist in the porous aquifer (e.g. Banks et al., 2002; Dames & Moore Norge, 2000), pollutants like heavy metals from mining and nutrients from wastewater might compromise the water quality in the near future.

Expanding the TEM surveys over the entire aquifer system. Nowadays it is possible to cover large areas using airborne geophysics. Considering the importance of this reservoir, it would be worthwhile to invest in such surveys since the technique has proven to be suitable for the local conditions. Outcomes from this type of study would be the quantification of water volumes contained in the entire porous aquifer.

Application of deep penetration geophysics (e.g. high power TEM, magnetotellurics, seismic reflection and gravity) to elucidate the connection between shallow hydrothermal flows with the deep geothermal sources. The hydrothermal flows around Capachos nowadays pose a risk of contamination for the freshwater aquifer; however, with broader knowledge of this matter, it can turn into a beneficial feature with economic advantages.

Another important point to expand the scope of this investigation is the exchange of information and experiences with other researchers and technicians working with similar studies in the region. Groundwater exploration applying geophysics is becoming more popular, engaging universities and institutions working in the field. Ideally, the information generated from such studies should be accessible for further investigations.

After improving and expanding the exploration of the porous aquifer, the next step in the management stage should aim for a numerical model of the aquifer including the physical characteristics of the study area, the hydraulic conditions (e.g. overabstraction around the well field) and the sources of potential contamination (e.g. mining tails, wastewater and saline intrusions).

7 References

Aarhus GeoSoftware, 2017a. Aarhus SPIA. URL https://www.aarhusgeosoftware.dk/spia---tem-software (accessed 7.07.19).

Aarhus GeoSoftware, 2017b. Aarhus Workbench. URL http://hgg.au.dk/software/aarhus-workbench/ (accessed 7.07.19).

Allen, J., 2016. Bolivia's Lake Poopó Disappears [WWW Document]. NASA. URL https://earthobservatory.nasa.gov/images/87363/bolivias-lake-poopo-disappears (accessed 2.25.19).

ANESAPA, 2019. Asociación Nacional de Empresas de Servicio de Agua Potable y Alcantarillado [WWW Document]. URL http://www.anesapa.org/ (accessed 6.10.19).

Aravena, R., Suzuki, O., Peña, H., Pollastri, A., Fuenzalida, H., Grilli, A., 1999. Isotopic composition and origin of the precipitation in Northern Chile. Appl. Geochemistry 14, 411–422. https://doi.org/10.1016/S0883-2927(98)00067-5

Banks, D., Holden, W., Aguilar, E., Mendez, C., Koller, D., Andia, Z., Rodriguez, J., Saether, O.M., Torrico, A., Veneros, R., Flores, J., 2002. Contaminant source characterization of the San Jose Mine, Oruro, Bolivia. Geol. Soc. London, Spec. Publ. 198, 215–239. https://doi.org/10.1144/GSL.SP.2002.198.01.14

Boiero, D., Godio, A., Naldi, M., Yigit, E., 2010. Geophysical investigation of a mineral groundwater resource in Turkey. Hydrogeol. J. 18, 1219–1233. https://doi.org/10.1007/s10040-010-0604-2

Broman, V., Svensson, E., 2017. TEM and ERT Investigations in Challapampa Aquifer, Bolivia. MSc Thesis, Engineering Geology, Lund University. ISRN LUTVDG/(TVTG--5152)/1-50/(2017).

Canaviri, B., 2011. Estimación de la vulnerabilidad intrínseca a la contaminación del aquífero libre en el sistema acuífero de Challapampa Oruro (Estimation of the intrinsic vulnerability to contamination of the unconfined aquifer in the Challapampa aquifer system Oruro). Tesis de grado (Bachelor thesis). Universidad Técnica de Oruro. Oruro, Bolivia.

Canedo-Rosso, C., Hochrainer-Stigler, S., Pflug, G., Condori, B., Berndtsson, R., 2019. Drought risk in the Bolivian Altiplano associated with El Niño Southern Oscillation using satellite imagery data. Nat. Hazards Earth Syst. Sci. Under revi. https://doi.org/https://doi.org/10.5194/nhess-2018-403

Christiansen, A.V., Auken, E., 2012. A global measure for depth of investigation. GEOPHYSICS 77, WB171-WB177. https://doi.org/10.1190/geo2011-0393.1

Christiansen, A.V., Auken, E., Sørensen, K., 2009. The transient electromagnetic method, in: Kirsch, R. (Ed.), Groundwater Geophysics: A Tool for Hydrogeology. Springer

Berlin Heidelberg, Berlin, Heidelberg, pp. 179–226. https://doi.org/10.1007/978-3-540-88405-7_6

Coudrain, A., Olive, P., Quintanilla, J., Sondag, F., Cahuaya, D., 1995. Salinity and isotopic dynamics of the groundwater resources on the Bolivian Altiplano, in: Application of Tracers in Arid Zone Hydrology (Proceedings of the Vienna Symposium August 1994). Vienna, pp. 267–276.

Craig, H., 1961. Isotopic Variations in Meteoric Waters. Sci. New Ser. 133, 1702–1703.

Dahlin, T., 2001. The development of DC resistivity imaging techniques. Comput. Geosci. 27, 1019–1029. https://doi.org/10.1016/S0098-3004(00)00160-6

Dahlin, T., Zhou, B., 2006. Multiple-gradient array measurements for multichannel 2D resistivity imaging. Near Surf. Geophys. 4, 113–123. https://doi.org/10.3997/1873-0604.2005037

Dames & Moore Norge, 2000. Estudio hidrogeológico de la mina San José y los acuíferos que suministran agua a la ciudad de Oruro (Hydrogeological Study of the San Jose Mine and Adjacent Aquifers Supplying Water to the City of Oruro): Report 1,2,3. Corporacion Minera de Bolivia COMIBOL. PMAIM-Subproyecto No 7.

D'Elia, M., 2013. Asesoramiento para el Diseño e Implementación de la Red de Monitoreo de Aguas Subterráneas en la Cuenca del Lago Poopó (Advice for the design and implementation of the groundwater monitoring network in the lake Poopó basin). Gobierno Autónomo Departamental De Oruro. Programa de Gestión Sostenible de los Recursos Naturales de la Cuenca del Lago Poopó Convenio No. DCI-ALA/2009/021-614, Oruro.

Ekmekçi, M., Günay, G., 1997. Role of public awareness in groundwater protection. Environ. Geol. 30, 81–87. https://doi.org/10.1007/s002540050135

Fetter, C.W., 2001. Applied hydrogeology / C.W. Fetter. Upper Saddle River: Prentice Hall, cop. 2001, New Jersey 07458.

Fiorella, R.P., Poulsen, C.J., Pillco, R., Barnes, J.B., Tabor, C.R., Ehlers, T.A., 2015. Spatiotemporal variability of modern precipitation δ18O in the central Andes and implications for paleoclimate and paleoaltimetry estimates. J. Geophys. Res. Atmos. 120, 1–27. https://doi.org/10.1002/2014JD022893.

GEOBOL, Swedish Geological AB, 1992. Carta Geológica de Bolivia - Hoja Oruro (Geological map of Bolivia - Sheet Oruro). Publicación SGB Serie I-CGB-11.

GITEC, C.G., COBODES Ltda., 2014. Formulación del Plan Director de la cuenca del lago Poopó (Poopo Lake Basin Management Plan Formulation). Informe final. Programa de gestion sostenible de los recursos naturales de la cuenca del lago Poopo. Gobierno Autónomo Departamental de Oruro. Agosto 2014, Oruro, Bolivia (CTO-SERV-03/2013).

GOB, 2009. Constitución Politica del Estado [WWW Document]. Gac. Of. Boliv. Minist. la Pres. Boliv. URL http://www.gacetaoficialdebolivia.gob.bo/index.php/normas/descargar/154183 (accessed 6.10.19).

GOB, 2016. Decreto Supremo Nro 2987 [WWW Document]. Gac. Of. Boliv. Minist. la Pres. Boliv. URL http://www.gacetaoficialdebolivia.gob.bo/index.php/normas/descargar/154121 (accessed 5.22.19).

Gómez, E., Barmen, G., Rosberg, J.-E., 2016. Groundwater Origins and Circulation Patterns Based on Isotopes in Challapampa Aquifer, Bolivia. Water 8, 207. https://doi.org/10.3390/w8050207

Guérin, R., Descloitres, M., Coudrain, A., Talbi, A., Gallaire, R., 2001. Geophysical surveys for identifying saline groundwater in the semi-arid region of the central Altiplano, Bolivia. Hydrol. Process. 15, 3287–3301. https://doi.org/10.1002/hyp.284

Haile, T., Abiye, T.A., 2012. The interference of a deep thermal system with a shallow aquifer: The case of Sodere and Gergedi thermal springs, Main Ethiopian Rift, Ethiopia. Hydrogeol. J. 20, 561–574. https://doi.org/10.1007/s10040-012-0832-8

Hubbard, S.S., Rubin, Y., 2005. Introduction to Hydrogeophysics, in: Hydrogeophysics. Water Science and Technology Library. Springer, Dordrecht, pp. 3–21. https://doi.org/https://doi.org/10.1007/1-4020-3102-5_1

IAEA, 2015. Global Network of Isotopes in Precipitation (GNIP) - Water Resources Programme. International Atomic Energy Agency (IAEA) [WWW Document]. URL http://www-naweb.iaea.org/napc/ih/IHS_resources_gnip.html (accessed 5.24.19).

Kimura, M., Masuhara, N., Baba, K., 2018. Making Social Networks Visible: Shared Awareness Among Stakeholders on Groundwater Resources 273–286. https://doi.org/10.1007/978-981-10-7383-0_19

Kirsch, R., Yaramanci, U., 2009a. Geoelectrical methods, in: Kirsch, R. (Ed.), Groundwater Geophysics. Springer Berlin Heidelberg, Berlin, Heidelberg, pp. 85–117. https://doi.org/10.1007/978-3-540-88405-7_3

Kirsch, R., Yaramanci, U., 2009b. Geophysical characterisation of aquifers, in: Groundwater Geophysics. Springer Berlin Heidelberg, Berlin, Heidelberg, pp. 491–509. https://doi.org/10.1007/978-3-540-88405-7_17

Kumar, D., Thiagarajan, S., Rai, S.N., 2011. Deciphering Geothermal resources in Deccan trap region using electrical resistivity tomography technique. J. Geol. Soc. India 78, 541–548. https://doi.org/10.1007/s12594-011-0123-3

Lizarazu, J., Aranyossy, J.F., Orsag, V., Salazar, J.C., 1987. Estudio Isotopico de la cuenca de Oruro-Caracollo, Bolivia (Isotopic study in the Oruro-Caracollo basin, Bolivia), in: Isotope techniques in water resources development. IAEA-SM-299/11 301-314. Vienna, Symposium March 1987.

Loke, M.H., 2004. Rapid 2-D Resistivity & IP inversion using the least-squares method. Man. Res2dinv, version.

Loke, M.H., Acworth, I., Dahlin, T., 2003. A comparison of smooth and blocky inversion methods in 2D electrical imaging surveys. Explor. Geophys. 34, 182–187.

Maliva, R., Missimer, T., 2012. Arid Lands Water Evaluation and Management, Arid Lands Water Evaluation and Management SE - 8, Environmental Science and Engineering. Springer Berlin Heidelberg. https://doi.org/10.1007/978-3-642-29104-3_8

Marengo, J.A., Espinoza, J.C., Alves, L.M., Ronchail, J., 2017. Drought in Bolivia: The worst in the last 25 years. "State Clim. - Bull. Am. Meteorol. Soc. 98, S188–S189. https://doi.org/10.1175/2017BAMSStateoftheClimate.1

Mazáč, O., Kelly, W.E., Landa, I., 1985. A hydrogeophysical model for relations between electrical and hydraulic properties of aquifers. J. Hydrol. 79, 1–19. https://doi.org/10.1016/0022-1694(85)90178-7

Mook, W.G., 2000. Environmental isotopes in the hydrological cycle - Principles and applications, IHP-V Tech. ed, International Hydrological Programme. Paris, France: Unesco, 2000.

Nabighian, M., 1991. Electromagnetic Methods in Applied Geophysics: Volume 2, Application, Parts A and B, Newmont Ex. ed. Society of Exploration Geophysicists, Denver, Colorado, US. https://doi.org/10.1190/1.9781560802686

Navarro, J.Á.S., López, P.C., Perez-Garcia, A., 2004. Evaluation of geothermal flow at the springs in Aragón (Spain), and its relation to geologic structure. Hydrogeol. J. 12, 601–609. https://doi.org/10.1007/s10040-004-0330-8

Niwas, S., Tezkan, B., Israil, M., 2011. Aquifer hydraulic conductivity estimation from surface geoelectrical measurements for Krauthausen test site, Germany. Hydrogeol. J. 19, 307–315. https://doi.org/10.1007/s10040-010-0689-7

Olsson, P.I., Dahlin, T., Fiandaca, G., Auken, E., 2015. Measuring time-domain spectral induced polarization in the on-time: Decreasing acquisition time and increasing signal-to-noise ratio. J. Appl. Geophys. 123, 316–321. https://doi.org/10.1016/j.jappgeo.2015.08.009

Olsson, P.I., Fiandaca, G., Larsen, J.J., Dahlin, T., Auken, E., 2016. Doubling the spectrum of time-domain induced polarization by harmonic de-noising, drift correction, spike removal, tapered gating and data uncertainty estimation. Geophys. J. Int. 207, 774–784. https://doi.org/10.1093/gji/ggw260

Pacheco-Guerrero, A., González-Trinidad, J., Júnez-Ferreira, H., Bautista-Capetillo, C., Hernández-Antonio, A., Olmos-Trujillo, E., Ávila-Sandoval, C., 2019. Integration of isotopic (2H and 18O) and geophysical applications to define a groundwater conceptual model in semiarid regions. Water 11. https://doi.org/10.3390/w11030488

Palacio, T., 1993. Geoelectric study for groundwater prospection in Oruro city. Santafe de Bogota. SeLA; PNUD; CAEM.

Palacky, G.J., 1987. Resistivity Characteristics of Geologic Targets, in: Electromagnetic Methods in Applied Geophysics. Society of Exploration Geophysicists, pp. 52–129. https://doi.org/10.1190/1.9781560802631.ch3

Perdomo, S., Kruse, E.E., Ainchil, J.E., 2018. Estimation of hydraulic parameters using electrical resistivity tomography (ERT) and empirical laws in a semi-confined aquifer. Near Surf. Geophys. 16, 627–641. https://doi.org/10.1002/nsg.12020

Reynolds, J.M., 2011. An introduction to applied and environmental geophysics. Wiley-Blackwell.

Rigsby, C.A., Bradbury, J.P., Baker, P.A., Rollins, S.M., Warren, M.R., 2005. Late Quaternary palaeolakes, rivers, and wetlands on the Bolivian Altiplano and their palaeoclimatic implications. J. Quat. Sci. 20, 671–691. https://doi.org/10.1002/jqs.986

Salina, I., Berger, D., 2008. Flow: For Love of Water (Documentary). http://www.environmentandsociety.org/mml/flow-love-water (accessed 7.07.19).

Satgé, F., Espinoza, R., Zolá, R.P., Roig, H., Timouk, F., Molina, J., Garnier, J., Calmant, S., Seyler, F., Bonnet, M.P., 2017. Role of climate variability and human activity on Poopó Lake droughts between 1990 and 2015 assessed using remote sensing data. Remote Sens. 9, 1–17. https://doi.org/10.3390/rs9030218

Scheihing, K., Moya, C., Struck, U., Lictevout, E., Tröger, U., 2017. Reassessing Hydrological Processes That Control Stable Isotope Tracers in Groundwater of the Atacama Desert (Northern Chile). Hydrology 5, 3. https://doi.org/10.3390/hydrology5010003

SCIDE, CORDEOR, GEOBOL, 1996. Informe de los pozos de producción - Proyecto de investigación y verificación de fuentes de abastecimiento de agua para la ciudad de Oruro (Report of the production wells - Project of investigation and verification of sources of water for supplying Oruro). GEOBOL - Servicio Geológico de Bolivia., Oruro. 159p.

Seiler, K.P., Gat, J.R., 2007. Groundwater Recharge from Run-Off, Infiltration and Percolation, Water Science and Technology Library. Springer Netherlands, Dordrecht. https://doi.org/10.1007/978-1-4020-5306-1

SELA, 2018. Servicio Local De Acueductos Y Alcantarillado - Oruro [WWW Document]. URL http://selaoruro.gob.bo/ (accessed 1.10.18).

SENAMHI, 2015. Servicio Nacional de Meteorologia e Hidrologia de Bolivia [WWW Document]. URL http://senamhi.gob.bo/ (accessed 9.4.15).

Slater, L.D., Lesmes, D., 2002. IP interpretation in environmental investigations. Geophysics 67, 77–88. https://doi.org/10.1190/1.1451353

Soupios, P.M., Kouli, M., Vallianatos, F., Vafidis, A., Stavroulakis, G., 2007. Estimation of aquifer hydraulic parameters from surficial geophysical methods: A case study of Keritis Basin in Chania (Crete - Greece). J. Hydrol. 338, 122–131. https://doi.org/10.1016/j.jhydrol.2007.02.028

Suarez Soruco, R., 2000. Compendio de Geología de Bolivia (Bolivian Geology Compendium). Rev. Tec. Yacimientos Pet. Fisc. Boliv.

Swedish Geological AB, 1996. Impacto de la contaminación minera e industrial sobre agua subterráneas (Impact of mining and industrial pollution on groundwater). Ministerio de Desarrollo Sostenible y Medio Ambiente. Secretaria Nacional de Mineria. Proyecto Piloto Oruro., (Report) ID: R-Bo-E-9.45-9702-PPO96I6.

Tizro, A.T., Voudouris, K.S., Salehzade, M., Mashayekhi, H., 2010. Hydrogeological framework and estimation of aquifer hydraulic parameters using geoelectrical data: a case study from West Iran. Hydrogeol. J. 18, 917–929. https://doi.org/10.1007/s10040-010-0580-6

Uribe, J., Muñoz, J.F., Gironás, J., Oyarzún, R., Aguirre, E., Aravena, R., 2015. Assessing groundwater recharge in an Andean closed basin using isotopic characterization and a rainfall-runoff model: Salar del Huasco basin, Chile. Hydrogeol. J. 1–17. https://doi.org/10.1007/s10040-015-1300-z

Yin, L., Hou, G., Su, X.S., Wang, D., Dong, J., Hao, Y., Wang, X., 2011. Isotopes (δD and δ18O) in precipitation, groundwater and surface water in the Ordos Plateau, China: Implications with respect to groundwater recharge and circulation. Hydrogeol. J. 19, 429–443. https://doi.org/10.1007/s10040-010-0671-4

Paper I

water

MDPI

Article

Groundwater Origins and Circulation Patterns Based on Isotopes in Challapampa Aquifer, Bolivia

Etzar Gómez [1,2,*], Gerhard Barmen [1] and Jan-Erik Rosberg [1]

1 Engineering Geology, Lund University, Box 118, Lund SE-221 00, Sweden; gerhard.barmen@tg.lth.se (G.B.); jan-erik.rosberg@tg.lth.se (J.-E.R.)
2 Institute of Hydraulic & Hydrology, San Andres Major University, La Paz, Bolivia
* Correspondence: etzar.gomez@tg.lth.se; Tel.: +46-222-7425

Academic Editor: Luc Lambs
Received: 25 January 2016; Accepted: 10 May 2016; Published: 18 May 2016

Abstract: Aridity and seasonality of precipitation are characteristics of the highland region in Bolivia. Groundwater becomes an important and safe source of water when surficial bodies are intermittent and affected by natural and anthropogenic contamination. Decades of exploitation of the Challapampa aquifer, combined with lack of information required to understand the groundwater circulation, represent a challenge for reservoir management. This study analyzes isotopic compositions of deuterium and oxygen-18 in different stages in the hydrologic cycle to assess flow patterns in the aquifer, especially in the alluvial fan of River Paria, where records are more extensive in space and time. Interpretations are based on existing and new data. Some implications, such as the age of water, the evaporation effect in groundwater and some thermal intrusions are supported by stable isotopes, tritium, radiocarbon, and electrical conductivity records. New results confirm that modern precipitation over the mountains surrounding the study area is the most important origin of water for shallow aquifers until exploited depths, 100 m below surface. The origin of water in deeper depths, 400 m, seems related to infiltration at higher altitudes and longer residence times.

Keywords: stable isotopes; groundwater; highland; Andes; Bolivia

1. Introduction

In the Bolivian Altiplano, as in other arid and semi-arid regions over the world, groundwater is an important component of the available water resources [1]. The region has a long history of mining activities since pre-colonial times [2], promoting the growth of cities like Oruro, where the most important water reservoir is the Challapampa aquifer system. The identification of the recharge areas, estimation of the inlet volumes, and general understanding of the circulation patterns are crucial for the management of this and any reservoir. For these purposes, various types of data and techniques can be used to study groundwater systems [3], among them, the environmental isotopic approach.

Previous studies proposed general theories about the circulation patterns in the Challapampa aquifer system, e.g., the most productive porous aquifers are contained in Quaternary sediments, which fill the flat and lower lands in the region. The main recharge originates in the annual rainfall over the mountain range, at the eastern and northern limits of the study area. It runs off and reaches the aquifer system mainly through alluvial fans. The regional groundwater flows towards Lake Poopo, the lowest and predominant discharge zone in the enclosed catchment, though high extraction rates may be causing some shallow systems to flow towards a well-field in the middle of the study area [4–7]. Even if the conceptual description above has been established in previous basic studies, the region has been scarcely researched in the last decades. Earlier attempts, analyzing isotopes, considered different stages in the hydrologic cycle like only precipitation [8,9] or only groundwater [10–12]. Also, increased

demand for water and changes in climatic conditions over the last thirty years have not been taken into account in the circulation models.

This study presents an updated and combined analysis of environmental isotopic data in precipitation, surface water, and groundwater, in order to elucidate and verify hypotheses about origins, circulation patterns, and flow systems in the Challapampa aquifer. The investigation is based on all available isotopic information, in order to propose a conceptual circulation model. Furthermore, new data provided so far by this research enhances novel interpretations and results.

2. Study Area

The Altiplano is a high plateau about 150 km wide and 1500 km long [13]. Bolivia has a third of its territory located in that region (Figure 1a). This land has distinctive characteristics in terms of geomorphology, climate, and resources. The Bolivian Altiplano hosts a substantial part of the biggest enclosed catchments in the continent, called the TDPS system. Its name is an acronym of the four sub-systems of which it is comprised, Lake Titicaca, River Desaguadero, Lake Poopo, and the salt flats (Figure 1a,b) [14,15].

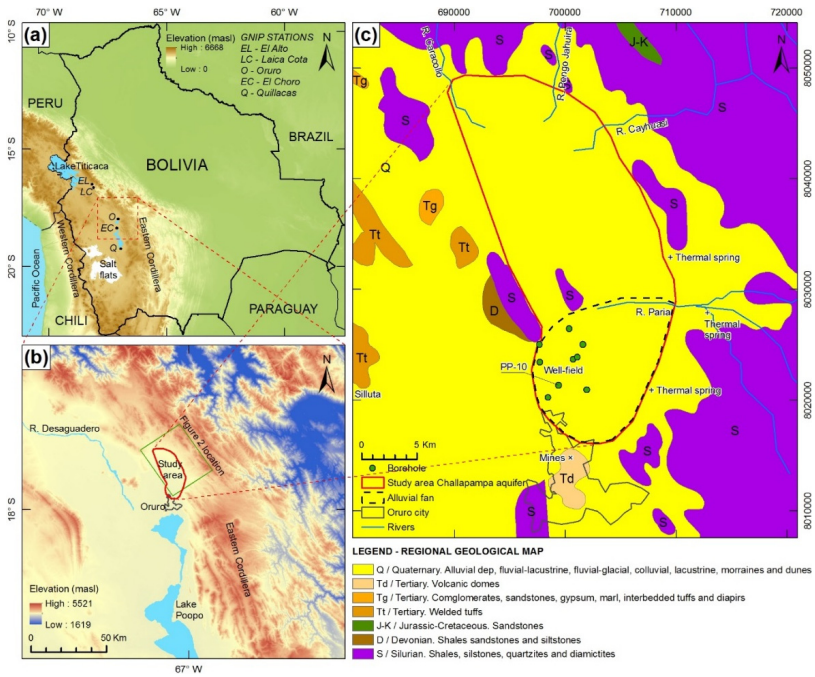

Figure 1. Location of the study area. (**a**) The Bolivian Altiplano and TDPS system; (**b**) Northern part of the Lake Poopo enclosed catchment; (**c**) Regional geological map. Modified from Geobol & Swedish Geological AB (1992) [16].

The study area is bounded by latitudes 17°35′ S–18°00′ S and longitudes 66°59′ W–67°12′ W, and it covers about 500 km^2 (Figure 1b,c). The average elevation in the plateau is about 3700 m above sea level (masl). The surrounding landscape is mountainous, divided with ridges parallel to each other in NW–SE direction, reaching 5500 masl in high peaks [5]. The region is characterized by semiarid climate; the average temperature is about 10 °C and the rainfall is in the range of 300 to 500 mm/y with a markedly wet summer, from December to March, during which the high-reaching anticyclones over the subtropical Andes produce about 80% of the annual precipitation. The potential evaporation in the region is around 1.5 m/y [13,15].

The delimitation of the study area is based on geological features and outcrops which enclose a substantial part of the aquifer system; nevertheless, as the sedimentary deposits cover greater areas in the region, some flow systems could cross the assumed limits. The regional geological features are dominated by two units; the first composed by outcrops of Silurian rocks and the sporadic presence of Tertiary and Devonian sediments (purple and brown colors in Figure 1c); and the second by Quaternary deposits controlled by glacial, lacustrine, and fluvial processes (yellow color in Figure 1c). Sedimentary units were the result of weathering and erosion of rocks in the mountain range, where the action of water led to the formation of terraces and alluvial fans. Those Quaternary deposits, commonly including colluvium, colluvium-fluvial, fluvial, fluvial-lacustrine, fluvial-glacial, and terraces, composed by coarse to fine grained sediments (pebbles, gravel, sand, silt, and clay) cover most of the flat study area.

Fluvial-lacustrine deposits, composed of clay and silt, cover large areas in the plain and prevent direct infiltration of surface water, causing floods during the rainy season [4,5,10]. Water retained at the surface evaporates by intense radiation, high temperatures during daylight hours, and high vapor pressure deficit, leaving salts encrusted in the soil matrix. Furthermore, isotopic analysis reveals that evaporation occurs prior to infiltration in those areas [10]. The average groundwater velocity in the aquifer was estimated as 1 m/y [11], though this value rises to 10 m/y in recharge areas [17]. The occurrence of thermal waters is also important in the groundwater circulation systems. Gitec & Cobodes (2014) [7] identified 16 thermal springs in the Lake Poopo basin, three of them at the eastern limit of the study aquifer. The influence and patterns of thermal activity in the aquifer system is still unknown. However, some boreholes in the southern part of the study area appear to be in contact with thermal intrusions (e.g., PP-10 in Figure 1c), probably through fault systems [6,11] (Figure 2).

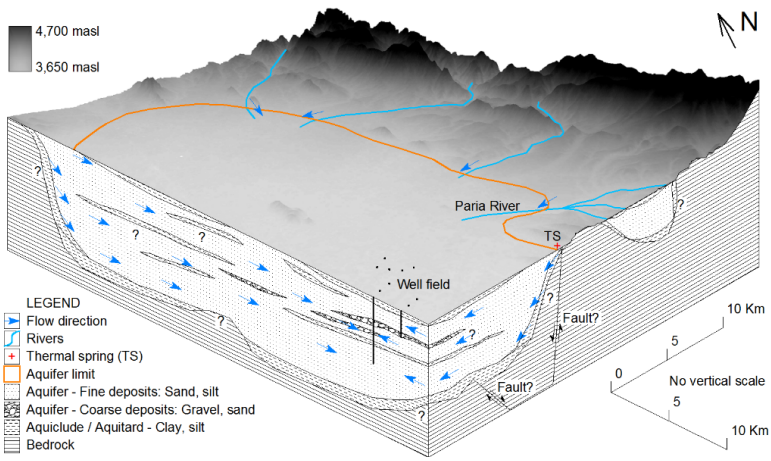

Figure 2. Schematic hydrogeological model of the Challapampa aquifer system (location in Figure 1b).

Lizarazu *et al.* (1987) [11] proposed the distinction of circulation patterns at different depths. However, their interpretation refers to a small area around the well field shown in Figure 2. The aquifer system is assumed to be a complex sedimentary unit, with horizontal and vertical continuity [2,4,6,7,12,17]. However, lenses with low hydraulic conductivity, mainly comprised of clay, exist in the stratification, but they are not large enough to isolate individual aquifers. Banks *et al.* (2002) [4] also proposed that the regional and deepest flow might be limited by a transition to a less permeable silty clay unit (Figure 2).

The Challapampa aquifer system is used to provide water for domestic consumption, agricultural and mining activities, and has hosted a well-field operated by SELA (a local public water supply

company in Oruro) for the last 50 years. Domestic water demand has doubled in the last 15 years. The average annual abstraction is 8,600,000 m^3 in this period [18]. The occurrence of groundwater in the region is related to the past and present climatic conditions over the TDPS system and the sedimentation processes that shaped the most important and extended porous aquifers. In the modern TDPS system, Lake Titicaca feeds by overflowing the lower Lake Poopo through the River Desaguadero (Figure 1a,b). During the Quaternary, the central Altiplano valley was the site of several lacustrine transgressions and regressions. Tauca was the earliest palaeolake covering the region, between 13,000 and 16,000 years BP. Some characteristics of that time, like high precipitation rates and melting of glaciers, are mentioned in previous studies [13,19–21]. Therefore, it is expected that hints of those characteristics will be found in groundwater at the deepest levels if it was recharged during that time.

3. Data, Sampling and Methods

Isotopic data used in this study is comprised of records of series and single measurements in different hydrologic cycle stages. Although stable isotopes of hydrogen and oxygen have been widely used in several climate and paleoclimate studies in the Bolivian Altiplano, the scarcity of data, gaps in series, and lack of consistent sampling methods are common problems reducing accuracy of the results [8,22]. This study includes records of oxygen-18 (^{18}O), deuterium (^{2}H), tritium (^{3}H), carbon-13 (^{13}C), and carbon-14 (^{14}C). However, besides the aforementioned issues, a substantial part of the sampling sites do not have clear position references or coordinates. Consequently, just part of the data is included on the maps and spatial analysis in this study.

Compositions of isotopes in precipitation were obtained from the International Atomic Energy Agency's (IAEA) Global Network for Isotopes in Precipitation (GNIP), which includes ^{18}O, ^{2}H, and ^{3}H records [9]. This study refers to five GNIP stations with similar characteristics as in the study area, regarding, for example, elevation and precipitation regimes. Those are Laica Cota, El Alto, Oruro, Quillacas and El Choro (Figure 1a). Sampling methodology for isotopes in precipitation follows the IAEA's procedures and recommendations; monthly precipitations were captured, stored, and transported to specialized laboratories to be analyzed (Laica Cota to IAEA laboratory Vienna, Austria; El Alto to Laboratoire de Geochimie et d'Hydrologie Isotopique, Université de Paris-Sud, Orsay, France; Oruro, Quillacas and El Choro to University of Michigan, Department of Earth and Environmental Sciences, USA) [8,9]. To estimate isotopic compositions, methods based on gas-source mass-spectrometry were applied (Oruro, Quillacas and El Choro using Picarro Cavity Ringdown Spectrometer L2120; Laica Cota and El Alto not reported) [3,8].

The isotopic data of surficial water and groundwater used in this study is comprised of data reported in three articles [7,11,12] and new data generated between 2014 and 2015 for this study (Table 1). The latter was analyzed at the Geological Survey of Denmark and Greenland's (GEUS) laboratory, applying the technique described before.

Table 1. Surficial water and groundwater isotopic data. Data from the present study are found in last line.

Reference	Sampling Year	Sampling Sites Reported	Sampling Sites Located	Isotopes Reported	Types of Sampling Sites
Lizarazu *et al.* (1987) [11]	1984–1985	61	25	^{18}O, ^{2}H, ^{3}H, ^{13}C, and ^{14}C	Boreholes, dug wells, springs, rivers, and mines
Swedish Geological AB (1996) [12]	1996	23	0	^{18}O	Boreholes and dug wells
Gitec & Cobodes (2014) [7]	2013	6	6	^{18}O, ^{2}H, ^{3}H and ^{14}C	Boreholes and rivers
Present study	2014–2015	17	17	^{18}O and ^{2}H	Boreholes, dug wells, and rivers

Stable isotopic compositions are reported in δ units as the per mil (‰) deviations with respect to the Vienna Standard Mean Ocean Water (VSMOW). No uncertainties were reported in previous studies, only in the present study the uncertainty is reported, ± 0.15 for ^{18}O and ± 1.51 for ^{2}H.

Tritium compositions are expressed in tritium units (TU) that corresponds to an abundance of 1 ^{3}H per 10^{18} ^{1}H atoms [23]. ^{13}C compositions are reported as the per mil (‰) deviations with respect to the Pee Dee Belemnite standard (PDB). Finally, ^{14}C activity refers the relation $^{14}C/^{12}C$, it is reported as percentage of Modern Carbon (pMC) with respect to the Oxalic Acid II standard [24].

4. Results and Discussion

4.1. Isotopic Compositions in Precipitation

The most intense rainy events occur from December to March (DJFM) [25], during the summer. In this season, precipitation over the region typically occurs when air masses from the Atlantic cross a large part of the continent, the Amazon, and pass over the Andes' Eastern Cordillera. That adiabatic transport promotes progressive reduction of heavy isotopes. Also, the elevation of the Altiplano promotes similar reduction. As a result, an inverse relation between stable isotopes and elevation is observed [8,26]. The rest of the year, with smaller precipitation, the atmospheric moisture source is the Pacific. This source is closer than the Atlantic. Consequently, the isotopic signature of precipitation from the Pacific is heavier. This study adopts the summer precipitation as the onset of the modern recharge process.

As shown in Figure 3a, the more depleted isotopic compositions are registered during DJFM in the selected GNIP stations. Four of them have $\delta^{18}O$ and $\delta^{2}H$ pair records used to obtain the Local Meteoric Water Line (LMWL) by linear regression (Figure 3b). The slopes of the LMWL and the Global Meteoric Water Line (GMWL) are similar. The later, estimated by Craig (1961) [27], follows the line $\delta^{2}H = 8 \times \delta^{18}O + 10$. However, the intercept of the LMWL in the $\delta^{2}H$ axis is higher. This tendency has been observed in precipitation at high altitudes across the continent [22,28]. This deuterium excess likely results from additional moisture promoted by fast evaporation of inland water bodies and movement of vapor in the upper troposphere down to the ground surface, both enriched in deuterium due to kinetic fractionation processes [8].

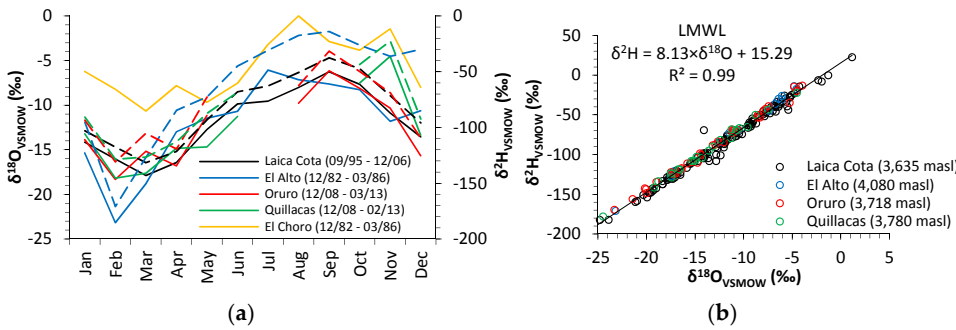

Figure 3. GNIP stations data. (**a**) Average isotopic compositions of precipitation by month ($\delta^{18}O$ in continuous lines and $\delta^{2}H$ in dashed lines. Nonexistent $\delta^{2}H$ records in El Choro) during indicated period (month/year); (**b**) LMWL [9].

Taking into account only the DJFM data, the isotopic relation is adjusted to $\delta^{2}H = 8.09 \times \delta^{18}O + 15.04$, which is comparable to the LMWL. A similar attempt was made for the rest of the months and the resulting equation is $\delta^{2}H = 8.24 \times \delta^{18}O + 16.06$. Consequently, a continuous correlation along the year is observed; the deuterium excess and the slope do not change significantly despite drastic seasonal changes in rainfall intensity. However, the GNIP data correspond to elevations between 3635 masl and 4080 masl (Figure 3b). In comparison to the high peaks of about 5500 masl in the surrounding tributary catchments (Figure 1b), the data exhibit insufficient information to identify signatures of rainfall at higher elevations.

4.2. Isotopic Compositions in Surface Water and Groundwater

Some studies in the Chilean Altiplano established gradients between −0.4‰ to −1.0‰ per 100 m height for $\delta^{18}O$ in precipitation [28,29]. Hence, the most depleted isotopic values in groundwater would represent recharge at higher altitudes. Conversely, water retained in the surface and shallow aquifers are significantly affected by evaporation [10,30]. As a consequence, the most enriched isotopic compositions are expected in samples of the aforementioned sites. Finally, $\delta^{18}O$ data corresponding to DJFM is assumed as the signature for the recharge process, the range between −12.6‰ and −17.5‰, defined by 25th and 75th percentile, respectively.

Isotopic data of surface water and groundwater in the study area and vicinity are scarce and a substantial part of it lacks complementary information like site locations, depths, sampling methods, and analysis procedures. Single $\delta^{18}O$ records are the largest available isotopic data. They are shown in Figure 4 *vs.* electrical conductivity (EC) as salinity parameter. Although just part of this data was located in the study area, most of the groundwater and surface water samples correspond to the range suggested as the typical signature of precipitation in the rainy season, dashed line range in Figure 4. Samples marked with "x" are different from those enclosed in a dashed rectangle. Although both groups correspond to the same place and the same mining activities at the southern limit of the study area. The first one represents groundwater pumped from deeper levels (400 mbs) to facilitate mineral extraction and the second one represents shallow levels where contaminants have been leaked after mineral refinement processes [12].

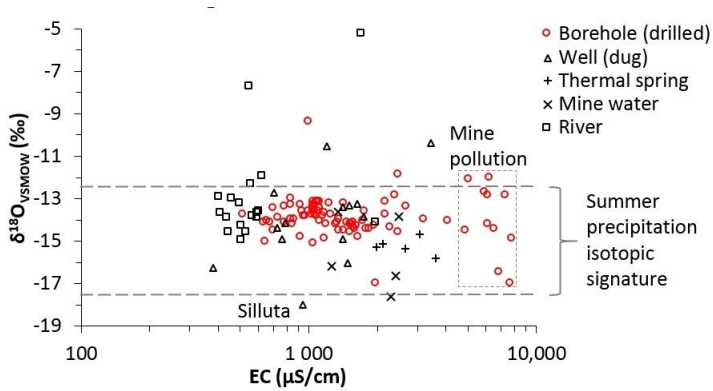

Figure 4. Isotopic data of all kinds in the region of Challapampa. EC (log) *vs.* $\delta^{18}O$. Modified from Gitec & Cobodes (2014), Lizarazu *et al.* (1987) and Swedish Geological AB (1996) [7,11,12].

The sampling sites which were located in the study area are shown in Figure 5. Part of the data presented in Figure 4 is excluded because it lacks location and coordinates, e.g., deep mine waters, dug wells, and thermal springs. The stable isotopic pair records of boreholes describe an evaporation trend line (Figure 5a), whose slope is less steep than that of the LMWL. The scattered point cloud fits with the water circulation conceptual model in the study area, along the arrow in Figure 5b. Summer precipitation over the catchments forms rivers (EC 500 µS/cm) running to the plain and recharging the aquifers. After infiltration, water travels throughout the Quaternary deposits, some flow systems are captured by boreholes in the range of 35–100 m below surface (mbs). The isotopic composition in these boreholes does not change significantly despite their increased salinity (EC 2000 µS/cm) due to mineral dissolution processes. As is shown in the potentiometric surface in Figure 5c, the lowest area is the well-field and some circulation systems flow towards it. Nevertheless, as this feature is based on potentiometric levels in wells and boreholes ranging from the surface until 100 mbs, deeper flows might cross this abstraction area and stream towards Lake Poopo, with NE–SW flow direction.

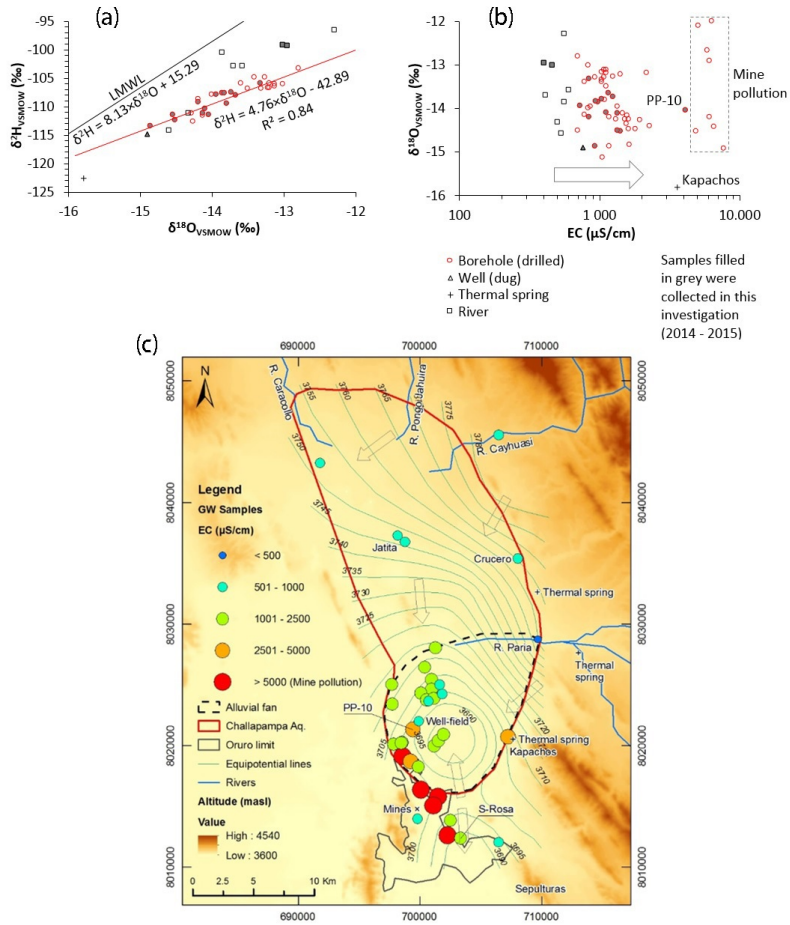

Figure 5. Isotopic data located in the Challapampa aquifer. (**a**) LMWL and the evaporation trend alignment for boreholes (red line); (**b**) EC (log) *vs.* $\delta^{18}O$ scatter plot. The arrow represents the increasing salinity along groundwater flows in the aquifer; (**c**) Location of groundwater samples, EC distribution, and the potentiometric surface. Red circles (shallow samples affected by pollution) and PP-10 (thermal intrusion) might not follow the increasing salinity arrow in (**b**). Modified from Gitec & Cobodes (2014) [7].

The range of $\delta^{18}O$ concentration is very broad in precipitation (Figure 3b); it is narrower taking into account surficial water and shallow groundwater in the study area (Figure 5a); and finally it is even narrower in borehole samples (red circles in Figure 5a). The more enriched values correspond to water affected by evaporation in rivers, shallow wells, and some boreholes where the average groundwater potential is 15 mbs in the alluvial fan. On the other hand, the more depleted values correspond to thermal springs (Kapachos) and deep groundwater samples in mines. Very depleted $\delta^{18}O$ values are also found, in some shallow wells near to Silluta village, 20 km west of the alluvial fan (Figure 1c). The depleted $\delta^{18}O$ values might indicate recharge at higher altitudes and even longer residence times. Glacier ice-cores from the peak of Sajama, 190 km to the east of the study area, preserve depleted $\delta^{18}O$ compositions; values of about −17‰ correspond to the last 11,000 y BP [31]. This isotopic fingerprint also hints at ancient recharge processes, when paleolakes flooded the area. The stable isotopic data of groundwater and rivers were updated in this investigation (Table 2).

Table 2. Isotopic composition of surficial water and groundwater samples collected in this study (2014 to 2015).

Sample	Depth * (mbs)	Type **	EC (μS/cm)	$\delta^{18}O$ (‰)	$\delta^{2}H$ (‰)	^{3}H *** (TU)	^{13}C *** (‰)	^{14}C *** (pMC)
PP-07	48–80	B/WF	979	−13.86	−107.72	1.0	−9.04	72.8
PP-09	38–71	B/WF	1172	−13.67	−108.05	BDL	−9.89	38.1
PP-10	39–84	B/WF	4130	−14.05	−111.46	0.4	−9.47	25.9
PP-11	36–84	B/WF	956	−13.83	−107.72	0.2	−8.63	40.5
PP-14	–	B/WF	1043	−13.80	−109.44	–	–	–
PP-17	22–79	B/WF	1339	−14.13	−111.18	–	–	–
PP-20	–	B/WF	1130	−14.09	−110.43	–	–	–
PP-21	–	B/WF	850	−14.19	−109.21	–	–	–
PP-22	–	B/WF	844	−13.32	−105.84	–	–	–
PP-23	32–97	B/WF	1251	−13.73	−107.47	–	–	–
Sela-2	38–53	B/WF	1357	−14.52	−112.50	0.2	−9.27	30.5
Crucero	–	B	932	−14.86	−113.51	–	–	–
Sta-Rosa	–	B	1432	−14.55	−111.39	2.4	−9.04	79.3
Jatita-I	65	B	760	−14.91	−114.85	–	–	–
Jatita-II	<10	D	734	−13.94	−107.85	–	–	–
Cayhuasi	0	R	460	−13.01	−99.24	9.3	–	–
Paria	0	R	407	−12.95	−99.34	7.4	–	–

Notes: * Obtained from drilling reports [7]; ** B = borehole (deep); WF = well-field; D = dug-well (shallow); R = river; *** Samples collected in 1984 and 1985, reported by Lizarazu *et al.* (1987) [11]. BDL = below detection limit.

The distribution of isotopic compositions over the study area is shown in Figure 6a,b. Some depleted values of $\delta^{18}O$ are located in the middle part of the aquifer, in the villages of Jatita and Crucero, those samples correspond to levels about 40 mbs. A sample collected from a shallow well in Jatita displayed a more enriched composition. The origin of groundwater at 40 mbs in the middle part of the aquifer seems not to be directly related to the infiltration of the rivers Cayhuasi or Pongo Jahuira, whose flows reduce after DJFM period. The origin of water in boreholes located in the alluvial fan has a more evident correlation with the isotopic signature of River Paria. In the southernmost region of the study area, samples of boreholes monitoring mine pollutants expose enriched compositions affected by evaporation. Most of the flow systems circulating from shallow levels until 100 mbs might have been recharged by modern precipitation following the circulation pattern described before.

Most of the boreholes in the well-field have similar characteristics with the exception of PP-10 (Figures 5 and 6), which is more saline and hot. The isotopic signature here is similar to those in the vicinity. Some deeper flows ascending and mixing with shallow and modern groundwater might explain the characteristics found in this borehole.

The distribution of tritium might confirm the regional circulation pattern. Higher values are recorded in river samples, Paria and Cayhuasi. Along the movement of water throughout the sediments, tritium concentrations display decay, diminishing to even nonexistent contents in boreholes at the middle and the distal part of the alluvial fan. However there are exceptions, the composition of a sample taken inside the city limit (Sta-Rosa) suggests a different origin of water for that specific area, not related to the infiltration of River Paria.

The age of groundwater in the study area can be estimated using tritium and radiocarbon concentrations. Tritium in the atmosphere had maximum records originating in the open-air nuclear weapon tests during 1955–1964 [9]. Nevertheless, the presence of the isotope was significantly lower in South America during the same peak-period. Of the five closest GNIP stations, only Laica Cota has tritium records in precipitation for the period 1995–2006. However, there are some gaps in the series. The average composition in that station was estimated to be 4.9 TU [9]. Although surficial water and groundwater samples in the study area were collected about 10 years earlier, it is possible to observe the decay of the isotope along the movement of water, from rivers (7.4 TU in Paria), to distant and deeper outlet points like boreholes where the tritium content is lower than the average in precipitation, as is shown in Figure 7. However, the circulation systems at intermediate levels seem to have residence times longer than the active life of tritium. As a consequence, values below the detection limit (close to zero) are common in boreholes.

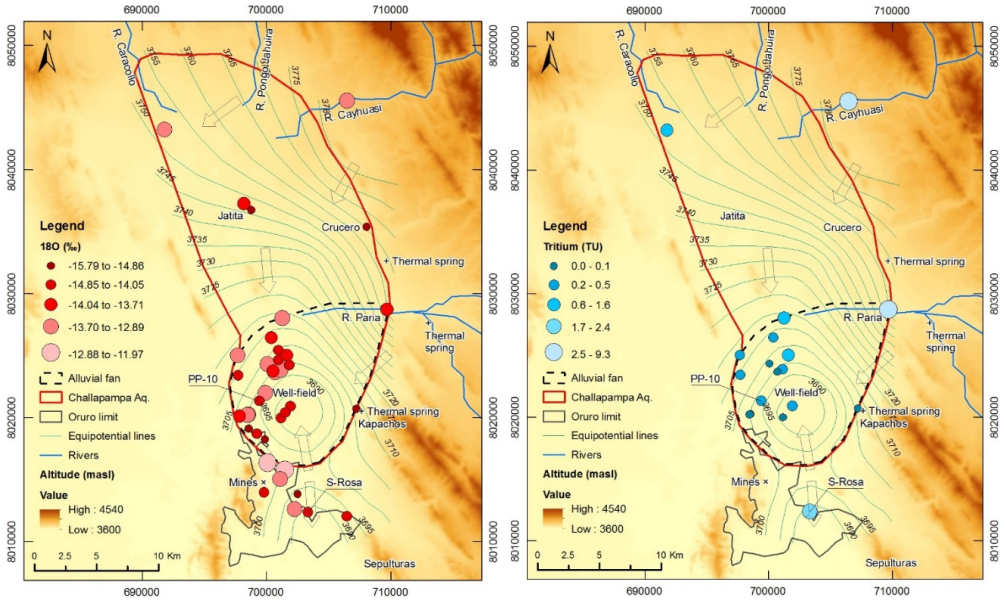

(**a**) (**b**)

Figure 6. Distribution of isotopic data over the study area. (**a**) $\delta^{18}O$ (‰); (**b**) Tritium (TU), compositions in 1984–1985. Arrows mark main groundwater flow directions. Modified from Gitec & Cobodes (2014), and Lizarazu *et al.* (1987) [7,11].

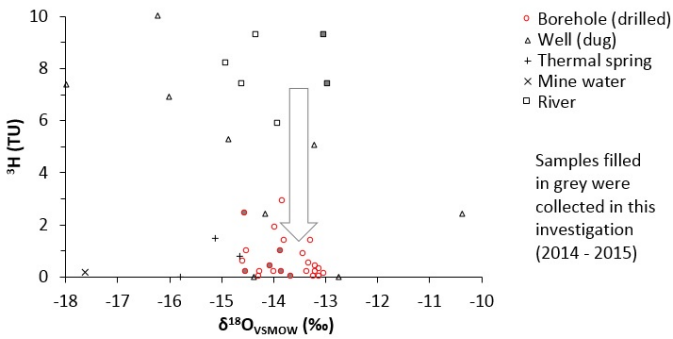

Figure 7. Tritium content in surficial water and groundwater samples between 1984 and 1985. The arrow indicates the decay of ^{3}H along the intermediate circulation flow system. Modified from Lizarazu *et al.* (1987) [11].

Isotopic compositions of ^{13}C and ^{14}C were also used to estimate groundwater ages from modern until 10,000 y BP in the region [7,11]. In the study area, the well-field shows dispersed ages, from modern in PP-07 until 7200 y BP in PP-10 [11]. In the latter borehole, the age agrees with the high salinity, exposing some deep flow patterns, probably ascending through faults. The modern age in the Sta-Rosa borehole, reported by Lizarazu *et al.* (1987) [11], might confirm the water divide in the south of the study area.

The analysis in this study is restricted by the sampling depth, ranging from the surface until about 100 mbs. Deep flow systems and their analyzes were compiled from previous studies [4,11].

The following interpretations are valid for the area of the alluvial fan of River Paria, where most of the sampling sites are located. As is shown in Figure 8, four circulation systems are proposed to distinguish origins, patterns, and characteristics: the first of these systems is on top, inluding local sub-systems from the surface until about 20 mbs. This system also enclose the unsaturated zone. The water here is infiltrated from surface after being retained by clay layers and part of it is evaporated. This process causes shallow groundwater to be saline (EC 1000 µS/cm) and enriched in heavy isotopes. Information about dug wells support this assumption (Figure 4). The residence time in the uppermost part of the groundwater flow system might be short, probably less than a year considering that the ponds and floods disappear some weeks after the rainy season. However, further investigations are needed to know this residence time more accurately. The second system, situated below the latter and reaching abstraction levels (100 mbs) is the intermediate one. A substantial part of the groundwater originates in modern precipitation over the mountains surrounding the aquifer system, transported by rivers and infiltrated in the alluvial fans. The constant abstraction in the well-field may create a depression cone of about 5 km radius around it, which is the main outlet for this system. The EC may vary from 600 to 2000 µS/cm. The $\delta^{18}O$ compositions are similar to those in rivers. The residence times might be some decades, according to the low or even nonexistent tritium compositions. Most of the samples collected in this study belong to this system. The results confirm the isotopic signature range identified in previous studies [4,7,11]. The third system is assumed as a transition between the modern flow system and an older, deeper one. This system might reach depths of 300 mbs or more. Although there are no boreholes pumping from this depth, resistivity and seismic tests suggest that the sediments might still be present at this level [4,12]. The geological units might include both the Quaternary sediments and the bedrock. Also, its salinity and isotopic characteristics might be a result of mixing between the overlying and underlying flows. The fourth and the deepest flow system is the regional one. Just a few samples reported by Lizarazu *et al.* (1987) [11] refer to characteristics at 400 mbs (see Figure 4, samples with "x"). Infiltration at high altitudes or recharge during the last paleolake event might be the origin of water in this level. The most depleted $\delta^{18}O$ values in groundwater correspond to this system, as well as high salinities far away from the pollution fingerprint. This system is likely flowing through the bedrock.

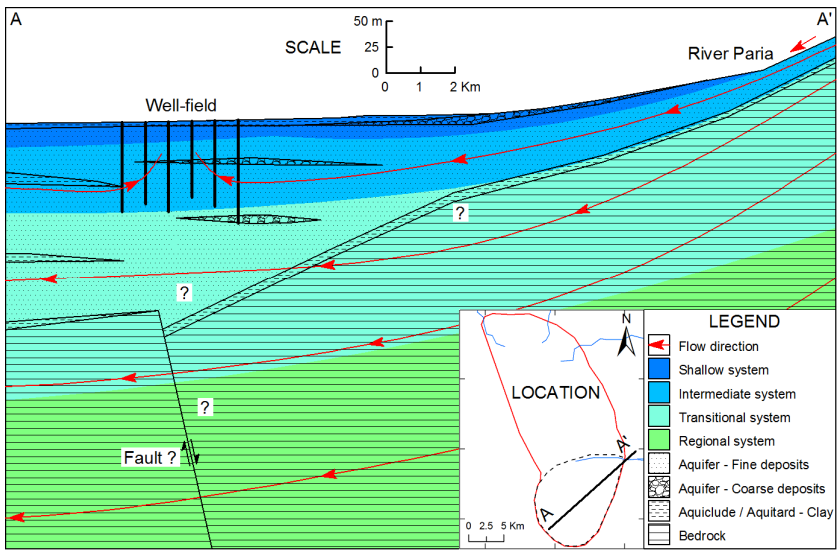

Figure 8. Schematic cross section (A–A') of the proposed four flow systems in the alluvial fan of River Paria.

5. Conclusions

The study of environmental isotopes in the Challapampa aquifer system aids understanding about the circulation patterns in the region. Nevertheless, due to the complexity of the geological settings, scarcity of data, and size of the study area, it is difficult to assess a simplified circulation model combining all criteria extracted from individual isotopic analyzes. The well-field, where the records are more abundant, exposes characteristics of the intermediate flow system. These characteristics are increased salinity, similar values regarding to stable isotopes, and tritium concentrations. Nevertheless, the same area shows some anomalies linked with thermal intrusions and even artesian conditions in at least one borehole (PP-10).

Summer precipitation represents 80% of the annual rainfall over the study area. It is comprised of the most depleted stable isotopic values along the year and this fingerprint remains similar in groundwater samples. The LMWL has a similar slope as the GMWL but with greater deuterium excess, as an effect of the site characteristics, e.g., altitude, amount of precipitation, and continental effect. The linear trend of stable isotopic compositions in groundwater samples expose the effect of evaporation.

The combination of the potentiometric surface, the degree of salinity, and the isotopic compositions reveal the circulation patterns flowing towards the well-field in the central part of the alluvial fan, owed in great part to the constant pumping in the area. Nevertheless, the latter is valid for systems until 100 mbs. The natural discharge zone of regional flow might be located outside the limits of the study area, perhaps in Lake Poopo.

Isotopic compositions in different stages of the hydrologic cycle hint at circulation patterns in the Challapampa aquifer system. This study differentiates four circulation systems. Most of the water exploited for consumption and irrigation is assumed as modern, originating in precipitation, transported by rivers, and recharged into the aquifers at the foothills and alluvial fans. Modern precipitation is the most important recharge source until about 100 mbs. Conversely, deeper levels seem to be recharged by different processes, possibly at higher altitudes or ancient times. Furthermore, it is recommended to extend the sampling of isotopes and hydrochemical parameters in precipitation over the entire elevation range to obtain the local gradient for stable isotopes, which should aid in the process of distinguishing recharge at higher elevations. Such extended sampling would also include groundwater at deeper levels, sampling stable isotopes to differentiate origins and radiocarbon isotopes to enhance the analysis regarding the age of water. Furthermore, some specific characteristics like thermal intrusion, artesian conditions, and migration of mining contaminants can be elucidated with isotopic techniques in the area.

Acknowledgments: The authors thank the following organizations for their help. The study was funded by the Swedish International Development Cooperation Agency (SIDA) and supported by Universidad Mayor de San Andrés in Bolivia and Lund University in Sweden. Part of the data used in this study was provided by the Bolivian State, Ministerio de Medio Ambiente y Agua (MMAyA) and the Project Water and Sustainable Development of the Altiplano coordinated by Ramiro Pillco. The isotopic samples were analyzed at the Geological Survey of Denmark and Greenland (GEUS).

Author Contributions: Gerhard Barmen, Etzar Gómez and Jan-Erik Rosberg conceived and designed this study. Etzar Gómez conducted the field-work; analyzed the data and prepared the initial manuscript. Gerhard Barmen and Jan-Erik Rosberg supervised the field-work, the data analysis and the manuscript preparation. All three authors finalized the research article together.

Conflicts of Interest: The authors declare no conflict of interest.

Abbreviations

The following abbreviations are used in this manuscript:

DJFM	December, January, February, and March
EC	Electrical conductivity
GMWL	Global Meteoric Water Line
GNIP	Global Network for Isotopes in Precipitation

IAEA	International Atomic Energy Agency
LMWL	Local Meteoric Water Line
PDB	Pee Dee Belemnite
PMC	Percentage of modern carbon
SELA	Servicio Local de Acueductos y Alcantarillado Oruro
TDPS	Titicaca, Desaguadero, Poopo, and the salt flats
VSMOW	Vienna Standard Mean Ocean Water

References

1. Subyani, A.M. Use of chloride-mass balance and environmental isotopes for evaluation of groundwater recharge in the alluvial aquifer, Wadi Tharad, western Saudi Arabia. *Environ. Geol.* **2004**, *46*, 741–749. [CrossRef]
2. Ramos, O.E.; Caceres, L.F.; Ormachea, M.R.; Bhattacharya, P.; Quino, I.; Quintanilla, J.; Sracek, O.; Thunvik, R.; Bundschuh, J.; Garcia, M.E. Sources and behavior of arsenic and trace elements in groundwater and surface water in the Poopó Lake Basin, Bolivian Altiplano. *Environ. Earth Sci.* **2011**, *66*, 793–807. [CrossRef]
3. Yin, L.; Hou, G.; Su, X.S.; Wang, D.; Dong, J.; Hao, Y.; Wang, X. Isotopes (δD and $\delta^{18}O$) in precipitation, groundwater and surface water in the Ordos Plateau, China: Implications with respect to groundwater recharge and circulation. *Hydrogeol. J.* **2011**, *19*, 429–443. [CrossRef]
4. Banks, D.; Holden, W.; Aguilar, E.; Mendez, C.; Koller, D.; Andia, Z.; Rodriguez, J.; Saether, O.M.; Torrico, A.; Veneros, R.; *et al.* Contaminant source characterization of the San Jose Mine, Oruro, Bolivia. *Geol. Soc. Lond. Special Publ.* **2002**, *198*, 215–239. [CrossRef]
5. Canaviri, B. Estimación de la Vulnerabilidad Intrínseca a la Contaminación del Aquífero Libre en el Sistema Acuífero de Challapampa Oruro. Bachelor's Thesis, Universidad Técnica de Oruro, Oruro, Bolivia, 2011.
6. D'Elia, M. *Asesoramiento para el Diseño e Implementación de la Red de Monitoreo de Aguas Subterráneas en la Cuenca del Lago Poopó*; Programa de Gestión Sostenible de los Recursos Naturales de la Cuenca del Lago Poopó Convenio No. DCI-ALA/2009/021–614; Gobierno Autónomo Departamental De Oruro: Oruro, Bolivia, 2013. (In Spanish)
7. Gitec-Cobodes, L.C.G. *Poopo Lake Basin Management Plan Formulation*; Programa de gestion sostenible de los recursos naturales de la cuenca del lago Poopo; Gobierno Autónomo Departamental De Oruro: Oruro, Bolivia, 2014.
8. Fiorella, R.P.; Poulsen, C.J.; Pillco, R.; Barnes, J.B.; Tabor, C.R.; Ehlers, T.A. Spatiotemporal variability of modern precipitation $\delta^{18}O$ in the central Andes and implications for paleoclimate and paleoaltimetry estimates. *J. Geophys. Res. Atmos.* **2015**, *120*, 1–27. [CrossRef]
9. Global Network of Isotopes in Precipitation. Available online: http://www.iaea.org/water (accessed on 11 May 2016).
10. Coudrain-Ribstein, A.; Talbi, A.; Loubet, M.; Gallaire, R.; Jusserand, C.; Ramirez, E.; Ledoux, E. Isotopic and chemical composition of groundwater in the Bolivian altiplano, present space evolution records hydrologic conditions since 11,000 Yr. In Proceedings of the Vienna Symposium Mai 1999, Vienna, Austria, 10–14 May 1999.
11. Lizarazu, J.; Aranyossy, J.F.; Orsag, V.; Salazar, J.C. Estudio Isotopico de la cuenca de Oruro-Caracollo (Bolivia). In Proceedings of Symposium of Isotope Techniques in Water Resources Development, Vienna, Austria, 30 March–3 April 1987.
12. Swedish Geological, A.B. *Impacto de la Contaminación Minera e Industrial Sobre agua Subterráneas*; Ministerio de Desarrollo Sostenible y Medio Ambiente, Secretaria Nacional de Mineria: Oruro, Bolivia, 1996. (In Spanish)
13. Coudrain-Ribstein, A.; Pratz, B.; Quintanilla, J.; Zuppi, G.M.; Cahuaya, D. Salinidad del recurso hídrico sobterráneo del Altiplano Central. *Le Bull. de l'Institut Fr. d'études Andin.* **1995**, *24*, 483–493. (In Spanish)
14. Calizaya, A. Water Resources Management Efforts for Best Water Allocation in the Lake Poopo Basin, Bolivia. Ph.D. Thesis, Lund University, Lund, Sweden, 2009.
15. Pillco, R.; Bengtsson, L. Long-term and extreme water level variations of the shallow Lake Poopó, Bolivia. *Hydrol. Sci. J.* **2006**, *51*, 98–114.
16. Carta Geológica de Bolivia. Hoja Oruro, Publicación SGB Serie I-CGB-11. Servicio Geológico de Bolivia. Geobol; Swedish Geological, A.B.: La Paz, Bolivia, 1992.

17. Zapata, R. Modelo Conceptual Hidrogeológico del Sistema Acuífero de un Abanico Aluvial en la Sub-Cuenca del río Poopó: Oruro-Bolivia. Master's Thesis, Universidad Mayor Real y Pontificia de San Francisco Xavier de Chuquisaca, Sucre, Bolivia, 2011.
18. Servicio Local de Acueductos y Alcantarillado de Oruro. Available online: http://selaoruro.gob.bo/ (accessed on 11 May 2016).
19. Fornari, M.; Risacher, F.; Féraud, G. Dating of paleolakes in the central Altiplano of Bolivia. *Palaeogeogr. Palaeoclimatol. Palaeoecol.* **2001**, *172*, 269–282. [CrossRef]
20. Rigsby, C.A.; Bradbury, J.P.; Baker, P.A.; Rollins, S.M.; Warren, M.R. Late Quaternary palaeolakes, rivers, and wetlands on the Bolivian Altiplano and their palaeoclimatic implications. *J. Quat. Sci.* **2005**, *20*, 671–691. [CrossRef]
21. Thompson, L.G.; Mosley-Thompson, E.; Henderson, K.A. Ice-core paleoclimate records in tropical South America since the Last Glacial Maximum. *J. Quat. Sci.* **2000**, *15*, 377–394. [CrossRef]
22. Gonfiantini, R.; Roche, M.A.; Olivry, J.C.; Fontes, J.; Zuppi, G.M. The altitude effect on the isotopic composition of tropical rains. *Chem. Geol.* **2001**, *181*, 147–167. [CrossRef]
23. Seiler, K.P.; Gat, J.R. *Groundwater Recharge from Run-Off, Infiltration and Percolation*; Springer: Berlin, Germany, 2007.
24. Isotope Methods for Dating Old Groundwater. Available online: http://www-pub.iaea.org/books/IAEABooks/8880/Isotope-Methods-for-Dating-Old-Groundwater (accessed on 11 May 2016).
25. Servicio Nacional de Meteorologia e Hidrologia de Bolivia. Available online: http://www.senamhi.gob.bo/ (accessed on 11 May 2016).
26. Gat, J.R. Oxygen and Hydrogen Isotopes in the Hydrologic Cycle. *Annual Rev. Earth Planet. Sci.* **1996**, *24*, 225–262. [CrossRef]
27. Craig, H. Isotopic Variations in Meteoric Waters. *Sci. New Series* **1961**, *133*, 1702–1703. [CrossRef] [PubMed]
28. Aravena, R.; Suzuki, O.; Peña, H.; Pollastri, A.; Fuenzalida, H.; Grilli, A. Isotopic composition and origin of the precipitation in Northern Chile. *Appl. Geochem.* **1999**, *14*, 411–422. [CrossRef]
29. Uribe, J.; Muñoz, J.F.; Gironás, J.; Oyarzún, R.; Aguirre, E.; Aravena, R. Assessing groundwater recharge in an Andean closed basin using isotopic characterization and a rainfall-runoff model: Salar del Huasco basin, Chile. *Hydrogeol. J.* **2015**, 1–17. [CrossRef]
30. Johnson, E.; Yáñez, J.; Ortiz, C.; Muñoz, J. Evaporation from shallow groundwater in closed basins in the Chilean Altiplano. *Hydrol. Sci. J.* **2010**, *55*, 624–635. [CrossRef]
31. Thompson, L.G.; Davis, M.E.; Mosley-Thompson, E.; Sowers, T.A.; Henderson, K.A.; Zagorodnov, V.S.; Lin, P.; Mikhalenko, V.N.; Campen, R.K.; Bolzan, J.F.; *et al.* A 25,000-Year Tropical Climate History from Bolivian Ice Cores. *Science* **1998**, *282*, 1858–1864. [CrossRef] [PubMed]

Paper II

Environmental Earth Sciences (2019) 78:84
https://doi.org/10.1007/s12665-019-8074-x

ORIGINAL ARTICLE

Alluvial aquifer thickness and bedrock structure delineation by electromagnetic methods in the highlands of Bolivia

Etzar Gómez[1,3] · Måns Larsson[2] · Torleif Dahlin[1] · Gerhard Barmen[1] · Jan-Erik Rosberg[1]

Received: 12 July 2017 / Accepted: 14 January 2019 / Published online: 28 January 2019

Abstract
The porous aquifers in the area called Challapampa are the most important groundwater reservoirs that supply drinking water to Oruro city in the highlands of Bolivia. They consist of unconsolidated fluvial–lacustrine deposits, resting on a complex sedimentary bedrock and covered by a thin surficial clay layer. The settings of these geological units and the structures governing the flow patterns have barely been investigated, despite this reservoir having been utilized during the last 50 years. This study applied transient electromagnetic (TEM) soundings and electrical resistivity tomography (ERT) in the middle part of the alluvial fan of River Paria to investigate the thickness of the porous aquifer and detect the relief of the bedrock. Likewise, some results expressed as resistivity models indicate the possible existence of geological structures below the unconsolidated sediments. The average depth of investigation reached in this study is between 200 and 250 m below the surface, for both the applied methods. The geological structures inferred have similar directions as the major faults in the vicinity, from southeast to northwest, which in turn are assumed as part of fractured aquifers underlying the porous aquifers. The geo-electrical techniques were successfully tested in the study area and the resistivity models from TEM complement very well those obtained from ERT. Therefore, extended investigations using the same techniques would help to develop a more complete description of the hydrogeological settings of the aquifer system.

Keywords Transient electromagnetic · Resistivity · Hydrogeology · Bolivia

Introduction

In the semi-arid Bolivian Altiplano, aquifers are the most important source of water, since rivers and lakes have been drying out in the recent years because of the climate change. The aquifer system in the area called Challapampa, close to Oruro city, supplies water for consumption to about 300,000 inhabitants, besides being used for agriculture, mining and industrial purposes. This reservoir requires a management plan to assure its sustainability in the future. However, important characteristics like delimitation, geometry, classification of aquifers, estimation of storage volumes and recharge processes are not fully understood yet. To provide the information and data required to build up a complete description of the aquifer system, long-term hydrogeological investigations are needed. Geophysical methods have proven to be efficient and inexpensive tools in obtaining fast information about the distribution of physical properties in the subsurface. They also have proven to be efficient ways to investigate features such as saline water interface, depth and thickness of geological units and depth to water table (Auken

✉ Etzar Gómez
etzar.gomez@tg.lth.se

Måns Larsson
mablarsson@gmail.com

Torleif Dahlin
torleif.dahlin@tg.lth.se

Gerhard Barmen
gerhard.barmen@tg.lth.se

Jan-Erik Rosberg
jan-erik.rosberg@tg.lth.se

[1] Engineering Geology, Lund University, Box 118, 221 00 Lund, Sweden

[2] Department of Geology, Lund University, Box 118, 221 00 Lund, Sweden

[3] Institute of Hydraulic and Hydrology, San Andres Major University, La Paz, Bolivia

et al. 2003; Corriols et al. 2009; Gonzales et al. 2016; Guérin et al. 2001; Nabighian 1991).

There are just a few geophysical studies conducted in the Altiplano. Guérin et al. (2001) performed 100 time-domain electromagnetic (EM) soundings to identify saline groundwater in sediments in a big area in the Central Altiplano (1750 km^2). That study mentions the existence of large shallow conductive layers and brines limiting a good deep resolution using direct current (DC) methods. Other studies in different environments, demonstrated the good correlation between EM and DC methods (Boiero et al. 2010; Metwaly et al. 2010). The present study aims to combine TEM and ERT methods to describe an area where the water is supposed to be relatively fresh (low salinity), despite the proximity of some hot springs to the east with more saline water.

Information obtained from technical reports (not published) including DC measurements and drilling protocols in sites nearby the present study area, show the characteristics of the first 100 m below the soil surface, at this depth the bottom of the porous aquifers was not reached yet. This study aims to investigate the thickness of the unconsolidated sediments and structural features below those sediments, in the central and southeastern parts of the alluvial fan of River Paria (Fig. 1). The TEM method, the most relevant in this study, was selected because its proven good resolution in depth and its simplicity to arrange the equipment in the field. The results of the study intend to improve the knowledge about the geometry of the Challamapa aquifer system by clarifying the shape of the bedrock, estimating the thickness of the alluvial sediments and for evaluating the applicability of electromagnetic methods to map the entire aquifer in the future.

Study area

The Challapampa aquifer system belongs to the Poopo enclosed basin, located to the west side of the Cordillera Oriental (eastern mountain range of the Andes), where the highest peaks reach 4600 m above sea level (masl) and the

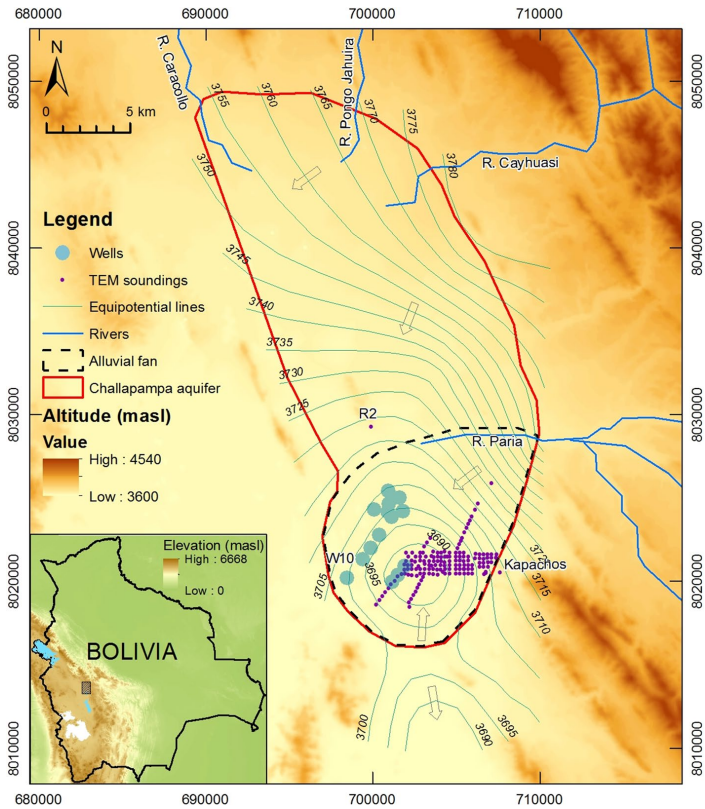

Fig. 1 Location of the Challapampa aquifer system in the Central Bolivian Altiplano. Part of it has been investigated applying TEM soundings. Arrows refer to the regional flow in the porous aquifers, within the first 100–160 m below the soil surface. Modified from GITEC and COBODES (2014); Swedish Geological (1996)

lowest and planar land is at 3700 masl (Fig. 1). In the Cordillera Oriental, the direction of the ridges is from northwest to southeast, which also defines the surrounding landscape and the bedrock relief below the porous aquifers.

The climate in the area is semi-arid, with scarce to non-existing vegetation. The average temperature is about 10 °C. Regarding precipitation, there is a big difference between summer and winter; about 80% of the mean annual 350 mm occurs from December to March (summer). In addition, the annual potential evaporation was estimated to be 1800 mm (SENAMHI 2015), evidencing the aridity of the region. During summer, intense precipitations create floods in the plateau, but the water is quickly evaporated leaving salt in the clayey soils. The land around the study area is mainly used for small-scale agriculture during the rainy season. Sporadic crops can be seen during the rest of the year in sites nearby the few wells used for irrigation in the vicinity. The alluvial fan of River Paria hosts a well field which abstracts water continuously, at a rate of about 300 l/s (SELA 2017), to supply Oruro. This situation has been affecting the piezometric levels in the irrigation wells and created social conflicts due to the limited access to water.

The Challapampa aquifer system is a generic name to refer all the geological formations yielding water in the region. The porous aquifers in the first ~ 100 m below the surface (mbs) are the main groundwater reservoirs near Oruro, characterized by the variety of the existing geological formations and the complexity of settings. The geological formations in the region can be divided into consolidated (rock) and unconsolidated (sediments). Among the first unit of rocks, sedimentary and metamorphic types are the most common in the bedrock (in purple in Fig. 2); also, igneous rocks are present in some volcanic intrusions (in orange in Fig. 2). The unconsolidated unit comprises sediments originated by erosional and depositional processes (in yellow in Fig. 2).

The consolidated rocks around and beneath the study area have folds and faults with northwest–southeast direction. Three Silurian formations have been identified in the bedrock and mountains (in purple in Fig. 2) where sandstones and siltstones are common. These formations are, from the oldest to the youngest, Llallagua, Uncia and Catavi (Suarez Soruco 2000). The Uncia and Catavi formations are exposed nearby the study site and according to the geological information, Uncia's bedrock underlies the Quaternary sediments. The bedrock might be comprised of green shales with beds of green sandstones and siltstones (GEOBOL and Swedish Geological 1992). Banks et al. (2002) include in their study a bedrock contour map (red lines in Fig. 2), based on drilling logs and geophysical tests like seismic refraction and vertical electrical soundings (VES), which in turn correspond to other previous studies not found in the present investigation. The deepest contact between sediments and bedrock might be located at 3540 masl (~ 160 mbs). Volcanic igneous rocks from the Tertiary are also part of the consolidated geological units; they are the so-called Oruro complex and Escalera volcanics. The first one, close to Oruro city, holds valuable minerals like silver, lead and others (Patureau 2007; Ramos et al. 2011). The second one, to the east of the study area, comprises rhyodacitic and porphyritic lavas (GEOBOL and Swedish Geological 1992). This intrusion might have a strong influence on the regional geothermal activity.

When it comes to the unconsolidated geological units, alluvial Quaternary sediments are the most extensive covering the relief of the bedrock and shaping the flat terrains. The grains in these deposits are mainly comprised of quartz and other silicates. They are largely variable in terms of grain size as well; pebbles, gravels, sands, silts and clays are all chaotically arranged because of the overlapping depositional processes. The well-rounded shape of pebbles and gravels lead to infer that they were transported long distances from the surrounding mountains by strong fluvial and glacial events. The finest sediments might correspond to lacustrine depositions, such is the case of the surficial clay layer (Rigsby et al. 2005). Figure 3 shows an example of how these sediments are arranged in a pit, in the first ~ 12 mbs. The thickness of the unconsolidated sediments of the porous aquifer may be from tenths to hundreds of meters, and the thickness of the surficial clay layer may be from tenths of centimeters to a couple of meters.

The most productive aquifers are the fluvial–lacustrine sediments of diverse thicknesses and settings. A few drilling logs, VES and debris excavations constitute the main sources of stratigraphic information in the study area, where the high vertical and lateral variability between different types of sediments is standing out, as shown in Fig. 3.

Hydrogeology

The Challapampa aquifer system has been studied at some drilling sites to obtain information to extract as much water as possible. However, most of that information was never properly saved and reported, and just a few investigations are available, e.g., Larsson (2016). The rest is partially or completely lost. In the study area, the geometry of the aquifer system was proposed by Banks et al. (2002) based on VES, seismic refraction and drilling logs (Dames & Moore Norge 2000; SCIDE et al. 1996). Unfortunately, just part of the information about stratigraphy is available. There are some drilling protocols around the well field area describing the stratigraphy of the first 100 mbs. These descriptions refer to the content of gravel, sand and clay at different levels. The stratigraphy obtained from those drilling reports is punctual and representative of few meters around the boreholes and not applicable to

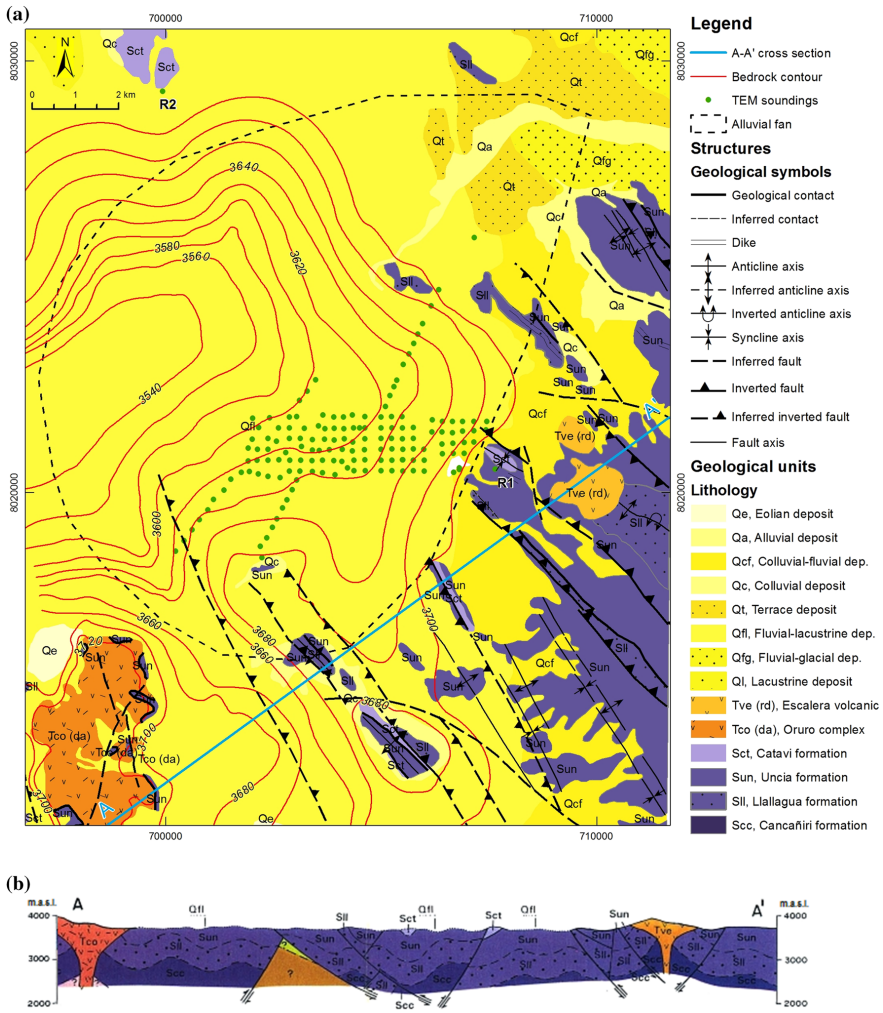

Fig. 2 **a** Geological map including bedrock contours and TEM soundings. **b** A–A′ cross-section. Quaternary sediments are not shown clearly due to the scale; the thickness of these units might be of a couple of meters in this section. Modified from Banks et al. (2002); GEOBOL and Swedish Geological (1992)

the rest of the alluvial fan, because of the high lateral and vertical variability in the arrangement of sediments. When it comes to the hydraulic conductivity, this variability ranges from 1.2E−5 to 5.8E−4 m/s in the unconsolidated sediments (Banks et al. 2002). Going deeper, the top, fractured and weathered part of the bedrock has values around $K = 1.0\text{E}{-5}$ m/s and for the consolidated sedimentary rock, it is about $K = 3.0\text{E}{-8}$ m/s (Dames & Moore Norge 2000).

According to the regional groundwater gradient (equipotential lines in Fig. 1), the flow seems to run from northeast to southwest in the porous aquifer. Precipitation in the mountains forms streams and rivers running towards the plane, which recharge the aquifers and then flows towards

Fig. 3 Excavation exposing about 12 mbs of sediments in the aquifer. This porous aquifer comprises gravel, sand and clay in different proportions according to the site and depth. However, clayey lenses are also interbedded in this geological package

the lowest site of the region, which might be the Lake Poopo, about 20 km south of the study area. However, the annual volumes of water extracted from the well field, about 9.5 million m^3 in 2016 (SELA 2017), have changed the natural flow direction and now it goes towards the central part of the alluvial fan, creating a cone of depression with a radius of influence of about 5 km around the well field (Banks et al. 2002).

In addition, hydrochemical and isotopic characteristics were used to propose four flow systems in the middle of the alluvial fan (Gómez et al. 2016), which are summarized in Table 1.

Geothermal activity also exists in the aquifer system, specifically to the east of the alluvial fan, in the site called Kapachos (Fig. 1). In this place, the water coming out from springs is hot and rich in total dissolved solids (high salinity), and the average temperature in the wells extracting from the porous aquifer is 15 °C and in the hot springs is ~ 50 °C. Salinity in terms of electrical conductivity (EC) in the wells extracting from the porous aquifers averages 1.0 mS/cm and in the hot springs is ~ 3.6 mS/cm. There are also boreholes, further away the present study site with thermal influence. For instance, in W10 in the wellfield (Fig. 1), the temperature is 30 °C and EC is 3.5 mS/cm. Flow paths and processes controlling the occurrence of the thermal water in the region remain unknown subjects out of the scope of this study.

Theory and methods

TEM is a point-based geophysical prospecting technique where a current flowing in a transmitter antenna generates a primary electromagnetic (EM) field. When that current is cut off, that primary EM field induces eddy currents flowing through the ground. Those eddy currents generate a secondary magnetic field detected by a receiver antenna. The receiver acquires time-dependent decaying voltage signals. During processing, those signals are transformed into electrical resistivity and vary as a function of the type of materials and how they are distributed in the ground (Christiansen et al. 2009; Reynolds 2011).

Water content and the type of water filling voids in the geological formations also determine the resistivity obtained by EM methods. Therefore, it is expected to find a distinction in terms of resistivity between saturated sediments

Table 1 Summary of flow systems and hydrogeological parameters in the Challapampa aquifer system (Banks et al. 2002; Dames & Moore Norge 2000; Gómez et al. 2016; Lizarazu et al. 1987)

Flow system depth (m)	Stratigraphic approach	Scheme	Hydraulic conductivity K (m/s)	Origin of water
0–20	Unconsolidated sediments	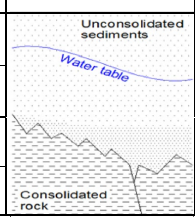	1.2E−5 to 5.8E−4	Direct infiltration
20–100	Unconsolidated sediments		1.2E−5 to 5.8E−4	Lateral recharge
100–400	Transition zone		1.0E−05*	Lateral recharge
> 400	Consolidated rock		3.0E−08	Unknown

*K in the transition zone is similar to that in the unconsolidated sediments, because the tests to obtain that value were conducted in the fractured top part of the rock, according to Dames & Moore Norge (2000)

(main aquifers) and the bedrock (see Table 1) to establish the thickness of the saturated alluvial sediments.

The equipment used for the TEM measurements was an ABEM WalkTEM, connected to two batteries of 12 V transmitting dual moment electrical pulses: about 18 A during the high moment (HM) and about 2 A during the low moment (LM). An offset array was used during the tests, where a transmitter loop (50 × 50 m cable AWG #12) is placed next to the equipment. In the centre of the transmitter, the RC-5 receiver (0.5 × 0.5 m) is placed and the RC-200 receiver (10 × 10 m) is 50 m offset from the centre of the transmitter. Although both receivers were able to register both low and high moments, the RC-5 was used for measuring LM for better shallow resolution, and the RC-200 was used for measuring HM for better depth resolution.

Raw TEM data contains sorted information of HM, LM and noise in specific channels for both receivers. Before the inversion, HM channels corresponding to RC-5 and LM corresponding to RC-200 were disabled. Thus, the shallow part of the models was resolved with the RC-5 LM, and the deepest part with the RC-200 HM. Typical data curves, combining LM and HM, need to be trimmed in some specific parts like before intersecting with the noise curves, at the begging of HM and at the end of LM, where they are not overlapping each other within an acceptable displacement defined by error bars, and at any sudden fluctuation out of the shift of the curve.

After conducting measurements and conditioning the TEM data, the next step is to find a model that might reproduce the obtained data and be representative of the resistivity distribution in the test site. The process to find that model is called inverse numerical modeling, and for TEM it is based on curve matching aided by mathematical relationships and algorithms to solve an inverse scattering problem (Nabighian 1991). Data residual is an indicator of how small the differences are between the measured and the modeled data after a curve matching process. Two types of models are used to match the data curves; a layered model, where mean resistivity values correspond to a few layers, and a smooth model where gradual transitions in resistivity correspond to a fixed number of layers increasing in thickness by depth (Christiansen et al. 2009). The limit at which the resistivity structure of a model is reliable is the depth of investigation (DOI), below that limit the geological interpretations might not be true (Christiansen and Auken 2012). Likewise, the method has a minimum depth of resolution depending on the earliest acquisition times and shallow resistivity, which means that the top part of subsoil cannot be resolved with TEM (Spies 1989).

The inverse numerical modeling requires a lot of computing capacity for TEM, so accurate electronic components are also needed to get signals from a wide dynamic range. These issues became achievable during the last decades, making this technique relatively young in groundwater mapping applications (Christiansen et al. 2009). The TEM data were processed with SPIA (Aarhus GeoSoftware 2017a), which runs one-dimensional inversions of individual soundings. Finally, the creation of maps and cross-sections based on inverted TEM data was done with Aarhus Workbench (Aarhus GeoSoftware 2017b), which carry out interpolations with the closest one-dimensional models by the Kriging method.

Resistivity, as a physical property of geological formations was also evaluated with the ERT technique. In principle, the resistivity distribution in the ground corresponding to the same site from TEM and ERT is expected to be similar, although each method has its own characteristics making them sensitive to external factors (3-D effects, DOI, high conductive structures and others). For this study, resistivity obtained from TEM and ERT is assumed equally valid. A thorough analysis of the differences between both techniques is out of the limits of this study. Complementary ERT measurements were performed to obtain two-dimensional resistivity profiles. This technique is based on the DC methods in which the apparent resistivity of the subsoil is estimated by injecting electrical currents through a pair of electrodes and measuring the potential difference between another pair of electrodes. The geometry and type of arrangement of the electrodes determine the measured value of the apparent resistivity, as well as the intensity of current injected during the tests. Modern multi-electrode systems and automatized acquisition systems improved the efficiency of this technique (Dahlin 2001; Dahlin and Zhou 2006). The ERT measurements were conducted using two ABEM Terrameter LS equipment, each one together with four cables of 21 takeouts and stainless steel electrodes and connectors. The type of array selected for the measurements was multiple gradient due to its high speed data acquisition, good signal-to-noise ratio and high data density (Dahlin and Zhou 2006). The roll-along technique was used to reach distances of 2400 and 2000 m to the north and to the south, respectively. Likewise, the current injected was 500 and 200 mA in the northern and southern profiles. Similarly to the TEM data, the ERT data need to be processed and inverted. The process consists of minimizing the difference between the pseudo-section (apparent resistivity from the measurements) and the resultant resistivity from a synthetic model by refining this later in each iteration round. The final and refined synthetic model is assumed as the most likely representation of the resistivity distribution in the ground (Dahlin 2001; Loke et al. 2003). The software used to invert the ERT data in this study was Aarhus Workbench (Aarhus GeoSoftware 2017b), 2-D inversions were selected applying the L1-norm (robust constrain inversion), STD 1.3 for lateral constrain and STD 2.0 for vertical constrain to obtain the resistivity models.

Results and interpretations

The TEM data include 145 soundings, conducted from May to July 2016 in the study area. Those tests were distributed in a rectangular grid (about 6 km × 1.5 km) with ~ 250 m separation between soundings. Not all of them were uniformly separated, because potential noise sources like power lines and houses were avoided. In addition, a number of soundings are aligned in two cross-sections, one of them overlapping both ERT profiles (See Fig. 4), which were conducted in March 2015.

The majority of the TEM soundings were conducted in the flat land, where sediments overlie the bedrock. In addition, two single TEM tests were conducted close to the bedrock outcrops to get the distinctive resistivity of those rocks. Figure 5 shows models corresponding to the

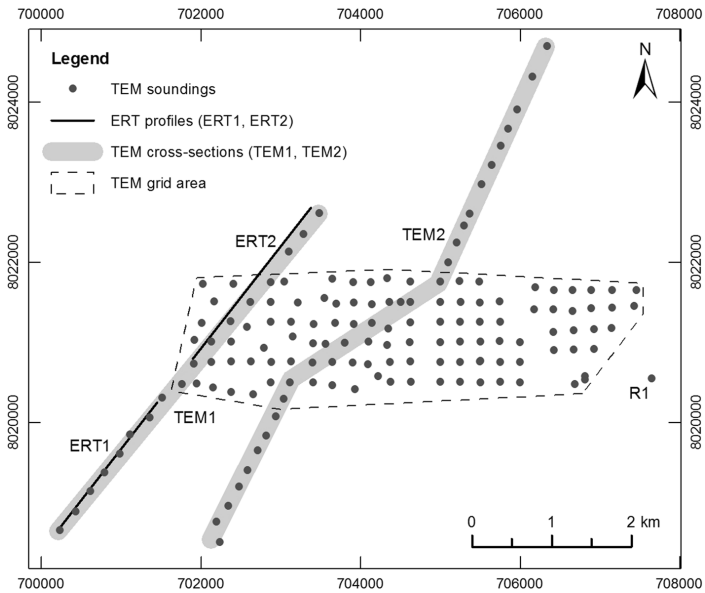

Fig. 4 Distribution of TEM and ERT measurements

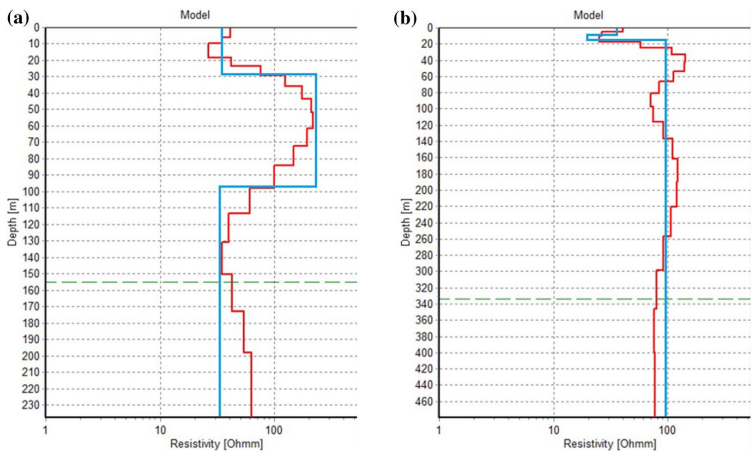

Fig. 5 TEM control soundings. Layered models in blue, smooth models in red. DOI in green dashed lines. **a** R1. Located close to the grid (see Fig. 4). **b** R2. Located up north of the study area (see Figs. 1, 2). R1 models show increasing resistivity below 29 m (bedrock); however, it decreases again below 97 m. However, it decreases to below 97 m. A more saline water flow or a different type of material at that level might be possible explanations. R2 models show a relatively constant high resistivity below 20 m

consolidated rock where values ≥ 100 Ω-m might be the characteristic of this type of geological unit.

The TEM soundings in the grid and nearby were similarly modeled by single one-dimensional inversions, which later were interpolated using the Kriging method to obtain horizontal resistivity maps and resistivity cross-sections. During the inversion process, a few soundings reached a DOI of 800 m which are assumed as outliers, while most of the soundings reached a depth between 100 and 400 m (see Fig. 6). Consequently, resistivity maps showed more blanks as they progress in depth (see Fig. 7).

A progressive resistivity visualization by depth is shown in Fig. 7. At the top slice, the map of resistivity distribution shows two distinctive parts; to the west, values about 30 Ω-m suggest dry sediments, although in the top 20 m from the surface, clay is more abundant, but the water content was small, because the tests were conducted from May to July (dry season). To the east, values between 5 and 10 Ω-m are in concordance with the presence of thermal springs and

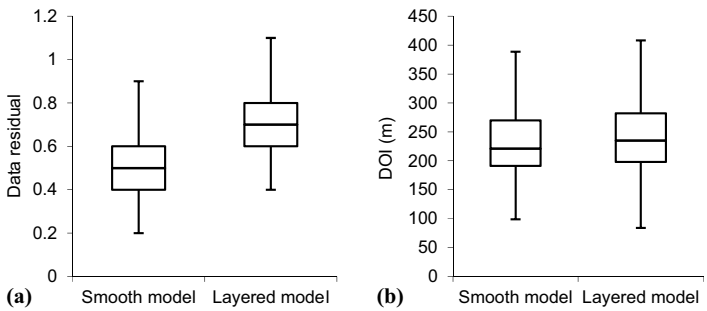

Fig. 6 Boxplots of **a** data residual and **b** DOI, for smooth and layered models corresponding to TEM data. Values in the boxplot represent the minimum, the first quantile, the median, the third quantile and the maximum. Soundings with data residual greater than 1 were removed. Most of the smooth models have smaller data residual than theirs correspondent layered models

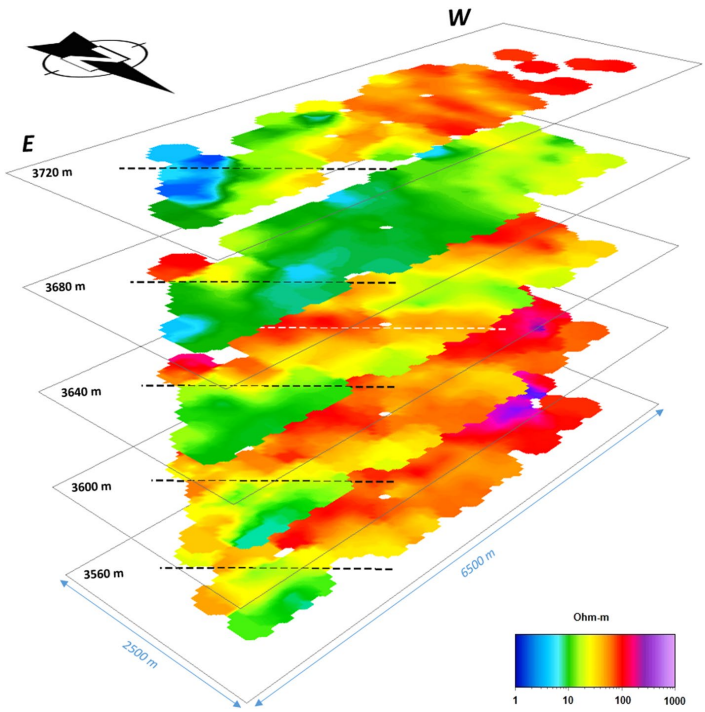

Fig. 7 Mean horizontal resistivity maps by depth (40 m separation), based on smooth models. Dashed lines marked in black indicate a trend of low values corresponding to the presence of saline water in a geological structure, and dashed line marked in white (slice 3640 m) indicate a bedrock fold, part of a complex bedrock relief

saline water disposed in this area. The next resistivity slice, at 3680 masl, is the most homogenous one, with values around 10 Ω-m, interpreted as fully saturated sediments. In addition, the most eastern part still exposes lower values linked with the hot springs. The next slice, at 3640 masl, starts showing higher values, which might indicate the relief of the bedrock exposing folds with southeast–northwest direction (white dashed line). For the rest of the slices below 3600 m, resistivity values remain almost constant, assumed as an indication of the DOI for most of the soundings not reaching these levels. Resistivity values ≥ 100 Ω-m in the western and central part of the grid, are characteristic of consolidated rock in this area. However, the most eastern part still shows lower values, suggesting in turn, the presence of ion-rich water. This trend is repeated in all the slices (black dashed line) which might be an indication of a geological structure, most likely a fault, where saline water is saturating the openings. Major faults in the region have the same direction, which lead to consider a possible connection.

The resistivity sections from the ERT tests are shown in Fig. 8. Profiles 1 and 2 (ERT1 and ERT2) show a thin surficial layer of a couple of meters with values around 80 Ω-m, this might indicate unsaturated sediments on top. Underlying the latter, lower values of around 20 Ω-m might indicate saturated sediments with a thickness varying from tens to hundreds of meters, following the relief of the bedrock. The bedrock has higher resistivity values ≥ 100 Ω-m. This interpretation is similar to those extracted from TEM results. However, ERT1 and ERT2 expose more detailed features, especially within the unconsolidated unit, because this technique generates a larger density of data for the tested profile in comparison to the TEM interpolations. For example, lenses of lower resistivity (~ 10 Ω-m), might indicate high clay content as it was seen in some pits in the area (Fig. 3).

The bedrock in ERT2 seems to sink into a depression to the northeast of the profile. To compare the resistivity distributions obtained from the ERT profiles, interpolations of TEM soundings are reported as cross-sections (TEM1 and TEM2). Figure 8 also shows two resistivity cross-sections based on smooth models and interpolated with the Kriging method, where it is possible to observe the uneven contact between basement rock and sediments. These cross-sections are perpendicular to the possible lengthening of some geological structures. The cross-section TEM1 overlaps the profiles ERT1 and ERT2 in the Fig. 8.

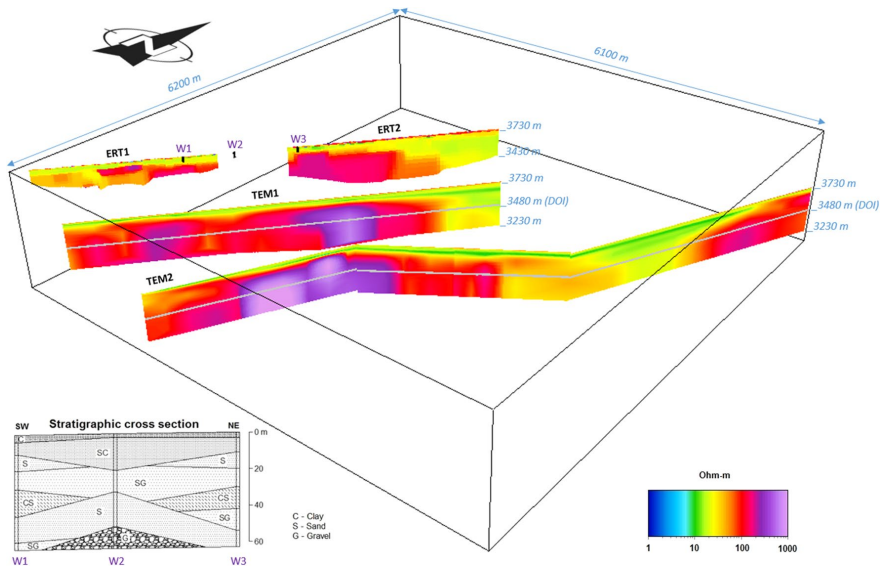

Fig. 8 3D image of resistivity sections from ERT and TEM. Profiles ERT1 and ERT2 are shown above TEM1 just for visualization purposes (ERT1, ERT2, TEM1 and wells W1, W2, W3 are located in the same line). ERT1 and ERT2 have different vertical resolution (DOI) because different electrode separations were used (10 and 20 m for ERT1 and ERT2, respectively). Stratigraphic cross-sections from drilling protocols describe the first 60 m corresponding to the unconsolidated sediments. The DOI for TEM1 and TEM2 is indicated as lines 250 m below the surface, although the resolution of both profiles reaches deeper levels because of the interpolation of the deepest soundings

The same resistive layer on top indicated in ERT1 and ERT2, is also shown in TEM1 and TEM2 as a thin layer. Values about 50 Ω-m might correspond to the surficial unsaturated sediments (as seen in Fig. 3). Just a few meters below the latter, the resistivity decreases to about 10 Ω-m, which might be an indication of saturated sediments. The thickness of these sediments varies according to the bedrock relief, from few meters to about 100 m. In the southwesternmost part of TEM2, the layer of saturated sediments is just a couple of meters, because the Silurian bedrock is outcropping nearby (see Fig. 2). Both TEM cross-sections show distinctive zones of high resistivity (≥ 500 Ω-m in purple), this feature might be an indication of consolidated bedrock with small to non-existent porosity and therefore low water storage. The big purple zones in TEM1 and TEM2 might correspond to the same structure, probably a buried ridge, which has similar direction (northwest–southeast) to the surficial outcrops, ridges and mountains in the region.

The settings and distribution of sediments (gravel, sand and clay) showed in the stratigraphic cross-section of Fig. 8 are difficult to distinguish just looking at the resistivity distribution in cross-sections ERT1, ERT2 and TEM1. The factors impeding a clear distinction might be the scale of the resistivity models and most important, the porosity and saturation degree of the sedimentary package, which makes the apparent resistivity being in the same range despite the difference in grain size distribution. Only the top clay layer differentiates itself from the rest of the unconsolidated materials due to its dryness.

Banks et al. (2002) reported the contact between sediments and bedrock located at 3580 masl in the northeast part of TEM1. In this cross-section, the resistivity corresponding to saturated sediments is still present even at 3300 m. Similarly, in a notorious part of TEM2, low resistivity might suggest the existence of deep valleys filled with sediments containing water. However, these hypothetical deep features do not coincide with the bedrock contour map (Banks et al. 2002), nor they do appear in the regional geological cross-section (Fig. 2b). The answer might be found in some structures and faults of the consolidated hard rock with southeast–northwest direction, which probably continue even below the unconsolidated sediments. Figure 9 shows the resistivity at 3650 m where the aligned distribution of low values coincides with the direction of two faults located to the southeast of the study area.

Discussion

The shallow resistivity to the east of the grid (Fig. 7a), about 5 Ω-m, is influenced by the high salinity of water coming out from the hot springs (EC ~ 3.6 mS/cm). A similar type of water might be present in the inferred faults (Fig. 9) and around them as well, playing a key role when it comes to determining the characteristic resistivity at different levels

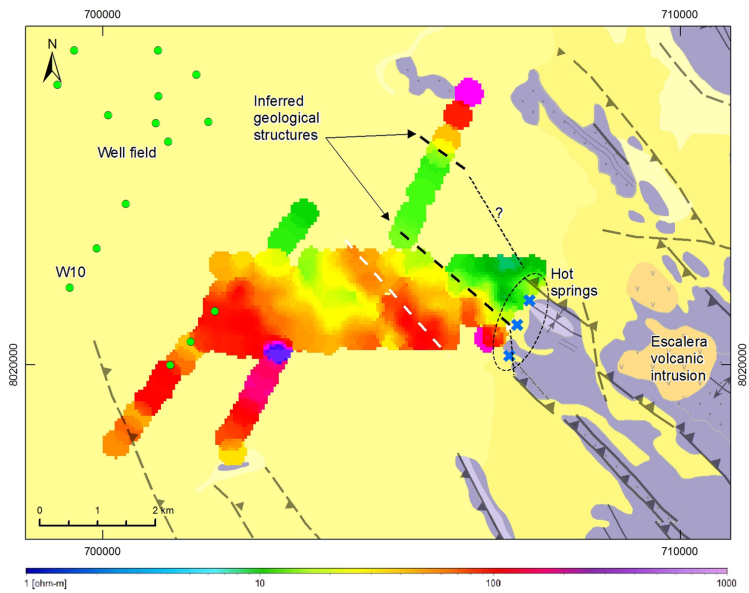

Fig. 9 Resistivity map at 3650 masl (about 70 mbs) from TEM soundings. Transparent geological map as the background (same as Fig. 2). The direction of the geological structures exposed in this map, from southeast to northwest, coincides with the alignment of the surficial ridges and faults indicated in the geological map. Hot springs are indicated with x close to the faults. Modified from GEOBOL and Swedish Geological (1992)

in the study area. The closeness of the Escalera volcanic intrusion might lead to think that this geological formation is contributing to the salinity enrichment and temperature rise of the groundwater especially in the faults. The process of dissolution and mixing of waters might happen further away from the limits of the investigation area or perhaps at greater depths. The geothermal sources in the region might be even more complex. An example of the last is the well W10 (Fig. 9), where the total penetration is 98 m, still within the porous aquifer. Its screen (from 65 to 85 mbs) seems to catch an ascending thermal flow, because the well presents artesian conditions and high salinity (3.5 mS/cm). Although the closest fault to W10 (left side in Fig. 9) does neither seem to be in contact with the Escalera volcanic intrusion nor with the Oruro complex, but an unknown geological formation indicated in Fig. 2b (brown color) might be the geothermal source.

The electromagnetic surveys in the study area aim to acquire characteristics of the subsurface at different depths expressed as resistivity; this feature is strongly influenced by the salinity of water stored in the voids. The average EC in the porous aquifer is 1.0 mS/cm (Gómez et al. 2016) and the resistivity of the unconsolidated and saturated sediments vary from 10 to 20 Ω-m, according to Fig. 7. In those parts where the groundwater is influenced by the geothermal activity, salinity increases (until 3.6 mS/cm) and therefore resistivity decreases (5 Ω-m) as it is observed around the hot springs (first slice of Fig. 7). The deeper the geophysical investigations reach, the lesser is the water content expected in the bedrock, as also indicated by the decreasing hydraulic conductivity with depth (Table 1). Low resistivity values of ~ 20 Ω-m are present at the bottom of the ERT2 profile and at the DOI mark of the cross-sections TEM1 and TEM2 (see Fig. 8), perhaps as indications of the presence of thermal and saline water in the inferred structures. The trend of the resistivity distribution coincides with the direction of faults projected below the study area.

Despite the influence of saline water, especially to the east of the TEM grid, the rest of the study area was surveyed consistently, distinguishing saturated alluvial sediments from the bedrock through their resistivity. The thickness of the sediments varies from a couple of meters (to the north and south ends of the TEM2 in Fig. 8) to about 80 m in the centre of the grid. Low resistivity values are found at deeper levels as well, however, they might be associated with the influence of saline water, as it was explained before. The slope of the bedrock, indicated by Banks et al. (2002), as an even depression from east to west in the grid area (see Fig. 2), seems to be more complex since there are indications of buried folds appearing at 40–80 mbs (see Fig. 10). These folds have the same direction as the rest of the structures in the subsoil, from southeast to northwest. Therefore, a detailed resolution of the bedrock relief was achieved with the geo-electrical methods used in this study. These methods can be used extensively to improve the understanding of the thickness of the sediments in the rest of the aquifer system.

Conclusions

Geophysical investigations applying transient electromagnetic soundings (TEM) and electrical resistivity tomography (ERT) methods in the area of the Challapampa aquifer system, made it possible to generate new information exposing geological structures like faults and buried folds, which were not previously identified. The findings of this study might

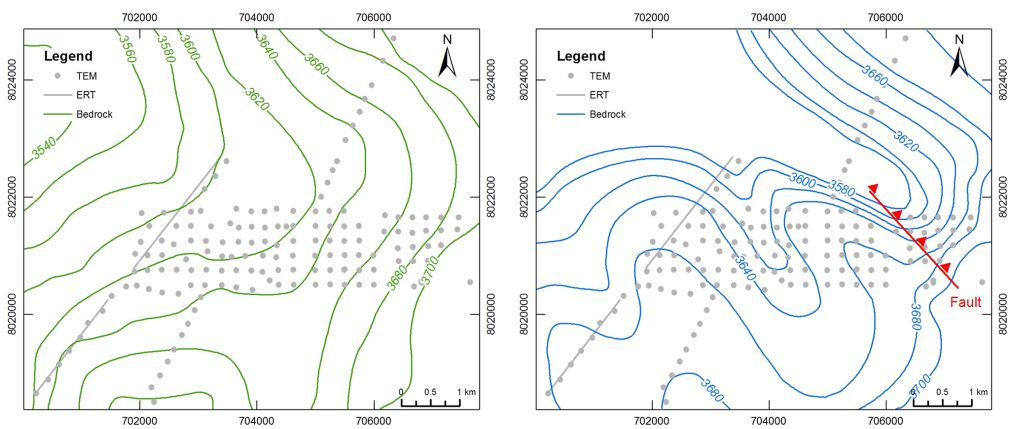

Fig. 10 Contour bedrock map from previous studies (Banks et al. 2002) to the left and inferred from geo-electrical methods to the right

help to improve the understanding of the hydrogeological characteristics of the aquifers in the region.

The ERT and TEM results complemented each other very well. Unconsolidated sediments, both dry and saturated, and consolidated rock have distinctive resistivity signatures, low values for the alluvium and high values for the bedrock. Although TEM investigations are recommended at sites where more conductive deep formations limit the DOI, some places with more resistive formations at lower limits were successfully interpreted with TEM methods like in the present study. In the study area, the typical resistivity values for the consolidated rock in the nearby outcrops are similar to those corresponding to the bedrock at about 80 mbs, under the unconsolidated sediments, in the grid area and in the resistivity cross-sections. However, the contact between sediments and hard rock looks irregular and complex, more than how it is shown in the bedrock contour lines in Fig. 2a from previous studies, maybe because similar geological processes might have shaped the superficial mountainous landscape and the buried bedrock.

The characteristics of water, especially the salinity, determine the resultant resistivity of the ground. The distribution of resistivity, at depths coinciding with the contact between the unconsolidated sediments and the bedrock, seems aligned with the trend of faults indicated in the geological map. These results suggest the existence of faults and other geological structures under the sediments, probably as lengthening of other structures to the southeast of the study area. The geological structures, like faults and folds, newly inferred and previously reported have a similar direction from southeast to northwest.

The two types of water influencing the resistivity images in the study area, fresh water in the unconsolidated sediments and more saline water close to some faults and structures in the bedrock, suggest the distinction of two different aquifers; a porous aquifer in the sediments on top (from the surface until the contact with the bedrock) and a fractured aquifer in the consolidated bedrock underlying the latter.

A more detailed resolution of the shape of the bedrock, and therefore the thickness of the alluvial sediments was evaluated in the study area. The thickness of the alluvial aquifer ranges from a couple of meters to about 120 m. These results improve the understanding of the geometry of the aquifer system. More extended investigations of this type are required to estimate the thickness of the porous aquifer in the rest of the reservoir, a parameter required in turn to evaluate the aquifer storage.

Acknowledgements The study was funded by the Swedish International Development Cooperation Agency (SIDA) and the Society of Exploration Geophysicists (SEG) through the Geoscientists Without Borders (GWB) programme. This work was also supported by Lund University (LU) in Sweden, Aarhus University (AU) in Denmark, and Universidad Mayor de San Andrés (UMSA) and Universidad Técnica de Oruro (UTO) in Bolivia. The TEM equipment was provided by Engineering Geology Division of Lund University with support from Guideline Geo AB. The ERT equipment was provided by UTO and Unidad de Saneamiento Básico y Vivienda (UNASVBI). We are grateful to Rafael Mendoza for helping in the field work, personnel of Corimex Ltda. for joining in field work for a couple of days. Conny Svensson from Engineering Geology, LU, for a thorough revision of the manuscript and also Esben Auken, Nikolaj Foged and other personnel of Hydrogeophysics Group Department of Geoscience, AU, for providing TEM setups, advice and support.

References

Aarhus GeoSoftware (2017a) Aarhus SPIA, Aarhus. 8000 Aarhus C, Denmark

Aarhus GeoSoftware (2017b) Aarhus Workbench, Aarhus. 8000 Aarhus C, Denmark

Auken E, Jørgensen F, Sørensen KI (2003) Large-scale TEM investigation for groundwater. Explor Geophys 34:188. https://doi.org/10.1071/EG03188

Banks D, Holden W, Aguilar E, Mendez C, Koller D, Andia Z, Rodriguez J, Saether OM, Torrico A, Veneros R, Flores J (2002) Contaminant source characterization of the San Jose Mine, Oruro, Bolivia. Geol Soc Lond Special Publ 198:215–239. https://doi.org/10.1144/GSL.SP.2002.198.01.14

Boiero D, Godio A, Naldi M, Yigit E (2010) Geophysical investigation of a mineral groundwater resource in Turkey. Hydrogeol J 18:1219–1233. https://doi.org/10.1007/s10040-010-0604-2

Christiansen AV, Auken E (2012) A global measure for depth of investigation. Geophysics 77:WB171–WB177. https://doi.org/10.1190/geo2011-0393.1

Christiansen AV, Auken E, Sørensen K (2009) The transient electromagnetic method. In: Kirsch R (ed) Groundwater geophysics: a tool for hydrogeology. Springer, Berlin, pp 179–226

Corriols M, Nielsen MR, Dahlin T, Christensen NB (2009) Aquifer investigations in the Leon-Chinandega plains, Nicaragua, using electromagnetic and electrical methods. Near Surf Geophys 7:413–425. https://doi.org/10.3997/1873-0604.2009034

Dahlin T (2001) The development of DC resistivity imaging techniques. Comput Geosci 27:1019–1029. https://doi.org/10.1016/S0098-3004(00)00160-6

Dahlin T, Zhou B (2006) Multiple-gradient array measurements for multichannel 2D resistivity imaging. Near Surf Geophys 4:113–123. https://doi.org/10.3997/1873-0604.2005037

Dames & Moore Norge (2000) Estudio hidrogeológico de la mina San José y los acuíferos que suministran agua a la ciudad de Oruro (Hydrogeological Study of the San Jose Mine and Adjacent Aquifers Supplying Water to the City of Oruro): Report 1,2,3., PMAIM-Subproyecto No 7. Corporacion Minera de Bolivia COMIBOL, Oruro, Bolivia, p 229

GEOBOL, Swedish Geological AB (1992) Carta Geológica de Bolivia - Hoja Oruro (Geological map of Bolivia - Sheet Oruro). Publicación SGB Serie I-CGB-11, p 6140

GITEC CG, COBODES L (2014) Formulación del Plan Director de la cuenca del lago Poopó (Poopo Lake Basin Management Plan

Formulation). Informe final. Programa de gestion sostenible de los recursos naturales de la cuenca del lago Poopo. Gobierno Autonomo Departamental de Oruro. Agosto 2014, Oruro, Bolivia (CTO-SERV-03/2013), p 561

Gómez E, Barmen G, Rosberg J-E (2016) Groundwater origins and circulation patterns based on isotopes in Challapampa aquifer. Bolivia Water 8:207. https://doi.org/10.3390/w8050207

Gonzales A, Dahlin T, Barmen G, Rosberg J-E (2016) Electrical resistivity tomography and induced polarization for mapping the subsurface of alluvial fans: a case study in Punata (Bolivia). Geosciences 6:51. https://doi.org/10.3390/geosciences6040051

Guérin R, Descloitres M, Coudrain A, Talbi A, Gallaire R (2001) Geophysical surveys for identifying saline groundwater in the semi-arid region of the central Altiplano, Bolivia. Hydrol Process 15:3287–3301. https://doi.org/10.1002/hyp.284

Larsson M (2016) TEM investigation on Challapampa aquifer, Oruro Bolivia. Geology Department, Lund University, MSc Thesis No 494, p 47

Lizarazu J, Aranyossy JF, Orsag V, Salazar JC (1987) Estudio Isotopico de la cuenca de Oruro-Caracollo, Bolivia (Isotopic study in the Oruro-Caracollo basin, Bolivia). Isotope techniques in water resources development IAEA-SM-299/11 301-314, Vienna, Symposium March 1987

Loke MH, Acworth I, Dahlin T (2003) A comparison of smooth and blocky inversion methods in 2D electrical imaging surveys. Explor Geophys 34:182–187

Metwaly M, El-Qady G, Massoud U, El-Kenawy A, Matsushima J, Al-Arifi N (2010) Integrated geoelectrical survey for groundwater and shallow subsurface evaluation: case study at Siliyin spring, El-Fayoum, Egypt. Int J Earth Sci 99:1427–1436. https://doi.org/10.1007/s00531-009-0458-9

Nabighian M (1991) Electromagnetic methods in applied geophysics: Volume 2, Application, Parts A and B. Newmont Exploration Limited ed. Society of Exploration Geophysicists, Denver, Colorado, US. https://doi.org/10.1190/1.9781560802686

Patureau N (2007) Contamination of the groundwater in Oruro city (Bolivia) and possible solutions to avoid polluting more in the future. MSc Thesis. No 069116458, School of Civil Engineering and Geosciences. Newcastle University, p 119

Ramos OE, Caceres LF, Ormachea MR, Bhattacharya P, Quino I, Quintanilla J, Sracek O, Thunvik R, Bundschuh J, Garcia ME (2011) Sources and behavior of arsenic and trace elements in groundwater and surface water in the Poopó Lake Basin, Bolivian Altiplano. Environ Earth Sci 66:793–807. https://doi.org/10.1007/s12665-011-1288-1

Reynolds JM (2011) An introduction to applied and environmental geophysics. Wiley, New York

Rigsby CA, Bradbury JP, Baker PA, Rollins SM, Warren MR (2005) Late Quaternary palaeolakes, rivers, and wetlands on the Bolivian Altiplano and their palaeoclimatic implications. J Quat Sci 20:671–691. https://doi.org/10.1002/jqs.986

SCIDE, CORDEOR, GEOBOL (1996) Informe de los pozos de producción - Proyecto de investigación y verificación de fuentes de abastecimiento de agua para la ciudad de Oruro (Report of the production wells - Project of investigation and verification of sources of water for supplying Oruro). GEOBOL - Servicio Geológico de Bolivia, Oruro, p 159

SELA (2017) Servicio Local De Acueductos Y Alcantarillado—Oruro. http://selaoruro.gob.bo/ Accessed 01 Jul 2017

SENAMHI (2015) Servicio Nacional de Meteorologia e Hidrologia de Bolivia. http://senamhi.gob.bo/. Accessed 9 Apr 2015

Spies BR (1989) Depth of investigation in electromagnetic sounding methods. Geophysics 54:872–888. https://doi.org/10.1190/1.1442716

Suarez Soruco R (2000) Compendio de Geología de Bolivia (Bolivian Geology Compendium), vol 18. Revista técnica de Yacimientos Petrolíferos Fiscales Bolivianos, Cochabamba, Bolivia, pp 213

Swedish Geological AB (1996) Impacto de la contaminación minera e industrial sobre agua subterráneas (Impact of mining and industrial pollution on groundwater). Ministerio de Desarrollo Sostenible y Medio Ambiente. Secretaria Nacional de Mineria. Proyecto Poloto Oruro. ID: R-Bo-E-9.45-9702-PPO96I6, Oruro, Bolivia, p 117

Paper III

Journal of South American Earth Sciences 91 (2019) 214–226

Contents lists available at ScienceDirect

Journal of South American Earth Sciences

journal homepage: www.elsevier.com/locate/jsames

Tracking of geological structures and detection of hydrothermal intrusion by geo-electrical methods in the highlands of Bolivia

Etzar Gómez[a,b,*], Emil Svensson[a], Torleif Dahlin[a], Gerhard Barmen[a], Jan-Erik Rosberg[a]

[a] Lund University – Engineering Geology, John Ericssons väg 1, 223 63, Lund, Sweden
[b] Universidad Mayor de San Andrés – Instituto de hidráulica e hidrología, Calle 30 Cota Cota, La Paz, Bolivia

ARTICLE INFO

Keywords:
Electrical resistivity tomography
Transient electromagnetic sounding
Faults
Altiplano
Bolivia

ABSTRACT

Oruro city in the Bolivian highlands depends solely on groundwater to supply domestic consumption and irrigation. The top porous aquifer currently exploited is not fully understood in aspects like geometry, hydrogeological properties and interaction with other aquifers in the region. Recent studies detected traces of fractures in the bedrock beneath the porous aquifer; these geological structures seem to be part of a fractured aquifer in contact with thermal sources. The present study aims to fill the gap between those recently detected fractures and the well-mapped fault system to the east of the study area and identify hydrothermal flows by using geo-electrical methods like Electrical Resistivity Tomography and Transient Electromagnetic soundings. Thirteen tomographic lines, placed transversely to the direction of three main faults, were meant to identify prolongations of those structures by tracking distinctive low resistivity in sectors where saline water saturates the subsoil. This type of water is also present in some hot springs near Capachos, where hydrothermal flows discharge under artesian conditions. Two of the investigated faults seem extending to the northwest, in agreement with the expected linkage towards the recently detected fractures. These two faults appear to reach a volcanic formation since the hydrothermal flows, going mainly upwards, align with their strikes. The remaining fault seems not to be connected to any hydrothermal source. The study presents new information, data and interpretations intending to improve the knowledge about the geological structures in a sensitive part of the local aquifer system.

1. Introduction

The existence of faults with saline water underlying the main fresh water reservoir in Oruro was found from some drillings reaching deep levels at which the water is not suitable for consumption nor irrigation. Therefore, improving the hydrogeological knowledge is crucial for the water resources management in the region. Geo-electrical methods can be useful tools in hydrogeological investigations, addressing subjects like delineation of saline interface, distinction of different geological formations and mapping groundwater resources (e.g. Auken et al., 2003; Corriols et al., 2009; Gonzales et al., 2016; Gopinath et al., 2018).

The volcanic formations around Oruro are most likely driving the hydrothermal activity in the region (Lizarazu et al., 1987; Suarez Soruco, 2000). The faults nearby these formations could be channels for the hydrothermal flows at deeper levels; however, they are mapped just outside the study area, eastwards of the border of the porous aquifer. On the other hand, recent geophysical investigations found traces of low resistivity linked to saline water intrusions, below the top porous aquifer to the north of the study area. The existence of possible connections between this sector and the faults to the southeast are investigated applying geo-electrical methods in the present study.

The different types of geological formations, their saturation degree and the type of fluid in their voids influence the resistivity obtained from the geo-electrical measurements. The data is later analysed and interpreted to map buried geological structures as it was demonstrated in similar studies around the world (e.g. Meidav and Furgerson, 1972; Pagano et al., 2003; Kumar et al., 2011; Rossi et al., 2017; Gopinath et al., 2018).

Because of the importance of the top porous aquifer as the main groundwater reservoir for Oruro (SELA, 2018), some studies aimed to characterize different hydrogeological aspects (e.g. Palacio, 1993; Dames and Moore, 2000; D'Elia, 2013; GITEC and COBODES Ltda., 2014). Regarding the subject of the present study, the relief of the bedrock was assessed interpreting geophysical profiles and drilling logs by Banks et al. (2002), electromagnetic investigations indicated the existence of folds and faults in the bedrock underlying the porous aquifers, just like on the surface (e.g. Guérin et al., 2001). A well field located in the central part of the alluvial fan of Paria River has been

* Corresponding author.Box 118, 221 00, Lund, Sweden.
E-mail address: etzar.gomez@tg.lth.se (E. Gómez).

https://doi.org/10.1016/j.jsames.2019.02.002
Received 10 July 2018; Received in revised form 26 January 2019; Accepted 1 February 2019
Available online 06 February 2019

exploiting groundwater since the 70's (SCIDE, 1996). The abstraction rate has been increasing over the years, e.g. 9,5 million m^3 in 2016, lowering the potentiometric surface and creating a cone of depression of ~5 km radius around the well field (Banks et al., 2002; D'Elia, 2013; GITEC and COBODES Ltda., 2014). Close to the eastern limit of that cone of depression, at a site called Capachos, hydrothermal activity is present as hot springs. According to in situ measurements, the water in this area is more saline than in the rest of the porous aquifer, e.g. the Electrical Conductivity (EC) is 3.6 mS/cm around Capachos and typically < 1.0 mS/cm in the rest of the aquifer. Consequently, there is a risk of contamination if the abstraction flows reach the hydrothermal zone (e.g. see Flores-Márquez et al., 2006; Haile and Abiye, 2012), which in turn, could increase the salinity of the water supplied to Oruro.

This study includes a description of the investigated area, especially on the hydrogeological background. The geo-electrical methods used in the study, Electrical Resistivity Tomography (ERT) and Transient Electromagnetic (TEM) soundings, are also described in aspects like data acquisition and processing. In the results and interpretation part, the resistivity images are analysed and confronted with the background information. The discussion part indicates how combining the resistivity interpretation with complementary information addresses the study case. Finally, the conclusion includes a summary of the most relevant aspects of the study, pointing the connection found between the two sectors of interest and the importance of the results to improve the geological knowledge in the region.

2. Study area

The western side of Bolivia owes its high altitude to the subduction of the Nazca plate rising and folding the South American plate, creating mountains and valleys (Froidevaux and Isacks, 1984; Suarez Soruco, 2000; O'Driscoll et al., 2012). The most extensive of these valleys filled with unconsolidated material is the Altiplano, the highest flat land in the continent (Suarez Soruco, 2000; Condom et al., 2004; Rigsby et al., 2005). The same subduction process is the origin of a continental volcanic arc along the Andes (Suarez Soruco, 2000; O'Driscoll et al., 2012). Valuable minerals have been found around some magmatic outcrops, supporting the settlement of towns and cities with the mining activity, such as the case of Oruro, which nowadays is one of the biggest cities in the Bolivian Altiplano (Fig. 1).

There are three groups of geological units in the investigated area (see Fig. 2). 1) Hard and consolidated rocks in the mountains, outcrops and bedrock (purple colours in Fig. 2). These formations are, from the oldest to the youngest: Cancañiri, Llallagua, Uncía and Catavi. The last three are exposed in the surrounding outcrops. They consist mainly of sedimentary rocks like sandstones, siltstones and shales; quartzite also exists in the oldest formations (GEOBOL and Swedish Geological AB, 1992; Suarez Soruco, 2000). The primary porosity in these rocks is assumed negligible. However, because of the orogeny and the volcanic activity in the region, the secondary porosity is assumed the most important at different scales, from small cracks to large faults. 2) Volcanic formations like the Escalera volcanics (orange colour in Fig. 2) comprising rhyodacitic and porphyritic lavas (GEOBOL and Swedish Geological AB, 1992; Suarez Soruco, 2000). The type and degree of porosity in these rocks at deeper levels is unknown. 3) Unconsolidated units, deposited during the Quaternary, consisting of clays, silts, sands, gravels and pebbles sorted in complex arrangements, especially in the central part of the aquifer system where these units are thicker (yellow colours in Fig. 2) (GEOBOL and Swedish Geological AB, 1992; Suarez Soruco, 2000; Rigsby et al., 2005). The primary porosity is dominant in these geological units; it can vary from one site to another depending on the grain size and the type of sedimentation process behind their formation. These sediments are likely to be interconnected, forming a single porous aquifer, which is assumed heterogeneous and anisotropic since the grains were transported and deposited with different types of events (e.g. fluvial, lacustrine, and colluvial). The last big lacustrine event deposited a thin clay layer on top, some tenths of centimetres thick, covering the porous aquifers and reducing significantly the vertical infiltration (Rigsby et al., 2005).

With regard to the type of water in the aquifers, the porous aquifer is mainly recharged by lateral infiltration from rivers and streams, which in turn receive the runoff from the surrounding mountains (Gómez et al., 2016). This aquifer is the main reservoir currently exploited with shallow and deep wells until ~100 m below surface (mbs). The water in this aquifer can be considered fresh since its typical EC value is < 1.0 mS/cm, according to in situ measurements on samples from the well field (done as part of the present study). Although water from shallow levels in some sites might have higher EC, e.g. ~1.5 mS/cm in dug wells 7 km northwards the study area, where salts encrusted in the fine sediments on top (traces of the last lake evaporation) might be dissolved by the small amount of water infiltrating and reaching the water table. On the other hand, the water circulating in fractures and faults of the consolidated formations might have similar meteoric origin, especially at the weathered and fractured levels in contact with the porous aquifers (top of the bedrock). Going deeper, the salinity of water is higher at greater depths, suggesting a different origin and longer residence times; e.g. the EC is ~2.5 mS/cm in samples coming from the Oruro mine at 400 mbs (Lizarazu et al., 1987). Samples from sites where the water is driven by hydrothermal flows usually have elevated temperature and high EC (e.g. see Navarro et al., 2004). There are three sites with hot springs in Capachos where the hot water is canalized to two public pools and used for recreation purposes (see Fig. 2a). The water is continuously circulating and after being used in the pools it is disposed in the vicinity, creating swamp areas (see Fig. 3). The EC of water in these hot-springs is ~3.5 mS/cm and the water temperature is ~50 °C.

3. Methods

The area of interest was investigated using ERT, IP and TEM methods. Thirteen tomographic lines of different lengths, from 800 to 3600 m and named alphabetically from A to M, were deployed transversely to the direction of three of the longest and deepest faults around Capachos (see Fig. 2a), aiming to track those structures by following changes in resistivity and normalized chargeability. Saturated and unconsolidated sediments are expected to have different resistivity than dry and hard rock. Likewise, the salinity of water in contact with the thermal sources in the area is thought to give a characteristic low resistivity in those parts where it is present (Pagano et al., 2003; Flores-Márquez et al., 2006; Wamalwa and Serpa, 2013) and therefore make it possible to distinguish the non-fractured rock from the faults with saline water. In addition, forty-nine TEM soundings complemented the study for comparison purposes. The data acquisition was done during March and April 2017 (Broman and Svensson, 2017).

The ERT technique is based on the principles of Direct Current (DC) resistivity surveying, in which the resistivity distribution in the ground is evaluated by injecting current through a pair of electrodes and measuring the potential difference in another pair of electrodes. The injected current and the type of arrangement of the quadrupole (set of electrodes) together with the resistivity distribution of the ground, determine the measured potential difference. Variations in the injected current or in the quadrupole arrangement affect the potential but the resistivity remains constant. Depending on the type of investigation, target features, sensitivity, resolution and logistics, some electrode configurations are more suitable than others. Modern multi-electrode

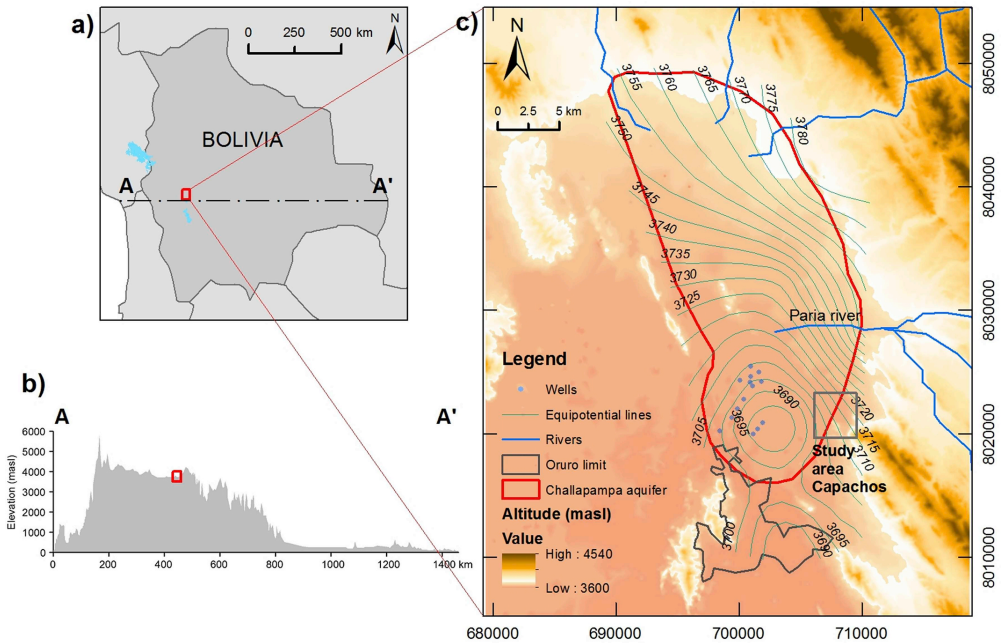

Fig. 1. Location of the study area. a) Bolivia; b) Topographic cross section A-A′, c) Challapampa aquifer system, Oruro and the study area Capachos.

and multi-channel equipment have improved the technique making it more efficient in terms of resolution, time and cost (Dahlin and Zhou, 2006).

Geological formations are capable of retaining electrical charges after a current is removed. That capacity is a function of the lithology and the conductivity of the fluid in the formation. The phenomenon is known as Induced Polarisation (IP) and is commonly expressed as chargeability (Slater and Lesmes, 2002). This property can be determined either in time or in frequency domain. In this study, IP was not directly measured in the field; it was extracted from the full waveform data recorded during the resistivity measurements, which also contains IP decay signals in time domain, following the procedure proposed by Olsson et al. (2015). The IP data can be calculated from the decay curve; where potentials are measured at different gates (times) during the "on" or "off" of the current (Olsson et al., 2016). In this study, the IP data were extracted only from the "on" of the current since the full waveform recorded 100% duty cycle (no "off" time). Acquisition of the full waveform data involves measurements of small voltage differences in short integration times, and hence it is prone to be affected by poor electrode-to-ground contacts and various sources of noise. This aspect must be taken into account since part of the measurements suffered from high resistances spoiling IP data quality of at least three profiles located in the rocky and dry outcrops in the east sector of the study area. Finally, another way of analysing IP is dividing the chargeability by the resistivity to obtain the Normalized IP (NIP), which is a parameter proportional to the surface conductivity (Slater and Lesmes, 2002). In this study, NIP was found to be a useful tool to examine those parts with strong influence of saline water close to the surface and in the bedrock fractures.

The ERT measurements were done with an ABEM Terrameter LS equipment including four cables (each one with 21 take outs and 10 m electrode separation) reaching a total spread length of 800 m. The input filters of the instrument were modified to be identical in frequency response to those of Terrameter LS2, and full waveform data were saved with a data rate of 3750 samples per second, to allow post processing with advanced filtering and extraction of IP data. The survey used a Multiple Gradient array, which was selected given its good signal-to-noise ratio and stable and fast field data acquisition (Dahlin and Zhou, 2006). Eight of the traverses were extended using the roll-along procedure, which consists of placing a new cable at the end of the line after the measurements are completed in one station. The positions of the electrodes were determined in the field with a GPS device. This is an important aspect in places where the topography is not horizontal, such as the case of the study site, because changes in the terrain can induce anomalies distorting the resistivity profiles (Loke, 2004).

After the data acquisition and signal processing were completed, 2D resistivity and IP images were obtained by applying an inverse numerical modelling process. It consists of an iterative method, based on finite elements or finite differences, comparing the apparent resistivity sections from an assumed model and from the field data (pseudo section). The inverse numerical modelling calculates differences (residual errors) between these two sections, then the model is refined aiming to minimize those differences until obtaining the most likely representation of the resistivity distribution in the final model (Dahlin, 2001; Loke et al., 2003). In this study, the inversion processes for ERT and IP sections were carried out using Res2Dinvx64 (v. 4.05), which uses finite elements to solve the inverse modelling. The robust constraint inversion (L1–norm) was selected in order to be able to handle sharp transitions in the models, for example in those parts with low resistivity, linked to the hydrothermal activity. The vertical to horizontal flatness ratio of 1.0 was selected in the software settings, since both vertical and horizontal changes in resistivity and chargeability were expected.

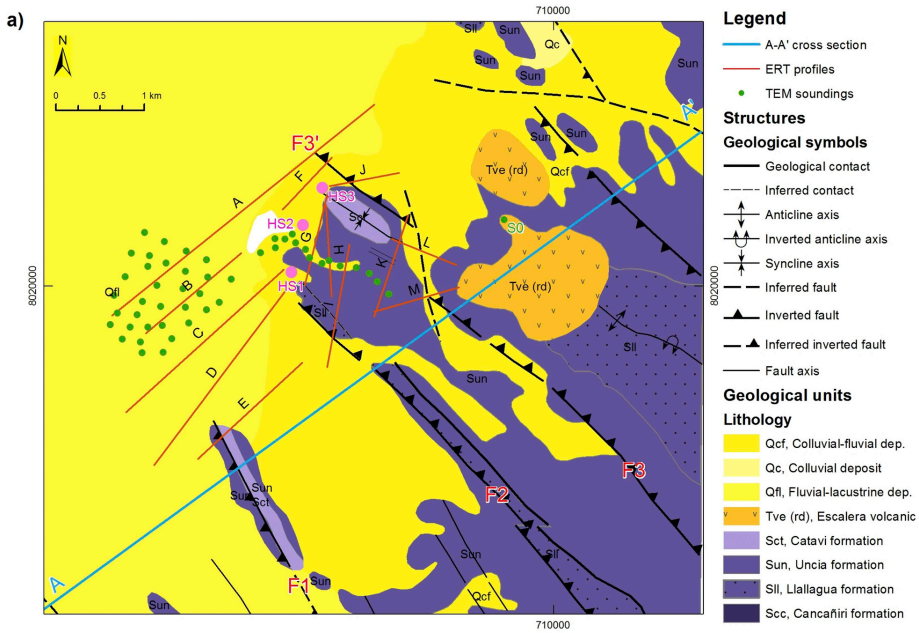

Fig. 2. Geological map of the study area at Capachos. a) Location of the ERT (red lines) and TEM (green dots) measurements. HS1, HS2 and HS3 are hot springs. F1, F2 and F3 are major faults. F3′ is assumed to be an extension of F3 slightly displaced to the north. b) Cross section A-A′, whose location is shown in Fig. 2a. Fault F4 is indicated as a second order fracture connected to F2. The Quaternary sediments are not shown in this cross section due to the scale; the thickness of these units in this part might be just of a couple of meters given their closeness to the hard rock outcrops. Modified from GEOBOL and Swedish Geological AB, (1992) and Banks et al. (2002). (For interpretation of the references to colour in this figure legend, the reader is referred to the Web version of this article.)

Regarding the other geo-electrical method applied in this study, TEM soundings were conducted in the west part of the investigated area, forming a scattered point region. Additional TEM soundings were completed eastwards, aligned erratically in between two rocky outcrops (see Fig. 2a). This technique is based on the generation of a primary electromagnetic field by sending a current through a transmitter antenna placed on the ground. When the electric pulse is stopped, eddy currents flow in the subsurface, which in turn generate a secondary magnetic field detected at the surface by a receiver antenna. The decay of that signal in logarithmic time intervals describes a characteristic curve depending on the type of geological materials and their distribution. In this study, TEM data were acquired using an ABEM WalkTEM equipment including a transmitter antenna (loop 50 × 50 m) and a receiver antenna (loop 0.5 × 0.5 m) placed at the centre of the transmitter. Numerical modelling, based on curve matching applying algorithms to solve inverse scattering problems (Nabighian, 1991) was performed using SPIA (Aarhus GeoSoftware, 2017a), which runs 1D inversions interpolated later with Aarhus Workbench (Aarhus GeoSoftware, 2017b) to obtain resistivity images in maps and vertical profiles.

4. Results and interpretation

The field measurements for this study were conducted during the dry season; hence, dry soil conditions were common especially in rocky terrains. Consequently, high contact resistances affected some ERT/IP profiles, although water and additives were used to improve the contact between electrodes and the soil. The depth of investigation achieved

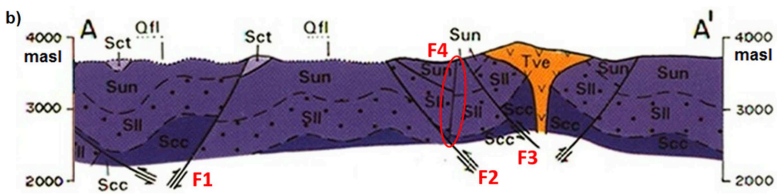

Fig. 2. (*continued*)

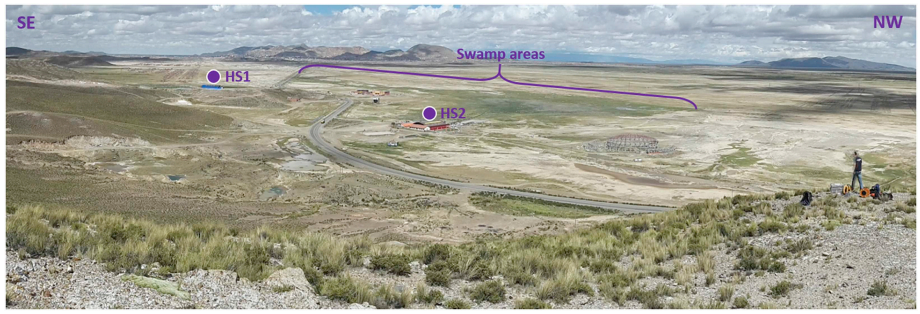

Fig. 3. View of the study area. HS1 and HS2 are pools and next to them flooded areas (swamps). Rocky and mountainous terrain to the left of the road. Unconsolidated sediments forming flat terrains to the right of the road.

with the ERT/IP profiles was ~170 m. On the contrary, the TEM soundings were not affected by the aridity of the terrain and good penetrations, ~200 m, were achieved. The data quality in all the resistivity models was good enough to make reliable interpretations (residuals < 4%). On the other hand, three of the chargeability models presented residuals > 10%, most likely affected by the high contact resistances and dryness of the rocky outcrops; profiles H, I and M expose possible "artifacts" or patches of high chargeability protruding abruptly from a lower background. Other sections, also in the rocky part, present similar presumed artifacts although the residuals of these sections are lower. Appendix 1 contains a summary of parameters regarding data quality and characteristics of the ERT/IP models obtained after running the inversions in Res2dinvx64.

Results from ERT and TEM yield similar resistivity values, corresponding to the type of geological formations and fluid content. Although, it must be acknowledged that each method has its own characteristics, sampling different subsurface volumes and having different sensitivities (Metwaly et al., 2010). A suggested classification of geological formations related to their resistivity in the study area is presented in Table 1; high values for hard rock with low porosity and low values for saturated unconsolidated sediments and fractured rocks. The lowest values most likely correspond to hydrothermal flows in vertical features and in shallow horizontal parts where saline water is present. This classification is based on measurements conducted in sites of well-defined geological characteristics like the top of nearby rocky outcrops (e.g. S0 in Fig. 2a) and around the hot springs. Geological interpretations from geophysical tests in previous studies were also taken into account for the resistivity classification (e.g. Palacio, 1993; Dames and Moore, 2000; Guérin et al., 2001; Canaviri, 2011; GITEC and COBODES Ltda., 2014; Broman and Svensson, 2017).

In those models with low residuals, the IP results vary in a range from 0 to ~10 mV/V for chargeability. Parts with values > 10 mV/V are assumed as artifacts. High chargeability is assumed to be associated with mineralization (precipitation of minerals) in those parts where saline water circulates, and probably due to the existence of clay minerals. However, attenuation of IP signals may have occurred in very conductive zones, such as the swamp areas where saline water saturates shallow parts of the ground. Inverted IP sections do not show any distinction of features like the surficial saturated clay layer or flow paths associated with the hydrothermal circulation, most likely due to that attenuation effect, making them not helpful in revealing the hypothesised geological features. On the other hand, most of the inverted NIP sections are in accordance with some hydrogeological features (shown also on the inverted resistivity profiles); high NIP values close and below the hot springs as well as on the top clay layer. The range of stable values of NIP is between 0.1 and 1 mS/m.

The results of the geo-electrical measurements are analysed and grouped in two zones (as shown in Figs. 2 and 4). Zone 1 corresponding to the NE part of the study area, where the sedimentary rocks are outcropping and the faults F2 and F3 are located, the latter are assumed to host flow paths connecting the closest volcanic intrusion with the hot springs. Zone 2 is mostly flat to the SW of the study area, also including a sedimentary fold (hill) along the fault F1.

4.1. Zone 1

Three of the transverses; profiles K, L and M, were located on top of the sedimentary outcrops, also close to the volcanic intrusion (see Fig. 2a). The ground at this sector is rocky and mainly resistive, although small conductive patches can be appreciated in the valleys, corresponding most likely to shallow unconsolidated sediments (small green parts in profiles K, L and M). According to the geological map, an inferred fault is located along this valley (see Fig. 2a). However, this inferred feature cannot be identified on the resistivity sections; if it

Table 1
Geological formations related to resistivity values in the study area.

Resistivity (ohm-m)	Classification	Geological characteristics
< 5	Very conductive	Soils saturated with saline and thermal waters, also in contact with preferential flow paths where this type of water is present
5 to 20	Conductive	Fully saturated formations, mainly unconsolidated sediments. High content of saline water coming from the hydrothermal flows or very shallow levels of saturated sediments where vertical infiltration dissolved salts encrusted close to the surface
20 to 80	Medium	Porous aquifers and top parts of the fractured bedrock. Water in these geological formations is assumed less saline than the hydrothermal one, therefore this might correspond to meteoric water laterally infiltrated
80 to 200	Resistive	Hard rocks (sedimentary and volcanic) with low effective porosity and therefore low water content
> 200	Very resistive	Dry hard rock with very little to insignificant porosity

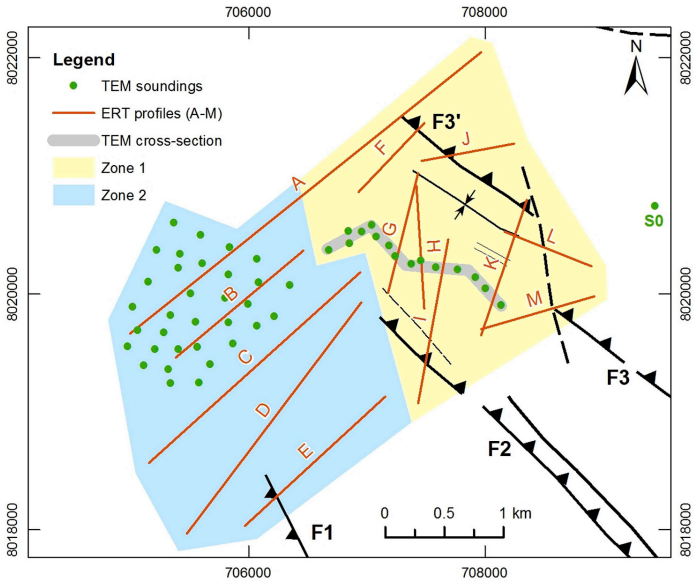

Fig. 4. Location of the TEM and ERT measurements. Data are divided and shown later in two separated zones (black marks are faults and structures, same as in Fig. 2a).

exists, it seems not to be saturated with saline water that would otherwise reduce the resistivity in this part.

Profiles G, H and I are located mainly in the rocky terrain, the first one (G) was deployed close to the hot springs HS1 and HS2. High resistivity is still the characteristic of the sedimentary rocks; however, conductive parts appear near the hot springs, as it is shown in profile G (Fig. 5a). In addition, the southern part of profile I exposes conductive areas at the intersection with fault F2.

The last three profiles A (the north-eastern half), F and J, belong to the flat terrain where sediments are thicker and partly saturated with saline water. Very conductive parts (almost vertical) are assumed as indications of faults crossing profiles A and F and aligning to a similar feature in the profile G. This fault is not aligned with F2, F3 or F3' (see Figs. 2 and 4). Therefore, it could be a different fault holding preferential flow paths corresponding to the local hydrothermal intrusion. It is termed F4 in Fig. 5a.

NIP images are also in accordance with the suggested alignment of fault F4 crossing profiles A, F and G in those parts where the normalized chargeability is higher than the background, as it is shown in Fig. 5b. The normalized chargeability in profile G is mostly low because it corresponds to the rocky part of the study area; however, parts with higher values might indicate fractures in the rock. The profile F is located at the foot of the outcrops and the NIP model suggests that the content of saline water is higher around the middle of the section; just in front of the hot spring HS3. Finally, profile A is the most distant from the rocky outcrops and it exposes a similar range of normalized chargeability values as in F.

The TEM soundings in this part of the study area (see Fig. 4) show models in agreement with the resistivity distribution from the ERT images, in accordance as well with the type and settings of geological formations. In Fig. 6, the rocky soils, to the east, have high resistivity values. To the west, where the unconsolidated sediments become thicker (300–500 m in distance from the west), the resistivity decreases close to the surface (parts with yellow to orange colours in Fig. 6). However, the most notorious feature in Fig. 6 is the deepest western part with very low resistivity at about 3500 masl in elevation. This feature is close to the hot spring HS1, which also seems to be aligned with the same direction as the fault F2.

4.2. Zone 2

This part of the study area, where the water from the Capachos hot springs infiltrates and saturates shallow levels of the subsoil, contains the western half of profile A, along with profiles B, C, D and E and the scattered TEM soundings. High resistivity values at ~50 m depth in profiles A, B, C and D (see Fig. 7a) might indicate a bedrock fold aligned from north to south (red shadow in Fig. 7a). This feature might constrain the thickness of the porous aquifer, since low resistivity values corresponding to saturated sediments are only present in the first ~50 mbs. In the profile C, there is a very conductive part to the most NE side, close to the hot spring HS1, it is assumed as an extension of the fault F2, hosting preferential hydrothermal flows in this area. Although the latter agrees with the expected feature in this part, it might require complementary measurements to corroborate its location and depth. Distinctive low resistivity trending downwards is shown on profile E, coinciding with the fault F1; however, it is less evident on profile D and no trace of it in other profiles to the NE. Therefore, this structure seems no larger than how is indicated in the geological map (see Fig. 2a).

The normalized chargeability distribution in the five profiles belonging to Zone 2 looks similar among them: high values on top, in the

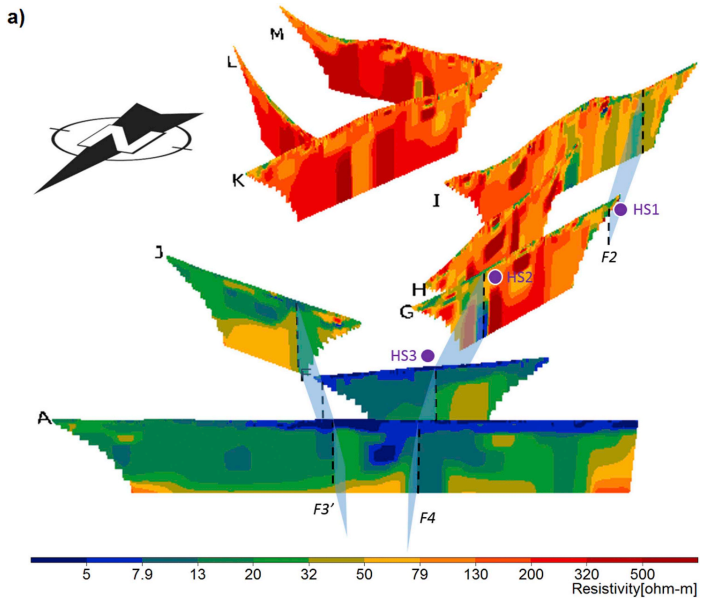

Fig. 5. a) 3-D view of resistivity models corresponding to Zone 1 of the study area. Notice that the image is rotated (from NW to SE) in order to show the most relevant features in front. Profiles F (800 m), G (1000 m), H (1000 m), I (1400 m), J (800 m), K (1200 m), L (800 m), M (1000 m) and half A (1800 m). Average thickness of the profiles 170 m. HS1, HS2 and HS3 are hot springs. Dashed lines indicate inferred faults; lines in profiles I and the southernmost part of G align with the fault F2 (see Fig. 2a), lines in profiles A, F and the northern part of G are aligned with the fault F4 (see Fig. 2a), blue shadows indicate possible faults. b) 3-D view of NIP models of the profiles A (half), G and F where an inferred fracture crosses at zones with high normalized chargeability. (For interpretation of the references to colour in this figure legend, the reader is referred to the Web version of this article.)

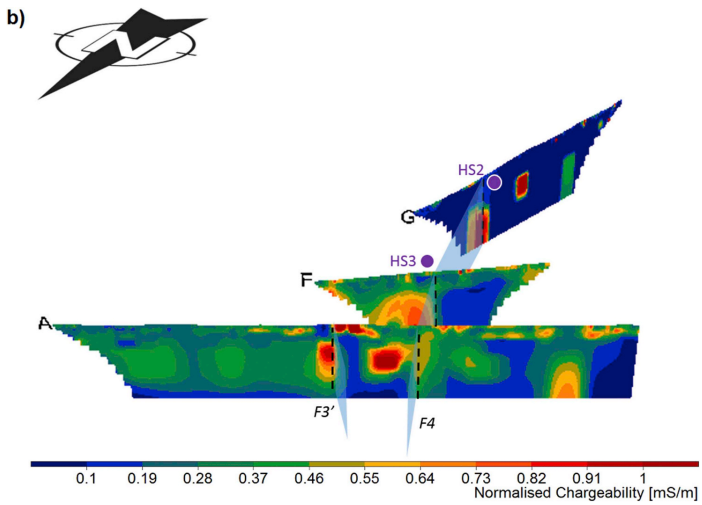

Fig. 5. (*continued*)

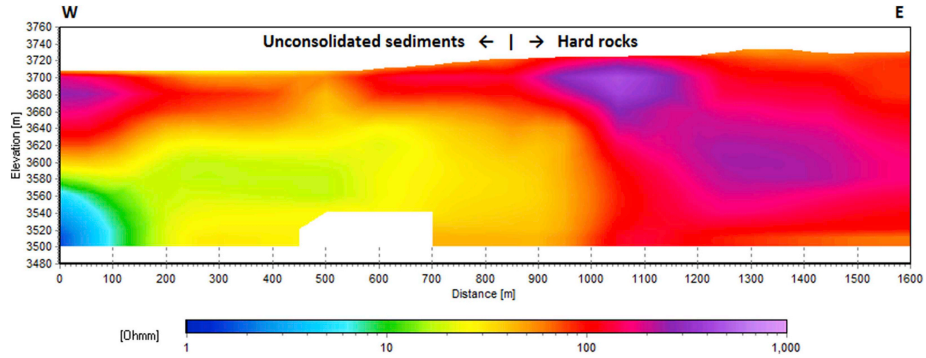

Fig. 6. Resistivity profile from TEM soundings (see its location in Fig. 4).

first 50 mbs, interpreted as unconsolidated sediments saturated with saline water, overlying hard rock with assumed lower porosity in parts of low values of normalized chargeability, as it is shown in Fig. 7b. The profile A shows trending lower NIP which might be a fracture with similar type of water that is present in the sediments overlying the bedrock. High normalized chargeability is also shown at the extreme north-eastern part of profile C, coinciding with the inferred feature shown on the resistivity profile C (Fig. 7a). Finally, a fault line appears on the NIP model of profile E, the same as on the resistivity model; higher values seem to correlate with this feature.

In addition to the ERT and IP surveys, 33 TEM soundings were conducted in the northern part of Zone 2. These tests reached slightly greater depths than the ERT, as it is shown in Fig. 8. Similarly to the ERT sections, the resistivity at the surface is low because of the presence of saline water, but it increases gradually with depth. At about 3580 masl (150 mbs) the resistivity decreases again to the east of the slice (Fig. 8). This feature might be an indication of fractures in the bedrock with saline water. The location of this zone does not coincide directly with a projection of the fault F2 (the closest one). However, it has the same elevation as another very conductive feature shown in Fig. 6 (also

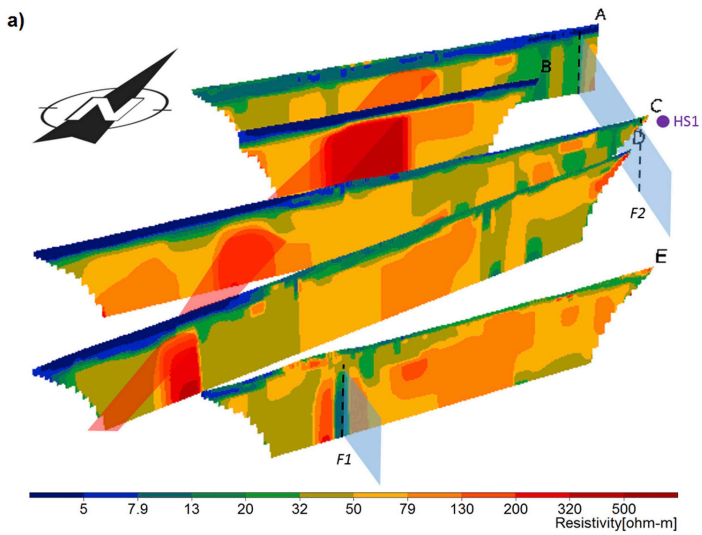

Fig. 7. a) 3-D view of the resistivity models corresponding to Zone 2 of the study area. Half A (1800 m), B (1400 m), C (2400 m), D (2400 m) and E (1600 m). Average depth of the profiles 170 m. HS1 is a hot spring. Dashed lines indicate inferred faults; in A and C aligning with the fault F2; in E aligning with the fault F1 (see Fig. 2a). Blue shadows indicate the direction of the inferred faults. Red shadow indicates an alignment of a bedrock fold in profiles A, B, C and D. b) 3-D view of NIP models of the profiles half A, C and E. Inferred faults cross at zones with high normalized chargeability values, marked with dashed lines; in C as an extension of the fault F2, in E as the location of fault F1.

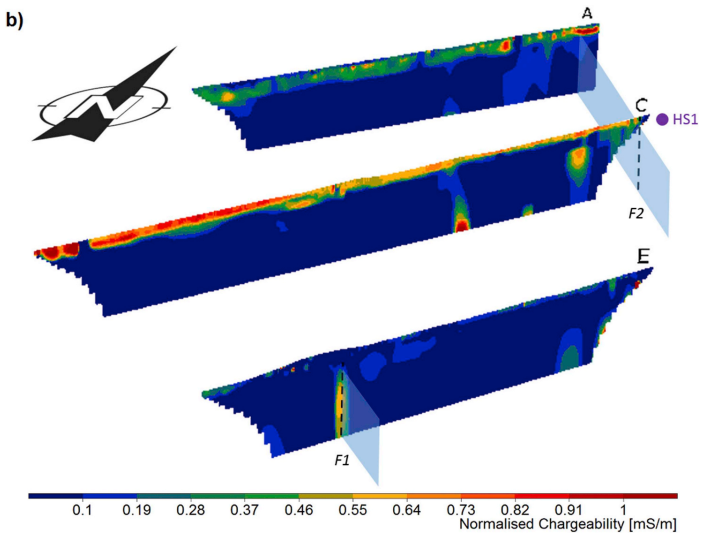

Fig. 7. (*continued*)

from TEM soundings), which is closer to the projection of the fault F2. Unfortunately, the description of the characteristics of this very conductive zone, away from the direction of one of the main faults, is out of the scope of this study because of limitations on the depth of investigation (~170 mbs). This anomaly seems to continue at greater depths and is assumed as an indication of the existence of fractures linked with the hydrothermal activity in the area.

5. Discussion

The geo-electrical properties of the ground around Capachos facilitate the distinction of different types of geological formations, based on the rock and soil characteristics, porosity and type of water stored in the voids. The existence of the hydrothermal activity in the study area is most likely driven by the nearest volcanic intrusion: the Escalera formation (see Fig. 2). The application of ERT was limited by the arid conditions in some places. On the other hand, the rough topography and uneven surfaces were not appropriate for the application of TEM. Despite those obstacles in some parts of the study area, most of the measurements and the data acquired have good quality for further processing and interpretation. A single TEM sounding was conducted on top of a consolidated hard rock formation (see the point marked as "S0" in Figs. 2 and 4) to obtain the characteristic resistivity of the outcrops. The resultant 1-D model revealed that the top and bottom parts are highly resistive (> 300 Ω-m). However, the resistivity declines at about 40 mbs (to a value ~40 Ω-m); probably due to a three-dimensional effect of a stream downhill the sounding site. It was not possible to conduct more tests near the volcanic intrusion due to the rough terrain and steep topography.

The geo-electrical response in the study area is highly controlled by the type of water saturating the testing sites, especially where the hydrothermal flows were detected. There are small hot springs nearby the sites indicated as HS2 and HS3 (see Figs. 2a, 3 and 5). The average EC of water measured in these sites was ~3.5 mS/cm; although the calculated value is higher, ~4.5 mS/cm, considering the content of dissolved ions and temperature (see Appendix 2). Even higher EC-values were measured in the puddles of the swamp area (see Fig. 3), reaching values of ~7.4 mS/cm. This high conductivity of water is likely due to the existence of a thin clay layer covering the flat land and reducing significantly the vertical infiltration, propitiating the accumulation of salts after the water is evaporated. Assuming that water with similar composition to than in Appendix 2 is disposed and retained in the swamps, it is still able to dilute part of the salts retained at the surface (e.g. calculated Saturation Index for halite −5.26, based on Appendix 2 data). Consequently, the resistivity at shallow levels around the hot springs is expected to be low: < 5 Ω-m, according to field measurements. The chargeability, extracted from the full waveform data, does not show clearly these shallow parts, probably due to an attenuation effect attributed to the high conductance in the saturated clay-rich layer, which also covers large areas further away the location of the profiles (A to M). However, the normalized chargeability (obtained dividing the chargeability by the resistivity) shows more clearly these shallow conductive parts saturated with saline water (see Fig. 7b).

Besides the shallow horizontal parts of low resistivity and high normalized chargeability, some images show conductive zones aligned in vertical and inclined features (e.g. see Figs. 5a and 7a). They are interpreted as faults where thermal water is present. The three major faults in the investigated area were tracked (see Fig. 9a); F1 does not seem to continue to the north west further than the location of the profile E. In addition, a structure like a buried fold (red shadow with N–S direction in Fig. 7a and indicated in Fig. 9a) seems to be a barrier for flows passing above this structure. Indications of F2 are present in the profiles A, C, G and I. Anomalies showing conductive zones are located close to HS1 (see profiles C and G in Figs. 5a and 7a) and they are interpreted as a preferential hydrothermal flow going upwards in this site. F3 and the transition to F3′ were not detected in the rocky part of the study area, according to the resistivity models of the profiles L and M (see Fig. 5a). However, there are indications of the fault F3'

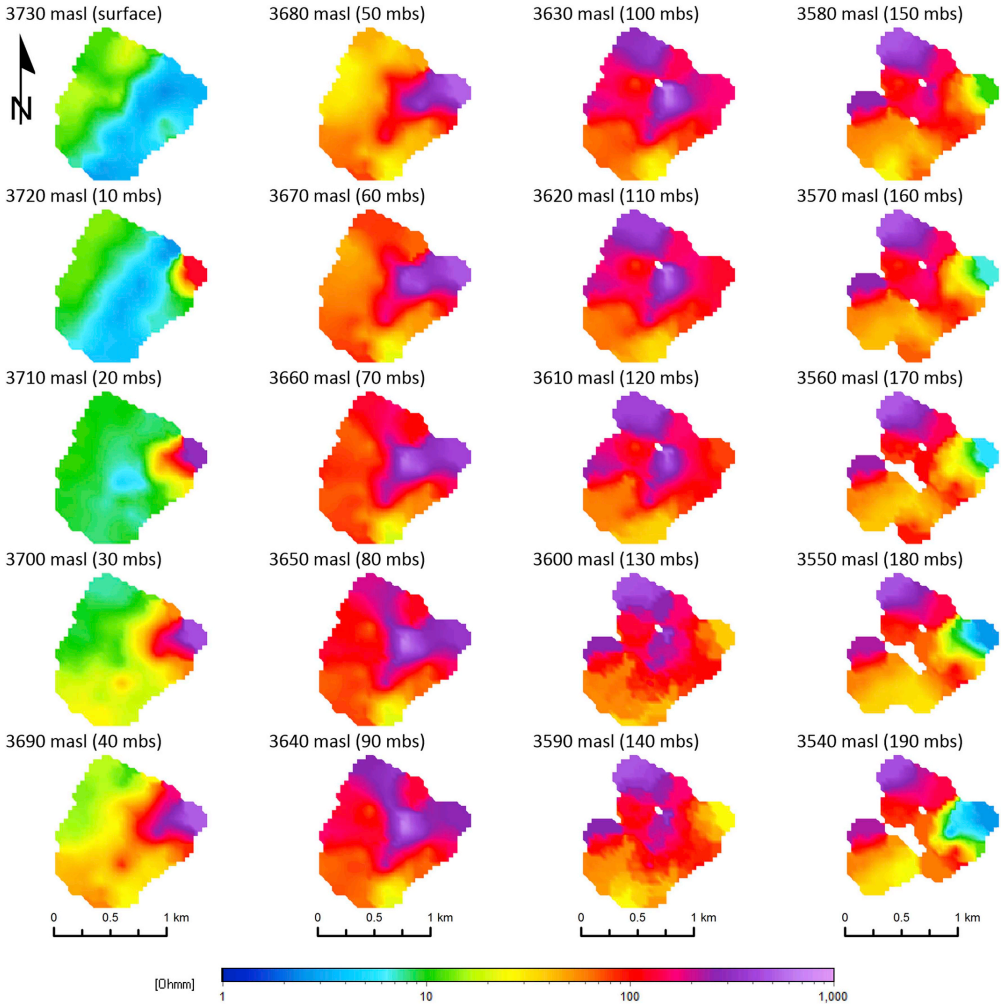

Fig. 8. Horizontal resistivity maps by depth (slices) from TEM soundings in the western part of the study area (location in Fig. 2a).

crossing profiles A, F and J (see Figs. 5a and 5b).

The most conductive parts in the profiles A, F and G (Fig. 5) might correspond to a second order fracture, indicated in the cross section of Figs. 2b and 9b as F4. The length of this fracture is not indicated in the geological map; however, it connects almost vertically with the fault F2, which in turn might reach the volcanic intrusion as indicated in Fig. 9b. According to this conceptual model, the location of the thermal source might be at deep levels (> 2000 mbs) and the hydrothermal flows might go upwards in fault F3 as well as in F2, the then partially deviated to F4.

6. Conclusions

The geological formations and structures like faults, folds and outcrops around Oruro, interact in complex ways with unconsolidated sediments and the regional groundwater. The present study aims to improve the understanding of the hydrogeological characteristics in Capachos, where three faults and their connection with hydrothermal flows were investigated with two geo-electrical methods: Electrical Resistivity Tomography and Transient Electromagnetic soundings.

The results evidence the geo-electrical methods are suitable for the

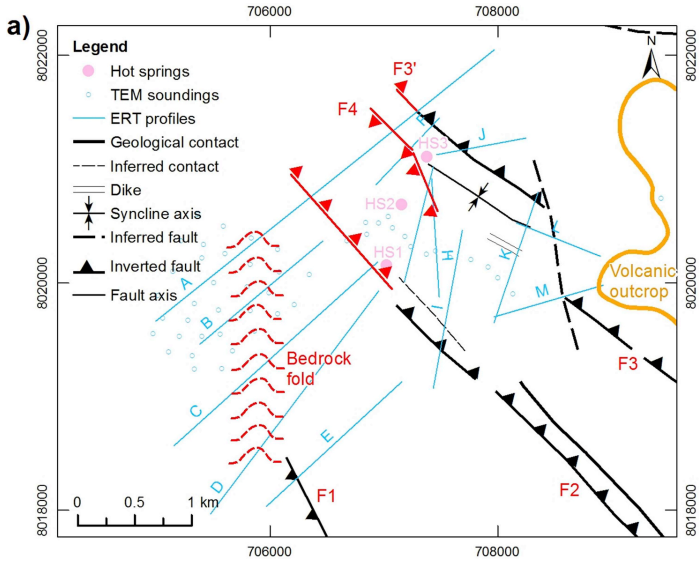

Fig. 9. a) Map of geological structures and faults found in the study area, structures in black belongs to the geological map (Fig. 2a), structures in red are inferred in this study. b) Conceptual model of the geothermal flow, red arrows indicate the hydrothermal flows, based on the geological map and cross section (Fig. 2b). (For interpretation of the references to colour in this figure legend, the reader is referred to the Web version of this article.)

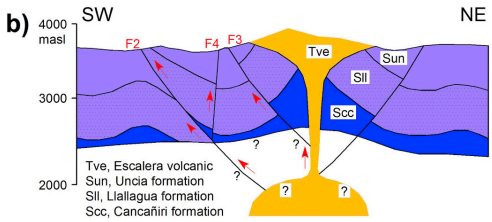

Fig. 9. (*continued*)

study area and show the resistivity models from ERT and TEM complement each other very well. In addition, the full waveform data recorded during the ERT measurements was used to obtain the IP characteristics, presented as normalized chargeability, used later to endorse the existence of features shown with resistivity.

The southernmost fault in the study area might not be longer than how it was described in the geological background information. On the contrary, the other two faults to the north seem longer, extending below the unconsolidated sediments. Low resistivity associated with water saturation indicate the prolongation of these structures to the NW, in apparent connection with similar structures inferred in recent studies. In addition, a fracture-free bedrock fold associated with high resistivity values was inferred in the western part of the study area.

The hydrothermal flows associated with very low resistivity values around the hot springs, align with the two most northern faults in the study area as well; these faults are assumed to reach the closest volcanic intrusion at deeper levels. This characteristic low resistivity was not detected at shallow depths, neglecting the existence of shallow horizontal flows between the volcanic intrusion and the hot springs. Therefore, the thermal waters in the area might circulate mainly upwards.

Resistivity images from TEM show concentrations of low values at levels > 170 m below surface; unfortunately, the depth of investigation of this method limit the resolutions of these features to only 20 m more in depth. Other methods, such as self potential, magnetotellurics, seismic or even ERT (with larger electrode separation) and TEM (with higher electrical pulses and larger antenna separation) might reveal deeper characteristics of the thermal flows as well as to improve the shallow resolution to obtain a better hydrogeological description of the area.

Acknowledgement

The study was funded by Styrelsen för internationellt utvecklingssamarbete (Swedish International Development Cooperation Agency - SIDA), Sweden (No. 5410004501); Geoscientists Without Borders/ Society of Exploration Geophysicists, United States (No. 201601005). The fieldwork was supported by Lund University, Sweden; Aarhus University, Denmark; Universidad Mayor de San Andrés, Bolivia; Universidad Técnica de Oruro, Bolivia; Guideline Geo AB, Sweden. Data acquisition was done in collaboration with Emil Svensson and Kamran Ahmad.

Appendix 1. Data complementary information

Common values for all the ERT/IP field measurements are:

- Electrode spacing: 10 m
- Number of stacking during the data acquisition: 3
- Chargeability delay time: 0.014 s

Common values for all the inverted ERT/IP models are:

- Number of layers for the inverted models: 15
- Width of the model cells: 5 m (the grid refinement option was used)
- Vertical to horizontal flatness ratio: 1.0

The rest of parameters regarding to the ERT/IP data are shown in the table below.

Line	Length (m)	Mean contact resistance (ohm)	Var. Coef. Contact resistance (%)	Pulse duration (s)[a]	Average current (mA)	Average variance (%)	Chargeability integration time (s)[a]	No. of data acquired	No. of data inverted	No. of iterations	No. of blocks	Resistivity mean residual (%)	Chargeability mean residual (%)
A	3600	217	40	1.8	317	0.36	1.778	14242	14202	9	10216	1.19	3.80
B	1400	179	15	1.8	501	0.30	1.778	4573	3510	10	3334	0.70	2.81
C	2400	191	39	2.0	463	0.29	1.898	8968	8914	7	6616	2.13	1.08
D	2400	200	27	2.0	501	0.21	1.898	8968	8967	14	6616	0.40	0.53
E	1600	644	129	1.8	391	0.39	1.778	5452	5445	11	4216	0.85	5.45
F	800	182	38	2.0	201	0.72	1.898	1936	1933	10	1816	0.75	1.45
G	1000	1180	84	1.8	233	0.59	1.778	2815	2805	17	2416	1.51	7.40
H	1000	1870	56	1.8	156	0.67	1.778	2815	2810	14	2416	2.58	11.98
I	1400	1880	64	1.8	168	0.26	1.778	4545	4509	9	3616	3.61	32.43
J	800	372	46	2.0	201	0.52	1.875	1936	1929	11	1816	0.74	2.58
K	1200	1600	61	1.8	196	0.17	1.778	3694	3680	12	3005	1.21	5.92
L	800	1350	44	1.8	212	0.07	1.778	1936	1935	13	1816	0.75	2.62
M	1000	1530	75	1.8	207	0.09	1.778	2815	2806	11	2416	1.43	10.34

[a] The difference in pulse duration and integration time for the chargeability was caused by different operator arrangements. This difference is relatively small and hence the effect on the integral chargeability is expected to be relatively limited as well.

Appendix 2. Major ions of a water sample from the hot spring HS2

Temp. °C	pH	Alkalinity mg/l	Ca^{2+} mg/l	Mg^{2+} mg/l	Na^{+} mg/l	K^{+} mg/l	SO_4^{2-} mg/l	Cl^{-} mg/l	Fe mg/l	NO_3^{-} mg/l
50	6.7	683.39	30.2	9.3	654	19.75	3	412.5	0.206	0.22

References

D'Elia, M., 2013. Asesoramiento para el Diseño e Implementación de la Red de Monitoreo de Aguas Subterráneas en la Cuenca del Lago Poopó (Advice for the design and implementation of the groundwater monitoring network in the lake Poopó basin). Gobierno Autónomo Departamental De Oruro. Programa de Gestión Sostenible de los Recursos Naturales de la Cuenca del Lago Poopó Convenio No. DCI-ALA/2009/021-614, Oruro.

O'Driscoll, L.J., Richards, M.A., Humphreys, E.D., 2012. Nazca-South America interactions and the late Eocene-late Oligocene flat-slab episode in the central Andes. Tectonics 31, 1–16. https://doi.org/10.1029/2011TC003036.

Auken, E., Jørgensen, F., Sørensen, K.I., 2003. Large-scale TEM investigation for groundwater. Explor. Geophys. 34, 188. https://doi.org/10.1071/EG03188.

Banks, D., Holden, W., Aguilar, E., Mendez, C., Koller, D., Andia, Z., Rodriguez, J., Saether, O.M., Torrico, A., Veneros, R., Flores, J., 2002. Contaminant source characterization of the san Jose mine, Oruro, Bolivia. Geol. Soc. London, Spec. Publ. 198, 215–239. https://doi.org/10.1144/GSL.SP.2002.198.01.14.

Broman, V., Svensson, E., 2017. TEM and ERT Investigations in Challapampa Aquifer. ISRN LUTVDG/(TVTG-5152)/1-50/(2017). MSc Thesis, Engineering Geology, Lund University, Bolivia.

Canaviri, B., 2011. Estimación de la vulnerabilidad intrínseca a la contaminación del aquífero libre en el sistema acuífero de Challapampa Oruro (Estimation of the intrinsic vulnerability to contamination of the unconfined aquifer in the Challapampa aquifer system Oruro). Tesis de grado (Bachelor thesis). Universidad Técnica de Oruro, Oruro, Bolivia.

Condom, T., Coudrain-Ribstein, A., Dezetter, A., Brunstein, D., Delclaux, F., Sicart, J.-E., 2004. Transient modelling of lacustrine regressions: two case studies from the Andean Altiplano. Hydrol. Process. 18, 2395–2408. https://doi.org/10.1002/hyp.1470.

Corriols, M., Nielsen, M.R., Dahlin, T., Christensen, N.B., 2009. Aquifer investigations in the Leon-Chinandega plains, Nicaragua, using electromagnetic and electrical methods. Near Surf. Geophys. 7, 413–425. https://doi.org/10.3997/1873-0604.2009034.

Dahlin, T., 2001. The development of DC resistivity imaging techniques. Comput. Geosci. 27, 1019–1029. https://doi.org/10.1016/S0098-3004(00)00160-6.

Dahlin, T., Zhou, B., 2006. Multiple-gradient array measurements for multichannel 2D resistivity imaging. Near Surf. Geophys. 4, 113–123. https://doi.org/10.3997/1873-0604.2005037.

Dames, Moore, Norge, 2000. Estudio Hidrogeológico De La Mina San José Y Los Acuíferos Que Suministran Agua A La Ciudad De Oruro (Hydrogeological Study of the San Jose Mine and Adjacent Aquifers Supplying Water to the City of Oruro). Report 1,2,3. Corporacion Minera de Bolivia COMIBOL. PMAIM-Subproyecto No 7.

Flores-Márquez, E.L., Jiménez-Suárez, G., Martínez-Serrano, R.G., Chávez, R.E., Pérez, D.S., 2006. Study of geothermal water intrusion due to groundwater exploitation in the Puebla Valley aquifer system, Mexico. Hydrogeol. J. 14, 1216–1230. https://doi.org/10.1007/s10040-006-0029-0.

Froidevaux, C., Isacks, B.L., 1984. The mechanical state of the lithosphere in the Altiplano-Puna segment of the Andes. Earth Planet. Sci. Lett. 71, 305–314. https://doi.org/10.1016/0012-821X(84)90095-5.

GEOBOL, Swedish Geological AB, 1992. Carta Geológica de Bolivia - Hoja Oruro (Geological map of Bolivia - Sheet Oruro). Publicación SGB Serie I-CGB-11, pp. 6140.

GeoSoftware, Aarhus, 2017a. Aarhus SPIA.

GeoSoftware, Aarhus, 2017b. Aarhus Workbench.

GITEC, C.G., COBODES, Ltda, 2014. Formulación del Plan Director de la cuenca del lago Poopó (Poopo Lake Basin Management Plan Formulation). In: Informe final. Programa de gestion sostenible de los recursos naturales de la cuenca del lago Poopo. Gobierno Autonomo Departamental de Oruro. Agosto 2014, Oruro, Bolivia, (CTO-SERV-03/2013).

Gómez, E., Barmen, G., Rosberg, J.-E., 2016. Groundwater origins and circulation patterns based on isotopes in Challapampa aquifer, Bolivia. Water 8, 207. https://doi.org/10.3390/w8050207.

Gonzales, A., Dahlin, T., Barmen, G., Rosberg, J.-E., 2016. Electrical resistivity tomography and induced polarization for mapping the subsurface of alluvial fans: a case study in Punata (Bolivia). Geosciences 6, 51. https://doi.org/10.3390/geosciences6040051.

Gopinath, S., Srinivasamoorthy, K., Saravanan, K., Suma, C.S., Prakash, R., Senthinathan, D., Sarma, V.S., 2018. Vertical electrical sounding for mapping saline water intrusion in coastal aquifers of Nagapattinam and Karaikal, South India. Sustain. Water Resour. Manag. 4, 833–841. https://doi.org/10.1007/s40899-017-0178-4.

Guérin, R., Descloitres, M., Coudrain, A., Talbi, A., Gallaire, R., 2001. Geophysical surveys for identifying saline groundwater in the semi-arid region of the central Altiplano, Bolivia. Hydrol. Process. 15, 3287–3301. https://doi.org/10.1002/hyp.284.

Haile, T., Abiye, T.A., 2012. The interference of a deep thermal system with a shallow aquifer: the case of Sodere and Gergedi thermal springs, Main Ethiopian Rift, Ethiopia. Hydrogeol. J. 20, 561–574. https://doi.org/10.1007/s10040-012-0832-8.

Kumar, D., Thiagarajan, S., Rai, S.N., 2011. Deciphering Geothermal resources in Deccan trap region using electrical resistivity tomography technique. J. Geol. Soc. India 78, 541–548. https://doi.org/10.1007/s12594-011-0123-3.

Lizarazu, J., Aranyossy, J.F., Orsag, V., Salazar, J.C., 1987. Estudio Isotopico de la cuenca de Oruro-Caracollo, Bolivia (Isotopic study in the Oruro-Caracollo basin, Bolivia). In: Isotope Techniques in Water Resources Development. IAEA-SM-299/11 301-314. Vienna, Symposium March 1987.

Loke, M.H., 2004. Rapid 2-D Resistivity & IP Inversion Using the Least-Squares Method. Man. Res2dinv, Version.

Loke, M.H., Acworth, I., Dahlin, T., 2003. A comparison of smooth and blocky inversion methods in 2D electrical imaging surveys. Explor. Geophys. 34, 182–187.

Meidav, T., Furgerson, R., 1972. Resistivity studies of the Imperial Valley geothermal area, California. Geothermics 1, 47–62. https://doi.org/10.1016/0375-6505(72)90012-0.

Metwaly, M., El-Qady, G., Massoud, U., El-Kenawy, A., Matsushima, J., Al-Arifi, N., 2010. Integrated geoelectrical survey for groundwater and shallow subsurface evaluation: case study at Siliyin spring, El-Fayoum, Egypt. Int. J. Earth Sci. 99, 1427–1436. https://doi.org/10.1007/s00531-009-0458-9.

Nabighian, M., 1991. Electromagnetic methods in applied geophysics. In: Application, Parts A and B, Newmont Ex, vol. 2 Society of Exploration Geophysicists, Denver, Colorado, US. https://doi.org/10.1190/1.9781560802686.

Navarro, J.Á.S., López, P.C., Perez-Garcia, A., 2004. Evaluation of geothermal flow at the springs in Aragón (Spain), and its relation to geologic structure. Hydrogeol. J. 12, 601–609. https://doi.org/10.1007/s10040-004-0330-8.

Olsson, P.I., Dahlin, T., Fiandaca, G., Auken, E., 2015. Measuring time-domain spectral induced polarization in the on-time: decreasing acquisition time and increasing signal-to-noise ratio. J. Appl. Geophys. 123, 316–321. https://doi.org/10.1016/j.jappgeo.2015.08.009.

Olsson, P.I., Fiandaca, G., Larsen, J.J., Dahlin, T., Auken, E., 2016. Doubling the spectrum of time-domain induced polarization by harmonic de-noising, drift correction, spike removal, tapered gating and data uncertainty estimation. Geophys. J. Int. 207, 774–784. https://doi.org/10.1093/gji/ggw260.

Pagano, G., Menghini, A., Floris, S., 2003. Electrical tomography and TDEM prospection in the Chianciano thermal basin (Siena, Italy). Ann. Geophys. 46, 501–512.

Palacio, T., 1993. Geoelectric Study for Groundwater Prospection in Oruro City. Santafe de Bogota. SeLA; PNUD; CAEM.

Rigsby, C.A., Bradbury, J.P., Baker, P.A., Rollins, S.M., Warren, M.R., 2005. Late Quaternary palaeolakes, rivers, and wetlands on the Bolivian Altiplano and their palaeoclimatic implications. J. Quat. Sci. 20, 671–691. https://doi.org/10.1002/jqs.986.

Rossi, M., Olsson, P.I., Johanson, S., Fiandaca, G., Bergdahl, D.P., Dahlin, T., 2017. Mapping geological structures in bedrock via large-scale direct current resistivity and time-domain induced polarization tomography. Near Surf. Geophys. 15, 657–667. https://doi.org/10.3997/1873-0604.2017058.

SCIDE, CORDEOR, GEOBOL, 1996. Informe de los pozos de producción - Proyecto de investigación y verificación de fuentes de abastecimiento de agua para la ciudad de Oruro (Report of the production wells - Project of investigation and verification of sources of water for supplying Oruro), vol. 159p GEOBOL - Servicio Geológico de Bolivia, Oruro.

SELA, 2018. Servicio Local De Acueductos Y Alcantarillado - Oruro. [WWW Document]. URL. http://selaoruro.gob.bo/ (accessed 1.10.18).

Slater, L.D., Lesmes, D., 2002. IP interpretation in environmental investigations. Geophysics 67, 77–88. https://doi.org/10.1190/1.1451353.

Suarez Soruco, R., 2000. Compendio de Geología de Bolivia (Bolivian Geology Compendium) Vol 18. Revista técnica de Yacimientos Petrolíferos Fiscales Bolivianos, Cochabamba, Bolivia, pp. 213.

Wamalwa, A.M., Serpa, L.F., 2013. The investigation of the geothermal potential at the Silali volcano, Northern Kenya Rift, using electromagnetic data. Geothermics 47, 89–96. https://doi.org/10.1016/j.geothermics.2013.02.001.

Paper IV

H2Open Journal

IWA PUBLISHING

H2Open Journal Vol 2 No 1
doi: 10.2166/h2oj.2019.007

Quantitative estimations of aquifer properties from resistivity in the Bolivian highlands

Etzar Gómez[a,b,*], Viktor Broman[a], Torleif Dahlin[a], Gerhard Barmen[a] and Jan-Erik Rosberg[a]

[a] Lund University – Engineering Geology, John Ericssons väg 1, 223 63 Lund, Sweden

[b] Universidad Mayor de San Andrés – Instituto de hidráulica e hidrología, Calle 30 Cota Cota, La Paz, Bolivia

*Corresponding author. E-mail: etzar.gomez@tg.lth.se

Abstract

Resistivity data constitute the largest part of the available information to assess the hydrogeological characteristics of the aquifer system near Oruro, in the central part of the Bolivian Altiplano. Two aquifers are part of this system; top unconsolidated sediments storing fresh water in their granular voids, overlying fractured hard rock formations where saline water was detected in connection to some faults. This study proposes an indirect and cost-effective way to estimate aquifer hydraulic properties for the groundwater management in the region. Hydraulic conductivity and transmissivity in the top aquifer were estimated using an empirical linear relationship between hydraulic conductivity and resistivity. This latter parameter, as well as the aquifer thickness, were obtained from the inverted models corresponding to the geoelectrical tests performed in the study area (electrical resistivity tomography, transient electromagnetic soundings and vertical electrical soundings). The highest estimated transmissivity values are $\sim 4.0 \times 10^{-2}$ m^2/s located in the centre of the study area, the lowest values are $\sim 3.4 \times 10^{-3}$ m^2/s, located around thermal intrusions to the south and where the top of the bedrock is shallow (~20 m depth) to the west. The methodology presented in this study makes wider use of resistivity measurements to identify promising groundwater production sites.

Key words: empirical linear correlation, geoelectrical methods, groundwater, hydraulic conductivity, resistivity, transmissivity

INTRODUCTION

Groundwater management and aquifer assessment rely on the reasonable knowledge of its hydrogeological characteristics, i.e., transmissivity (T), hydraulic conductivity (K), storativity (S) and specific storage (Ss) (Fetter 2001; Tizro *et al.* 2010). The conventional ways to estimate these parameters are through pumping tests, slug tests, permeameter measurements and grain size analysis (Fetter 2001). However, these tests can be expensive, time-consuming and depend on the existence of boreholes and sampling points conveniently distributed over a study area (Soupios *et al.* 2007; Perdomo *et al.* 2018). Likewise, values of hydrogeological parameters can vary over relatively short distances in heterogeneous aquifers, making the results from conventional methods valid only for small sectors of an aquifer (Perdomo *et al.* 2018). The correlation between resistivity and hydrogeological properties

H2Open Journal Vol 2 No 1
doi: 10.2166/h2oj.2019.007

in porous aquifers can be used to get cost-effective estimations of parameters like K and T from surface geoelectrical measurements (Tizro *et al.* 2010).

The porous aquifer to the north of Oruro (~300,000 inhabitants) supplies the total demand for domestic consumption, irrigation and industry. However, the hydrogeological knowledge of this reservoir needs to be improved in order to have a future management plan of water resources in the region (D'Elia 2013; GITEC & COBODES Ltda 2014). The aquifer has been investigated at small scales in the past, aiming to implement wells connected to the supply system (SCIDE *et al.* 1996). The information from these studies is partially available and corresponds only to a small part of the study area. With the purpose of obtaining preliminary aquifer parameters in an area bigger than where the wells are located, this study combines the available information from drilling reports, pumping tests and geoelectrical measurements to obtain values of K and T, based on an empirical linear petrophysical relationship between resistivity and hydraulic conductivity.

In order to expand K and T estimations, resistivity and aquifer thicknesses were obtained from inverted models corresponding to field measurements applying electrical resistivity tomography (ERT) and transient electromagnetic soundings (TEM), conducted between 2013 and 2017 as part of this study. Complementary data were retrieved from previous studies applying vertical electrical soundings (VES) (e.g., SCIDE *et al.* 1996; Dames & Moore Norge 2000; Canaviri 2011). The typical resistivity range corresponding to porous aquifers saturated with fresh water was used to estimate hydrogeological parameters, making wider use of the geoelectrical measurements in the study area. This study intends to improve the comprehensive knowledge of one of the most important groundwater reservoirs in the Bolivian Altiplano.

STUDY AREA

The study area is characterized by a semiarid climate and scarce vegetation. It belongs to the Poopo enclosed catchment where the lake of the same name receives the discharge of surficial and sub-surficial water bodies. However, this lake dried up in 2015 evidencing the decline of available water in the region (Satgé *et al.* 2017). In terms of groundwater, the most important reservoirs are porous aquifers lying beneath peneplain terrains surrounded by mountains, covering approximately 500 km^2 at an elevation of ~3,700 m above sea level (Figure 1). The selected study area is located in the alluvial fan of River Paria. The recharge of the aquifers mainly occurs by lateral infiltration of surface water coming from the rivers, which previously receive and transport the runoff from the mountains during the rainy season. The natural flow direction in the top porous aquifer was mainly to the south, in accordance with the topography. However, the large volumes extracted from a well field in the middle of the alluvial fan have been changing that original flow direction, lowering the water table around the wells and creating a cone of depression of about 5 km radius (Swedish Geological AB 1996; Banks *et al.* 2002; GITEC & COBODES Ltda 2014). The study area is considered hydraulically stressed due to the increasing abstraction of groundwater, ~9.5 million m^3/yr (SELA 2018), which in the future might threaten the hydrodynamic equilibrium in the whole aquifer system (D'Elia 2013), since the recharge, ~12.5 million m^3/yr coming from the River Paria, has also been declining (GITEC & COBODES Ltda 2014).

The geological units in the region consist of three main groups, from older to younger: sedimentary rocks (consolidated), volcanic outcrops (consolidated) and granular deposits (unconsolidated). In the study area, sedimentary rocks including sandstones, siltstones, shales and quartzite are part of the bedrock. The secondary porosity in this unit is assumed the most important for water storage. Overlying the latter, unconsolidated deposits of clay, silt, sand, gravels and pebbles are found in complex arrangements due to the overlapped depositional events (fluvial, lacustrine, glacial and colluvial) (Rigsby *et al.* 2005). The primary porosity is predominant in these formations, which are considered

H2Open Journal Vol 2 No 1
doi: 10.2166/h2oj.2019.007

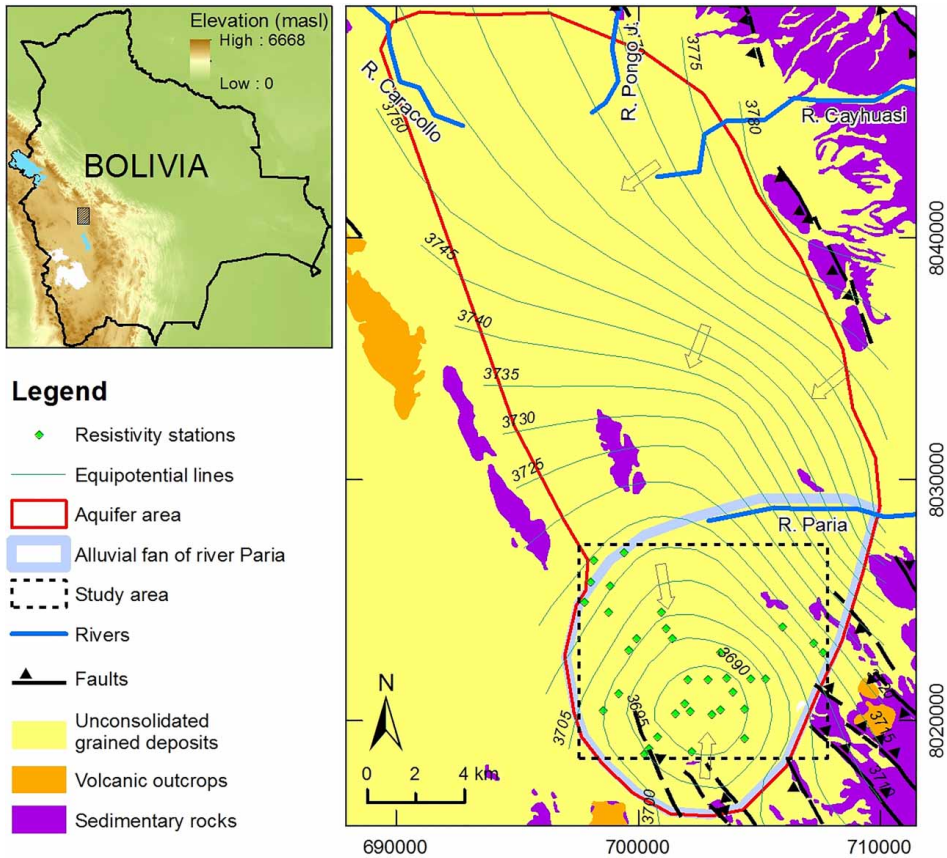

Figure 1 | Location of the study area and regional geological map. Modified from Banks *et al.* (2002), Dames & Moore Norge (2000), GEOBOL & Swedish Geological AB (1992), GITEC & COBODES Ltda (2014) and Swedish Geological AB (1996).

interconnected as a single porous aquifer (Dames & Moore Norge 2000; D'Elia 2013). A large part of the study area is covered with a thin clay layer which reduces the vertical infiltration (D'Elia 2013).

THEORY, METHODS AND MATERIALS

The flow of water and the flow of electrical current in porous media are governed by similar petrophysical parameters (e.g., porosity, grain size distribution, pore size distribution, mineralogy of grains, geometry of pores, tortuosity), making them related to each other (Soupios *et al.* 2007; Kirsch & Yaramanci 2009). Many authors have used the analogy of the governing factors for hydraulic and electrical conduction to establish empirical relationships and models (Börner 2009; Perdomo *et al.* 2018). For example, Archie's law relates bulk resistivity and fluid resistivity in a formation factor that depends on the tortuosity and the porosity (Glover 2016; Perdomo *et al.* 2018). Another approach is the Kozeny–Carman equation, which relates the hydraulic conductivity among the porosity with its hydraulic radius, the tortuosity and other structural parameters (Börner 2009). In this study, an empirical linear relationship is used to estimate hydraulic conductivity from resistivity, in the spirit of other field investigations that found an inverse correlation between these parameters in different groups of sediments (Mazáč *et al.* 1985; Kirsch & Yaramanci 2009).

H_2Open Journal Vol 2 No 1
doi: 10.2166/h2oj.2019.007

In order to find the relationship between K and ρ valid for the study area, data from previous studies were gathered. A few hydrogeological studies have been conducted around the aquifers near Oruro in the past; however, not all of them are available and the data usually lack precise location, complete record sets and calculations. Information from some boreholes and drilling protocols include stratigraphy, pumping tests and hydrochemical analysis (SCIDE *et al.* 1996). The mud rotary method was commonly used for drilling. Samples of cuttings are made each metre to get the stratigraphy of the unconsolidated sediments (presented as proportions of gravel, sand and clay). The boreholes reach depths in the range of 60 to 150 m, completed within the porous formations. In order to estimate hydraulic properties, pumping tests were performed at some boreholes and the reported K values are in the range of 5.5×10^{-5} to 2.9×10^{-4} m/s (SCIDE *et al.* 1996; Canaviri 2011). The hydrochemical analyses encompass major ion concentrations and *in situ* measurements, like pH and electrical conductivity (*EC*) (Lizarazu *et al.* 1987; Swedish Geological AB 1996; Gómez *et al.* 2016). The groundwater salinity in the study area, expressed as *EC*, is in the range of 0.8 to 3.5 mS/cm; however, only a few sites close to a fault reported the highest values, with the rest of the boreholes reporting values of $\leq$1.0 mS/cm.

Recent ERT and TEM measurements around the study area achieved good resolution and depth of investigation (DOI), confirming both methods are suitable for the local conditions (e.g., Larsson 2016; Broman & Svensson 2017). Although the methods have different sensitivity degree and resolution (Boiero *et al.* 2010), both were used to retrieve resistivity values and thickness of the porous aquifer from their inverted models. The ERT method evaluates resistivity by injecting currents and measuring potentials. The measurements using multi-electrode and multi-channel equipment, improve this method covering large distances with good resolution (Dahlin & Zhou 2006). 2-D resistivity sections can be obtained after applying an inverse numerical modelling; an iterative process aiming to reduce the differences between modelled data coming from a synthetic model and the field measurements (Dahlin 2001; Loke *et al.* 2003). The TEM technique also uses electrical currents, but in this case to generate primary electromagnetic fields that induce eddy currents passing through the ground. The signals of these currents are detected and transformed into resistivity (Christiansen *et al.* 2009; Reynolds 2011). 1-D resistivity models can be obtained after a numerical modelling process consisting of curve matching to solve inverse scattering problems (Nabighian 1991). The measurements were conducted in different campaigns between 2013 and 2017 using ABEM equipment: the Terrameter LS for ERT and the WalkTEM for TEM.

Finally and to expand the hydraulic conductivity estimations from resistivity, the study includes VES measurements and results reported in some previous studies (e.g., Swedish Geological AB 1996; Dames & Moore Norge 2000; Canaviri 2011; GITEC & COBODES Ltda 2014). Similarly to ERT, the VES method estimates the resistivity distribution in the ground by injecting currents and measuring potentials, but in this case the models are solved in 1-D. VES data do not follow standard procedures for data acquisition, inversion or results presentation, since the measurements were conducted at different times, using different equipment and inverted with different software. The distribution of the available data is shown in Figure 2. In order to handle consistent 1-D resistivity data from all the available sources, representative points and their correspondent vertical resistivity profiling, were taken from the ERT sections (originally solved in 2-D) (i.e., triangles are used for the further calculations instead of lines marked as ERT).

RESULTS AND INTERPRETATION

To estimate hydraulic parameters from geoelectrical tests using a linear relationship, the target aquifer should be clearly visible in terms of resistivity and thickness from the inverted models. For example, in the northwest part of the study area, the ERT profile A is coincident with the resistivity stations 1 and

H2Open Journal Vol 2 No 1
doi: 10.2166/h2oj.2019.007

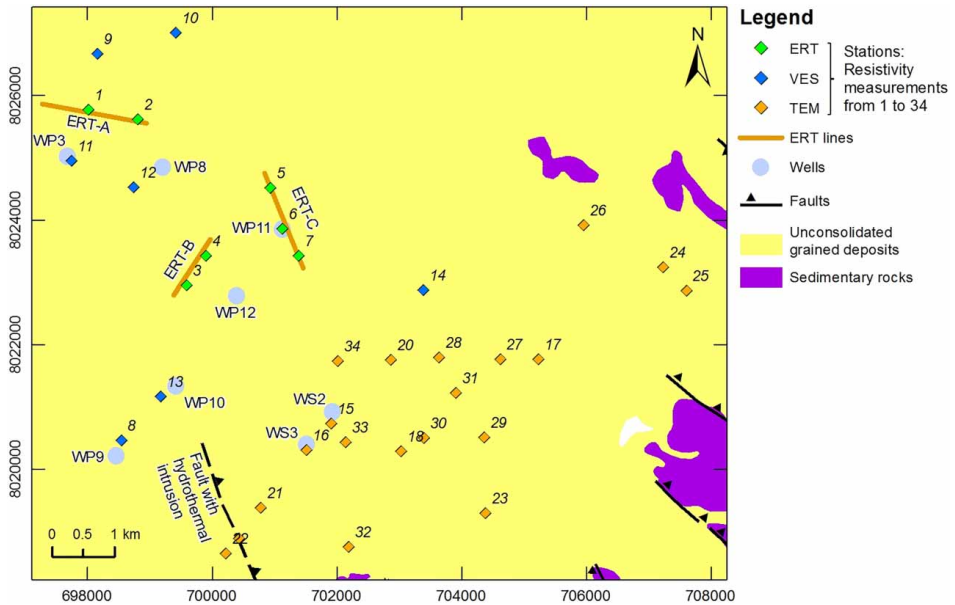

Figure 2 | Location of measurements and sources of information over the study area. Regional geological map as the background. Wells reported values of *T* and *K* from pumping tests. Modified from Banks *et al.* (2002), Canaviri (2011), Dames & Moore Norge (2000), GEOBOL & Swedish Geological AB (1992) and SCIDE *et al.* (1996).

2 (see Figure 2). As shown in Figure 3, the top part of the section until ~3,650 masl (~70 m thickness) is assumed as the porous aquifer with low resistivity signature (~20 ohm-m) overlying a more resistive layer (~100 ohm-m) corresponding to the bedrock with low or negligible water content. Two VES measurements are reported at the same sites of stations 1 and 2, their corresponding resistivity models are shown in Figure 3 as columns. These VES models also expose changes in resistivity from low values in the shallow part to higher values at similar levels shown in the ERT model. Despite this change in resistivity supports the inferred change in geological facies, the values shown in the VES models are not necessarily the same as on the ERT model due to the differences between these methods (different equipment, sensitivity, processing and inversion procedures). In this case,

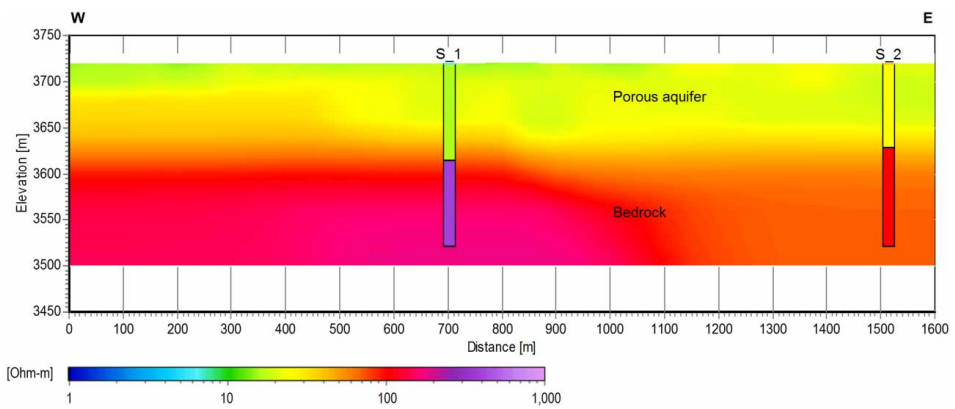

Figure 3 | 2-D resistivity model corresponding to the ERT line A. The profile includes two 1-D models corresponding to VES measurements. The resistivity scale is valid for both types of models.

H_2Open Journal Vol 2 No 1
doi: 10.2166/h2oj.2019.007

the resistivity coming from the ERT is assumed more reliable since the raw data were processed in this study, whereas the VES models were obtained from a thesis showing model results directly without raw data (Canaviri 2011), hence, the data quality of that study could not be assessed. The resistivity and target aquifer thickness for stations 1 and 2 come from the ERT line A.

The salinity of water influence greatly the resistivity measurements regardless the method applied to get that information. The top porous aquifer yields fresh water (EC <1.0 mS/cm), but the fractured aquifer might be saturated with saline water around some faults (EC >3.5 mS/cm). The knowledge about the fractured aquifer is limited; however, its high salinity and temperature can be attributed to the existence of deep thermal sources, most likely the volcanic intrusions mentioned in the regional geological background. Not all the faults in the region seem to reach thermal sources, but those that presumably do, have a distinctive low resistivity signature. The hydrothermal flows seem to go upwards in some parts along the faults; consequently, some sectors of the porous aquifer present hydrothermal intrusions with artesian conditions. For example, one of these faults with hydrothermal flows crosses the study area coming from the south. The well WP10 (see Figure 2) is apparently located along the projection of the mapped fault. The drilling depth in this well is ~100 m and the water is more saline (EC ~3.5 mS/cm) than in others in the vicinity. Although the salinity in WP10 is greater than the limit for consumption (1.5 mS/cm) (IBNORCA 2010), mixing this source with others from the porous aquifer keeps this parameter below the limit before being distributed. The closest ERT resistivity section (B) shows a feature with low resistivity that is assumed as corresponding to the hydrothermal intrusion (Figure 4).

The DOI of the ERT model B is ~220 m below the surface. The section seems completed within the porous aquifer, in a site that is also indicated as the deepest part of the porous aquifer according to previous studies (e.g., Banks *et al.* 2002). However, the hydrothermal intrusion precludes the use of the linear relationship due to the saline intrusion. In addition, the very shallow layer of the section has relatively high resistivity values (~80 ohm-m); it is interpreted as the part above the water table, i.e., unsaturated sediments. The same feature also appears on the ERT line C, but its resistivity value is slightly lower (Figure 5). Unlike ERT sections B and C, the unsaturated fringe does not appear in section A presumably because it is located outside of the influence of the cone of depression shown in Figure 1; therefore, the water table around section A might be shallow.

The target aquifer is also visible on the TEM inverted models. For example, station 28 (Figure 6) has the three main parts of the hydrogeological settings in the study area: the unsaturated fringe on top, the porous aquifer and the bedrock, each one with a distinctive resistivity.

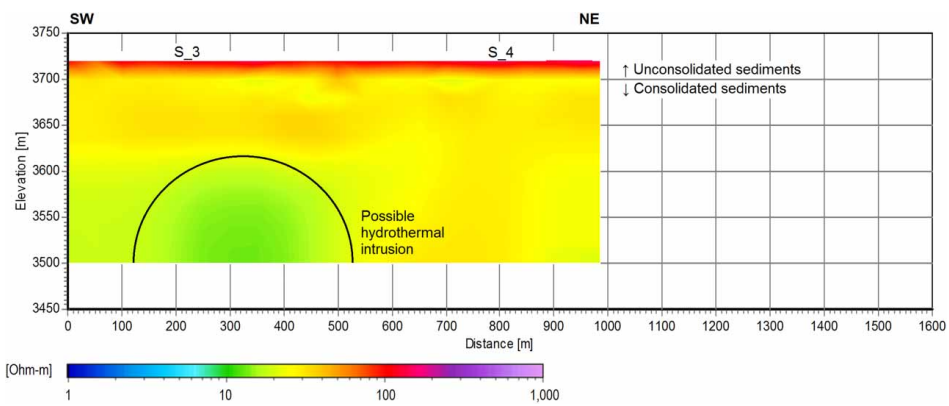

Figure 4 | 2-D resistivity model corresponding to the ERT line B. A hydrothermal intrusion characterized by low resistivity appears in the bottom of the section.

H_2Open Journal Vol 2 No 1
doi: 10.2166/h2oj.2019.007

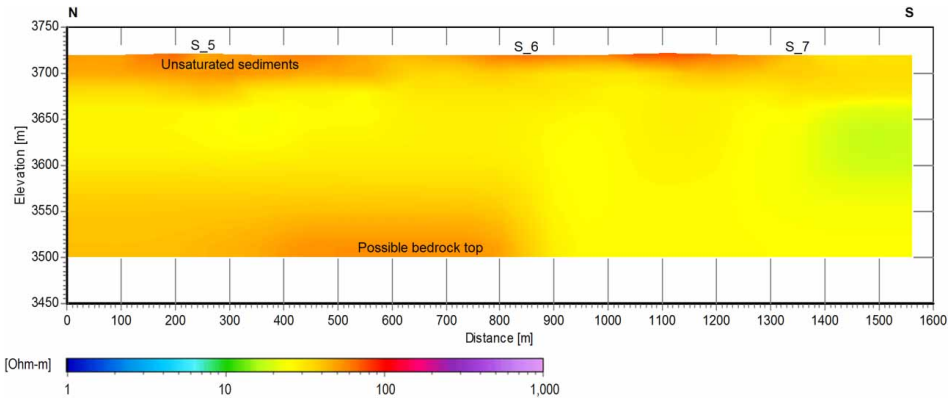

Figure 5 | 2-D resistivity model corresponding to the ERT line C. Unsaturated sediments characterized by relatively high resistivity can be seen at shallow parts of the section.

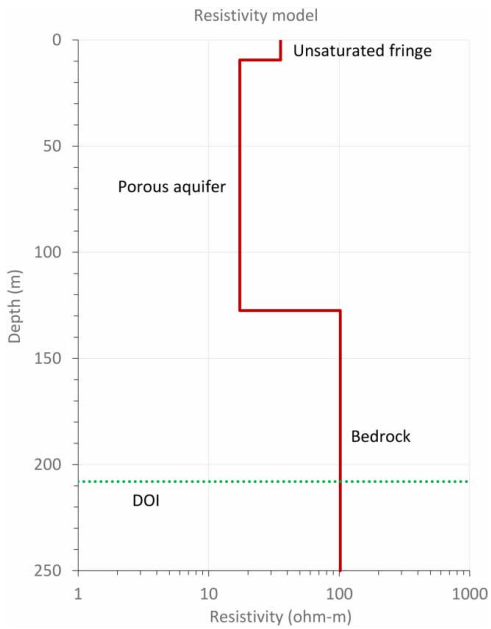

Figure 6 | 1-D resistivity model corresponding to station 28 (TEM). The model shows three layers, the same that appear on the northern part of the ERT model C.

The empirical relationship between K and ρ can be established using the hydraulic conductivity obtained from pumping tests conducted in wells located in the alluvial fan of River Paria, and found in technical reports (e.g., SCIDE *et al.* 1996; Dames & Moore Norge 2000). The corresponding resistivity was adopted from the closest geoelectrical station to each well (see Figure 2). Figure 7 shows K vs. ρ values fit in a linear correlation except for WP10. As mentioned before, the water in well WP10 is influenced by high salinity associated with hydrothermal intrusions because it is located along the projection of a fault that presumably reach thermal sources. The salinity of water in this place increases the electrical conductivity of the ground measured with VES (Canaviri 2011), making this point out of the linear tendency. The rest of the points were used to establish a linear

H2Open Journal Vol 2 No 1
doi: 10.2166/h2oj.2019.007

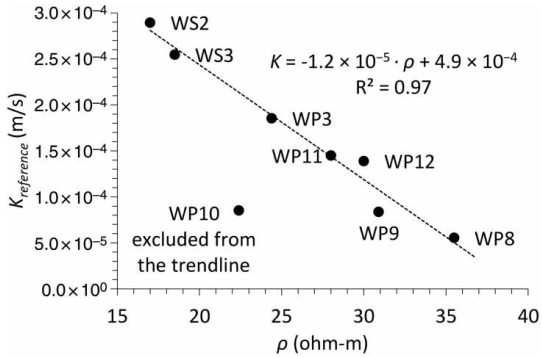

Figure 7 | Empirical linear correlation between hydraulic conductivity from pumping tests and resistivity from the closest geoelectrical station.

relationship indicated in Figure 7, which serves to predict K values in the rest of the study area based on ρ values from geoelectrical models.

The correlation between K and ρ in the study area is adjusted to a straight line described by the equation:

$$K = -1.2 \times 10^{-5} \cdot \rho + 4.9 \times 10^{-4}$$

Kirsch & Yaramanci (2009) present a similar linear relationship for a fine grained sand aquifer, which type of sediment is likely abundant in the present study area. Hydraulic conductivity in the rest of the geoelectrical stations were estimated using this linear equation. Furthermore, transmissivity was also estimated using the relationship $T = K \cdot h$ (Fetter 2001), where h is the thickness of the saturated porous aquifer; in some sites it is underlying an unsaturated fringe (as shown in Figures 4–6). The saturated thickness as well as resistivity were obtained from inverted resistivity models; in the case of VES and TEM these models are solved in 1-D, and ρ and h values can be directly obtained from them (as in Figure 6). For ERT models solved in 2-D, ρ and h values were obtained vertically (like 1-D) below the location of each station from the blocked inverted models, regardless of lateral changes in resistivity in the rest of the section. The last column $T_{\text{reference}}$ is obtained multiplying $K_{\text{reference}}$ by h.

The distribution of estimated T over the study area allows the most promising areas in terms of groundwater production to be identified; these values were interpolated with the Kriging method to obtain smooth transitions, as shown in Figure 8. The highest transmissivity is located in the middle of the study area, in agreement with previous studies indicating the same sector holds the thickest portion of the porous aquifer (e.g., Banks *et al.* 2002). On the other hand, the lowest values are located in the southwest part, where the top of the bedrock was detected at shallower levels and where the hydrothermal intrusion constrains the usable thickness around the fault shown in Figure 2. Interpolated values in the northern top and southeast parts of the study area may not be entirely reliable due to the less densified resistivity stations for interpolations.

DISCUSSION

The estimation of aquifer characteristics presented in this study is based on the relationships between hydraulic and electrical properties in unconsolidated sediments. The linear correlation found between $K_{\text{reference}}$ (obtained from pumping tests) and ρ (obtained from inverted geoelectrical models) is valid

H2Open Journal Vol 2 No 1
doi: 10.2166/h2oj.2019.007

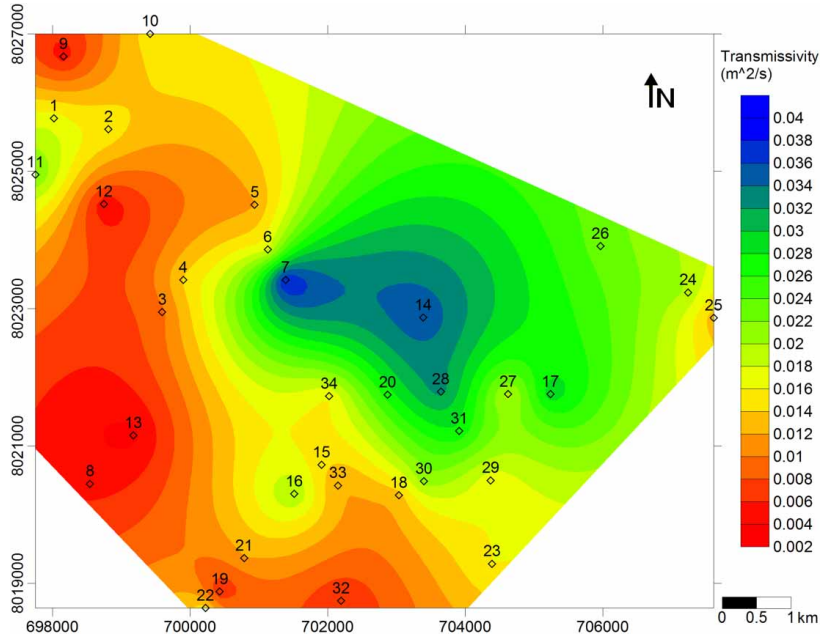

Figure 8 | Calculated transmissivity distribution corresponding to the top porous aquifer in the central part of the alluvial fan of the River Paria.

only for the study area, since this type of inverse correlation has been empirically established varying according to the rock type and the grain size (Mazáč *et al.* 1985; Kirsch & Yaramanci 2009). The factors governing the geoelectrical response are also critical when it comes to evaluating the validity of the method. In this aspect, the biggest uncertainty comes from the mixed use of results from ERT, TEM and VES, since these methods evaluate resistivity in different ways and have different sensitivities. However, in the spirit of making wider use of the available resources in the study area the proposed empirical petrophysical relationship can provide results worth analysing.

Regarding the thickness of the porous aquifer, in some parts of the study area the contact between unconsolidated sediments and bedrock can be identified on the resistivity models as transitions from relatively low values (~20 ohm-m) to greater values (e.g., ERT section A, Figure 3). Likewise, saline water intrusions can be seen as transitions to lower values (e.g., ERT section B, Figure 4), reducing the thickness of the aquifer saturated with fresh water. In cases where the bottom limit of the target aquifer cannot be identified due to limitations in the DOI of the geophysical methods, the results might have a degree of uncertainty. In the central part of the study area, stations 7 and 14 were assigned the maximum thickness of their respective DOI (see Table 1), although the thickness in these points may be greater in reality. Nevertheless, the same site was identified as having the deepest unconsolidated sediment sector in previous studies (e.g., Dames & Moore Norge 2000; Banks *et al.* 2002).

The density of geoelectrical stations plays a significant role in resolving hydrogeological properties in new areas. The greater the distance between stations, the less reliable is the interpolation of intervening regions. The access to some parts of the study area was restricted during the fieldwork due to conflicts between villagers and water well owners. Consequently, it was not possible to extend the measurements to cover blank spaces in between geoelectrical stations shown in Figure 8. The estimated transmissivity values in the study area vary between 3.4×10^{-3} and 4.0×10^{-2} m^2/s evidencing, in turn, the influence of the great variations in the aquifer thickness.

H_2Open Journal Vol 2 No 1
doi: 10.2166/h2oj.2019.007

Table 1 | Estimated hydraulic conductivity and transmissivity values obtained from an empirical linear relationship between K and ρ

Station	Source type	Reference well	$K_{reference}$ (m/s)	ρ (ohm-m)	K (m/s)	h (m)	T (m^2/s)	$T_{reference}$ (m^2/s)
1	ERT			20	2.43×10^{-4}	70	1.70×10^{-2}	
2	ERT			24	1.94×10^{-4}	80	1.55×10^{-2}	
3	ERT			30	1.19×10^{-4}	80	9.51×10^{-3}	
4	ERT	WP12	1.39×10^{-4}	30	1.19×10^{-4}	120	1.43×10^{-2}	1.67×10^{-2}
5	ERT			30	1.19×10^{-4}	100	1.19×10^{-2}	
6	ERT	WP11	1.45×10^{-4}	28	1.44×10^{-4}	120	1.73×10^{-2}	1.74×10^{-2}
7	ERT			24	1.94×10^{-4}	200	3.87×10^{-2}	
8	VES	WP9	8.37×10^{-5}	30.9	1.08×10^{-4}	63	6.78×10^{-3}	5.27×10^{-3}
9	VES			36.8	3.41×10^{-5}	144	4.91×10^{-3}	
10	VES			21.5	2.25×10^{-4}	68	1.53×10^{-2}	
11	VES	WP3	1.85×10^{-4}	24.4	1.89×10^{-4}	122	2.30×10^{-2}	2.26×10^{-2}
12	VES	WP8	5.54×10^{-5}	35.5	5.03×10^{-5}	80	4.02×10^{-3}	4.43×10^{-3}
13	VES	WP10	8.52×10^{-5}	22.4	2.14×10^{-4}	40	8.54×10^{-3}	3.41×10^{-3}
14	VES			19.6	2.48×10^{-4}	143	3.55×10^{-2}	
15	TEM	WS2	2.89×10^{-4}	17	2.81×10^{-4}	50	1.40×10^{-2}	1.45×10^{-2}
16	TEM	WS3	2.55×10^{-4}	18.5	2.62×10^{-4}	80	2.10×10^{-2}	2.04×10^{-2}
17	TEM			19.9	2.45×10^{-4}	120	2.94×10^{-2}	
18	TEM			13.4	3.26×10^{-4}	40	1.30×10^{-2}	
19	TEM			15.8	2.96×10^{-4}	20	5.92×10^{-3}	
20	TEM			17.9	2.70×10^{-4}	100	2.70×10^{-2}	
21	TEM			12.1	3.42×10^{-4}	35	1.20×10^{-2}	
22	TEM			12.6	3.36×10^{-4}	45	1.51×10^{-2}	
23	TEM			11.6	3.48×10^{-4}	46	1.60×10^{-2}	
24	TEM			11.2	3.53×10^{-4}	56	1.98×10^{-2}	
25	TEM			15.2	3.03×10^{-4}	42	1.27×10^{-2}	
26	TEM			19.4	2.51×10^{-4}	92	2.31×10^{-2}	
27	TEM			13.6	3.23×10^{-4}	59	1.91×10^{-2}	
28	TEM			17.3	2.77×10^{-4}	118	3.27×10^{-2}	
29	TEM			10.8	3.58×10^{-4}	46	1.65×10^{-2}	
30	TEM			15.5	3.00×10^{-4}	70	2.10×10^{-2}	
31	TEM			14.3	3.15×10^{-4}	88	2.77×10^{-2}	
32	TEM			14	3.18×10^{-4}	19	6.05×10^{-2}	
33	TEM			19.1	2.55×10^{-4}	47	1.20×10^{-2}	
34	TEM			17.9	2.70×10^{-4}	59	1.59×10^{-2}	

CONCLUSIONS

The central part of the alluvial fan of the River Paria is favourable for geoelectrical surveys given its clear distinction between geological facies, greatly influenced by the type of water saturating the aquifers. The top porous aquifer, used for fresh water supply, was evaluated in its hydraulic properties by using an empirical relationship between resistivity and hydraulic conductivity to identify suitable sites for groundwater production, which, in this case, is the central part of the investigated area.

Resistivity models from different geoelectrical measurements (electrical resistivity tomography, transient electromagnetic soundings and vertical electrical soundings) were evaluated in terms of

H2Open Journal Vol 2 No 1
doi: 10.2166/h2oj.2019.007

target aquifer thickness and resistivity from the inverted models. The distribution of the calculated transmissivity in the study area is also in good agreement with geological models from previous investigations; the highest values are located in the centre of the study area, at the same site where the porous aquifer is thicker. In sites where the top of the bedrock is shallow and where hydrothermal intrusions were detected, the estimated transmissivity has lower values.

Getting an early idea of hydrogeological properties like transmissivity and hydraulic conductivity, before conducting more demanding and costly tests, can be very valuable, identifying the most promising sectors for groundwater production. A more ambitious study may include extended surveys to cover larger areas (e.g., with airborne geophysics), necessary for groundwater management plans.

ACKNOWLEDGEMENTS

The study was funded by the Swedish International Development Cooperation Agency (SIDA) and the Society of Exploration Geophysicists (SEG) through the Geoscientists Without Borders (GWB) programme. This work was also supported by Lund University (LU) in Sweden, Aarhus University (AU) in Denmark, Universidad Mayor de San Andrés (UMSA) and Universidad Técnica de Oruro (UTO) in Bolivia. The TEM equipment was provided by Engineering Geology Division LU with support from Guideline Geo AB. The ERT equipment was provided by UTO. We are grateful to the people who helped to conduct the field measurements: Ramiro Pilco, Måns Larsson, Emil Svensson, Kamran Ahmad, Mauricio García, Rafael Mendoza, personnel of Instituto de hidráulica e hidrología (IHH-UMSA), Servicio Local de Acueductos y Alcantarillado de Oruro (SELA), Unidad de Saneamiento Basico y Vivienda (UNASVBI), Ministerio de Medio Ambiente y Agua (MMAyA) and Corimex Ltda, students from UTO and many other volunteers. Finally, we acknowledge the assistance of the facilitators at the workshop on scientific writing, arranged by Aalto University, Helsinki, Finland and IWA/YWP Finland in August 2018. This has considerably improved the content of the paper.

REFERENCES

Banks, D., Holden, W., Aguilar, E., Mendez, C., Koller, D., Andia, Z., Rodriguez, J., Saether, O. M., Torrico, A., Veneros, R. & Flores, J. 2002 Contaminant source characterization of the San Jose Mine, Oruro, Bolivia. *Geol. Soc. London, Spec. Publ.* **198**, 215–239. https://doi.org/10.1144/GSL.SP.2002.198.01.14.

Boiero, D., Godio, A., Naldi, M. & Yigit, E. 2010 Geophysical investigation of a mineral groundwater resource in Turkey. *Hydrogeol. J.* **18**, 1219–1233. https://doi.org/10.1007/s10040-010-0604-2.

Börner, F. 2009 Complex conductivity measurements. In: *Groundwater Geophysics: A Tool for Hydrogeology* (Kirsch, R., ed.). Springer, Berlin, Heidelberg, Germany, pp. 119–153. https://doi.org/10.1007/978-3-540-88405-7_4.

Broman, V. & Svensson, E. 2017 *TEM and ERT Investigations in Challapampa Aquifer, Bolivia*. MSc thesis, Engineering Geology, Lund University, Lund, Sweden. ISRN LUTVDG/(TVTG–5152)/1-50/(2017).

Canaviri, B. 2011 *Estimación de la vulnerabilidad intrínseca a la contaminación del aquífero libre en el sistema acuífero de Challapampa Oruro (Estimation of the Intrinsic Vulnerability to Contamination of the Unconfined Aquifer in the Challapampa Aquifer System Oruro)*. Tesis de grado (Bachelor thesis), Universidad Técnica de Oruro, Oruro, Bolivia.

Christiansen, A. V., Auken, E. & Sørensen, K. 2009 The transient electromagnetic method. In: *Groundwater Geophysics: A Tool for Hydrogeology* (Kirsch, R., ed.). Springer, Berlin, Heidelberg, Germany, pp. 179–226. https://doi.org/10.1007/978-3-540-88405-7_6.

Dahlin, T. 2001 The development of DC resistivity imaging techniques. *Comput. Geosci.* **27**, 1019–1029. https://doi.org/10.1016/S0098-3004(00)00160-6.

Dahlin, T. & Zhou, B. 2006 Multiple-gradient array measurements for multichannel 2D resistivity imaging. *Near Surf. Geophys.* **4**, 113–123. https://doi.org/10.3997/1873-0604.2005037.

Dames & Moore Norge 2000 *Estudio hidrogeológico de la mina San José y los acuíferos que suministran agua a la ciudad de Oruro (Hydrogeological Study of the San Jose Mine and Adjacent Aquifers Supplying Water to the City of Oruro).* Report 1,2,3. PMAIM-Subproyecto No. 7. Corporacion Minera de Bolivia COMIBOL.

D'Elia, M. 2013 *Asesoramiento para el Diseño e Implementación de la Red de Monitoreo de Aguas Subterráneas en la Cuenca del Lago Poopó (Advice for the Design and Implementation of the Groundwater Monitoring Network in the Lake Poopó*

H_2Open Journal Vol 2 No 1
doi: 10.2166/h2oj.2019.007

Basin). Programa de Gestión Sostenible de los Recursos Naturales de la Cuenca del Lago Poopó Convenio No. DCI-ALA/2009/021-614, Oruro, Bolivia. Gobierno Autónomo Departamental De Oruro.

Fetter, C. W. 2001 *Applied Hydrogeology*. Prentice Hall, Upper Saddle River, NJ, USA.

GEOBOL & Swedish Geological AB 1992 *Carta Geológica de Bolivia – Hoja Oruro (Geological map of Bolivia – Sheet Oruro)*. Publicación SGB Serie I-CGB-11.

GITEC, C.G. & COBODES Ltda 2014 *Formulación del Plan Director de la Cuenca del Lago Poopó (Poopo Lake Basin Management Plan Formulation)*. Informe final. Programa de gestion sostenible de los recursos naturales de la cuenca del lago Poopo. Gobierno Autónomo Departamental de Oruro. Agosto 2014, Oruro, Bolivia (CTO-SERV-03/2013).

Glover, P. W. J. 2016 Archie's law – a reappraisal. *Solid Earth* **7**, 1157–1169. https://doi.org/10.5194/se-7-1157-2016.

Gómez, E., Barmen, G. & Rosberg, J.-E. 2016 Groundwater origins and circulation patterns based on isotopes in Challapampa aquifer, Bolivia. *Water* **8**, 207. https://doi.org/10.3390/w8050207.

IBNORCA 2010 *Norma Boliviana NB 512 - Agua Potable Requisitos (Bolivian Norm NB 512 - Drinking Water Requirements)*. Instituto Boliviano de Normalización y Calidad. Cuarta Revisión ICS 13.060.20 Agua Potable. Diciembre 2010., La Paz, Bolivia.

Kirsch, R. & Yaramanci, U. 2009 Geophysical characterisation of aquifers. In: *Groundwater Geophysics: A Tool for Hydrogeology* (Kirsch, R., ed.). Springer, Berlin, Heidelberg, Germany, pp. 491–509. https://doi.org/10.1007/978-3-540-88405-7_17.

Larsson, M. 2016 *TEM Investigation on Challapampa Aquifer, Oruro Bolivia*. MSc thesis, Department of Geology, Lund University, Lund, Sweden. No. 494, p. 44.

Lizarazu, J., Aranyossy, J. F., Orsag, V. & Salazar, J. C. 1987 Estudio Isotopico de la cuenca de Oruro-Caracollo, Bolivia (Isotopic study in the Oruro-Caracollo basin, Bolivia). In: Symposium Isotope Techniques in Water Resources Development. IAEA-SM-299/11 301-314. Vienna, Austria, March 1987.

Loke, M. H., Acworth, I. & Dahlin, T. 2003 A comparison of smooth and blocky inversion methods in 2D electrical imaging surveys. *Explor. Geophys.* **34**, 182–187.

Mazáč, O., Kelly, W. E. & Landa, I. 1985 A hydrogeophysical model for relations between electrical and hydraulic properties of aquifers. *J. Hydrol.* **79**, 1–19. https://doi.org/10.1016/0022-1694(85)90178-7.

Nabighian, M. 1991 *Electromagnetic Methods in Applied Geophysics*, Vol. 2. Application, Parts A and B. Society of Exploration Geophysicists, Denver, CO, USA. https://doi.org/10.1190/1.9781560802686.

Perdomo, S., Kruse, E. E. & Ainchil, J. E. 2018 Estimation of hydraulic parameters using electrical resistivity tomography (ERT) and empirical laws in a semi-confined aquifer. *Near Surf. Geophys.* **16**, 627–641. https://doi.org/10.1002/nsg.12020.

Reynolds, J. M. 2011 *An Introduction to Applied and Environmental Geophysics*. Wiley-Blackwell, Chichester, UK.

Rigsby, C. A., Bradbury, J. P., Baker, P. A., Rollins, S. M. & Warren, M. R. 2005 Late Quaternary palaeolakes, rivers, and wetlands on the Bolivian Altiplano and their palaeoclimatic implications. *J. Quat. Sci.* **20**, 671–691. https://doi.org/10.1002/jqs.986.

Satgé, F., Espinoza, R., Zolá, R. P., Roig, H., Timouk, F., Molina, J., Garnier, J., Calmant, S., Seyler, F. & Bonnet, M. P. 2017 Role of climate variability and human activity on Poopó Lake droughts between 1990 and 2015 assessed using remote sensing data. *Remote Sens.* **9**, 1–17. https://doi.org/10.3390/rs9030218.

SCIDE, CORDEOR & GEOBOL 1996 *Informe de los pozos de producción – Proyecto de investigación y verificación de fuentes de abastecimiento de agua para la ciudad de Oruro (Report of the Production Wells – Project of Investigation and Verification of Sources of Water for Supplying Oruro)*. GEOBOL – Servicio Geológico de Bolivia, Oruro, Bolivia, p. 159.

SELA 2018 *Servicio Local De Acueductos Y Alcantarillado – Oruro [WWW Document]*. http://selaoruro.gob.bo/ (accessed 1.10.18).

Soupios, P. M., Kouli, M., Vallianatos, F., Vafidis, A. & Stavroulakis, G. 2007 Estimation of aquifer hydraulic parameters from surficial geophysical methods: a case study of Keritis Basin in Chania (Crete - Greece). *J. Hydrol.* **338**, 122–131. https://doi.org/10.1016/j.jhydrol.2007.02.028.

Swedish Geological AB 1996 *Impacto de la contaminación minera e industrial sobre agua subterráneas (Impact of Mining and Industrial Pollution on Groundwater)*. Ministerio de Desarrollo Sostenible y Medio Ambiente. Secretaria Nacional de Mineria. Proyecto Piloto Oruro, (Report) ID: R-Bo-E-9.45–9702-PPO96I6.

Tizro, A. T., Voudouris, K. S., Salehzade, M. & Mashayekhi, H. 2010 Hydrogeological framework and estimation of aquifer hydraulic parameters using geoelectrical data: a case study from West Iran. *Hydrogeol. J.* **18**, 917–929. https://doi.org/10.1007/s10040-010-0580-6.